Sri Gajanan Moudgalya Gogulapati

Development of Finite Element Models to study Pavement Widening



Development of Finite Element Models to study Pavement Widening

By

Sri Gajanan Moudgalya Gogulapati

in partial fulfilment of the requirements for the degree of

Master of Science

in Civil engineering

at the Delft University of Technology, to be defended publicly on 25-04-2024 at 16:00 h

Supervisor: Dr. Kumar Anupam (Chair) TU Delft Thesis committee: Ir. Cor Kasbergen TU Delft

Mr Saranga Premarathna
Dr. Zhen Yang
TU Delft
TU Delft
TU Delft
TU Delft
Rijkswaterstaat



External:



ACKNOWLEDGMENTS

I am sincerely grateful to TU Delft and Rijkswaterstaat for providing me with the opportunity to delve into this thesis topic. Their support and encouragement have been invaluable throughout my research journey, allowing me to contribute to the field of pavement engineering.

I extend my heartfelt appreciation to my university supervisors, Dr. Kumar Anupam and Ir. Cor Kasbergen, for their unwavering guidance and support. Dr. Anupam's involvement and dedication to my thesis were significant in shaping its direction, while Ir. Cor Kasbergen's expertise helped me develop a material model. Their mentorship has truly empowered me to think critically and approach challenges with confidence.

I am also indebted to Mr. Saranga Premarathna and Ir. Mohan Salil, whose mentorship and support were crucial during my thesis. Their willingness to address my queries and provide constructive feedback played a pivotal role in the successful completion of my research.

Furthermore, I extend my gratitude to Dr. Zhen Yang for graciously accepting the role of thesis committee member and evaluating my performance.

I am quite fortunate to have so many friends who supported me during my thesis, and I am grateful. I would like to thank my friends Sudharsan Bharatwaj, Kevin Khalife, Vikash Garib, Adam Barry, Sreedharan Nair, Ausaaf Ahmed Siddiqui, Nishant Gurrapadi and Abhinanda for supporting me since the beginning of my master's. They supported and motivated me throughout my master's journey at TU Delft.

Most importantly I would like to thank my family. Starting with my father, GV Pantulu, Mother, G Ramalakshmi, and Brother, GSV Harsha Vardhan and G Sowmya as they have been my supporting pillars throughout. Also, my cousins Chaitanya, Varun and Varshitha who have provided me their support in successfully completing my masters. My family gave me the support and the courage to keep moving forward and my journey would not have been possible without them.

Sri Gajanan Moudgalya Gogulapati April 15th, 2024

ABSTRACT

Sustainability has become a paramount concern in modern research, aligning with global efforts to reduce carbon emissions and embrace circular economy principles. The mentioned imperative extends to the field of pavement engineering, where the widening of existing pavements, a common practice to accommodate increasing traffic demands, necessitates sustainable solutions. The current thesis addresses the pressing need for pavement engineering practices that align with ambitious sustainability goals while ensuring structural integrity and performance.

Drawing upon the context of countries like the Netherlands, striving for zero carbon emissions and full circularity by 2030, the research explores avenues for sustainable pavement widening. This involves optimizing designs to minimize material usage, reduce emissions, incorporate recyclable materials, and extend the lifespan of road infrastructure. The challenges posed by non-uniform settlements and stress concentrations at widening joints are investigated, highlighting the importance of accurate material modelling and interface characterization.

Motivated by the need for sustainable pavement solutions, the research aims to guide decision-making in pavement design towards environmental sustainability while meeting functional requirements. The scope encompasses FEM models, EVP behaviour of asphalt surfaces, base layer variations, interface modelling, and comparative analyses between 2D and 3D models.

The current study undertakes a thorough examination of the implications of pavement widening on stress concentrations, material behaviour, and interface modelling, aiming for development of more sustainable and resilient pavement designs. Employing a comprehensive research framework encompassing theoretical modelling and numerical simulations, the study seeks to elucidate the issues inherent in widened pavement structures.

The main thesis objective is the development of an elasto-visco-plastic (EVP) material model, to capture the time-dependent behaviour exhibited by asphalt surfaces under varying loading conditions. Using the Finite Element Method (FEM), the developed material model serves as a foundational pillar for subsequent investigations, facilitating an examination of stress distribution patterns within widened pavement structures.

The Research provides a detailed framework for conducting the study on pavement widenings. It begins with the delineation of study parameters, including cross-sectional geometry, material properties, and simulation techniques. The development and validation of the EVP material model are elaborated, along with the implementation of finite element method (FEM) simulations to analyse stress distributions. Parametric analyses are conducted to investigate the effects of load variations, base layer characteristics, and interface modelling on widened pavement performance. The methodology also includes the utilization of cohesive zone modelling for interface characterization, enabling a more detailed representation of pavement layer interfaces.

The identification of critical stress concentrations emerges as a focal point of inquiry, necessitating a crucial to understand the interplay between load variations, base layer thickness, and material stiffness. Through various numerical analyses, the study seeks to unravel the intricate web of factors influencing stress propagation within widened pavement structures. Moreover, the implications of reduced recessing length and base layers in new pavement

designs are subjected to meticulous scrutiny, shedding light on potential trade-offs between structural integrity and resource optimization.

Overall, the current thesis contributes to advancing pavement engineering practices, promoting sustainable transportation infrastructure, and supporting global sustainability goals. Through rigorous analysis and modelling, the research seeks to enhance the understanding of critical factors influencing widened pavement performance, paving the way for safer, more efficient, and environmentally conscious road networks.

LIST OF FIGURES

Figure 1 Research Framework

Figure 2 Widened Pavement section and the joint interface along widened section.

Figure 3 Different types of joint configurations in pavement widening from the study[3]

Figure 4 Widened pavement section with stepped lap configuration between the old and new pavement[3]

Figure 5 Development of cracks at the joint in the widened section[16]

Figure 6 Stress and Strain response of Viscoelastic material over time.

Figure 7 Adhesive bond testing in a Stepped lap joint configuration from research[27]

Figure 8 Tack coat material between the layers of pavement for interlayer bonding.

Figure 9 Cross-Section of Widened pavement model analysed in the current research.

Figure 10 Framework for Research Methodology

Figure 11 Generalized Maxwell material model configuration.

Figure 12 Elastic Single Spring Mechanical Model

Figure 13 Elastic Spring in Parallel Configuration

Figure 14 Viscous Single Dashpot Mechanical Model

Figure 15 Single Plastic Slider Mechanical Model

Figure 16 Viscoelastic Maxwell Element

Figure 17 GM material model configuration.

Figure 18 Elasto-Plastic material model component.

Figure 19 Yield function HISS (Desai, 1986): (a) in space $I1 - \sqrt{I2d}[35]$

Figure 20 Drucker-Prager yield surface.

Figure 21 Replacing the elastic spring in Elasto-Plastic model with GM Model

Figure 22 Elasto-Visco-Plastic Material Model - Combined GM and Drucker-Prager

Figure 23 2D-widened pavement FEM models with (a) Reduced number of Base

layers and (b) Reduced Recessing/overlapping length in base layer.

Figure 24 2D-Widened Pavement FEM model with mesh, load location and boundary condition.

Figure 25 Mesh, Load and Boundary Condition of (a) 2D- & (b) 3D- Geometries used for material model validation.

Figure 26 Load Application

Figure 27 (a) Strain εxx and (b) Strain εyy over time for Elastic and EVP Material Models at the node under applied load in 2D-and 3D- models

Figure 28 Plastic Strains εxx in 2D-geometry validating the material model plastic behaviour.

Figure 29 Critical location in widened pavement.

Figure 30 (a) Stress (σxx) and (σyy) , (b) micro-strain $(\mu \varepsilon xx)$ and $(\mu \varepsilon yy)$ and (c)

Stress (σxy) and micro-strain $\mu \varepsilon xy$ in both unwidened (2D-UP) and widened pavement without reinforcement (2D-WP-NR) models.

Figure 31 (a) Stresses σyy and σxx and (b) Micro-strains $\mu \varepsilon xx$ and $\mu \varepsilon yy$ along the width of the pavement in widened pavement models with and without reinforcement.

Figure 32 (a) Stresses σyy and σxx and (b) Micro-strains $\mu \varepsilon xx$ and $\mu \varepsilon yy$ along the width of the pavement in widened pavement models with varying load location.

Figure 33 Micro-Strain $\mu \varepsilon xx$ along the width of the pavement in widened pavement models with varying material stiffness.

Figure 34 Micro-Strain $\mu \varepsilon xx$ along the width of the pavement in widened pavement models with varying material stiffness.

Figure 35 Micro-Strain $\mu \varepsilon xx$ along the width of the pavement in widened pavement models with reduced recessing length and reduced number of base layers. Figure 36 (a) Micro-Strain $\mu \varepsilon xx$ and (b) $\mu \varepsilon yy$ along the width of the pavement in widened pavement models with CZM and current design standards. Figure 37 (a) Micro-Strain $\mu \varepsilon xx$ and (b) $\mu \varepsilon yy$ along the width of the pavement in widened pavement models with surface layer EVP material and combined surface and base layer EVP material.

LIST OF TABLES

Table 1 Elastic Parameters of material in each pavement layer in a widened pavement model based on current design standards adopted in Netherlands[22]

Table 2 Viscoelastic Parameters for EVP material in widened pavement model

Table 3 Plastic Material parameters for EVP material model based on Drucker-Prager yield criteria.

Table 4 Material parameters for Cohesive Zone Modelling material at the joint in pavement widening.

Table 5 Model acronyms and description for FEM based Pavement Models

Table 6 Stress and Micro-Strains at the critical location in Unwidened and widened pavement models

Table 7 Stresses and Strains at the critical stress location for widened pavement models with and without reinforcement

Table 8 Stresses and Strains at the critical stress location for widened pavement model subjected to variation in load location.

Table 9 Stresses and Strains at the critical stress location for widened pavement model subjected to variation in base layer material stiffness.

Table 10 Stresses and Strains at the critical stress location for widened pavement model subjected to variation in base layer thickness.

Table 11 Stresses and Micro-Strains at the critical stress location for widened pavement model with reduced base layer recessing length

Table 12 Stresses and Micro-Strains at the critical stress location for widened pavement model with reduced number of base layers in widened part

Table 13 Stresses and Micro-Strains at critical location for widened pavement models 2D-WP-R and model with CZM modelling (2D-CZM-R) of the joint

Table 14 Stresses and Micro-Strains at critical location for widened pavement models 2D-WP-R with surface layer EVP material and combined surface + base layer with EVP material.

Contents

1.	Intr	oduction	12
	1.1	Problem Statement	13
	1.2	Research Motivation	13
	1.3	Research Scope	13
	1.4	Research Questions	13
	1.5	Research Outline	15
2	Lite	rature Review	17
	2.1	Pavement Widening	17
	2.1.	1 Types of Pavements widening	17
	2.1.	2 Current Failure mechanisms of Pavement Widening	19
	2.2	Pavement Materials and Material Models	21
	2.2.	1 Pavement Materials	21
	2.2.	2 Visco-Elastic Generalized Maxwell Material Model	22
	2.2.	3 Elasto-Visco-Plastic Material Model	23
	2.3	Cohesive Zone Modelling	23
	2.4	Conclusion.	25
3	Res	earch Methodology	26
	3.1	Cross Sectional geometry of widened pavements	26
	3.2	Study Parameters	28
	3.2.	1 Elastic Parameters	28
	3.2.	2 Viscoelastic Material Parameters	28
	3.2.	3 Plastic Material Parameters	29
	3.2.	4 Cohesive Material Parameters	29
	3.3	Material Model	30
	3.3.		
	3.3.	2 Combination of basic material models	33
	3.3.	3 Elasto-Visco-Plastic Material Model	37
	3.3.	4 Summary	46
	3.4	Design of Experiment	
	3.5	Finite Element Implementation	47
	3.5.		
	3.5.		
	3.6	Validation of material models	48
	3.6.	1 Viscoelastic Material Model Validation	48

4	Res	ults & Discussion	52
	4.1	Effect of Pavement Widening	52
	4.2	Effect of Reinforcement in Pavement Widening	54
	4.3	Effect of Load Location	56
	4.4	Effect of varying material stiffness of base layer in widened pavement	58
	4.5	Effect of varying base layer thickness in widened pavement	59
	4.6	Effect of varying Recessing/Overlapping length in base layer	61
	4.7	Effect of Reduction in Number of Base Layers in Widened Pavement	62
	4.8	Effect of Cohesive Zone Modelling (CZM)	63
	4.9	Effect EVP material in Base Layers	65
5	Cor	nclusions	67
6	Fut	ure Recommendations	71
7	Ref	erences	73

1. Introduction

Sustainability is key in modern research as it aligns with global goals to reduce carbon emissions and adopt circular economy principles. Countries like the Netherlands have set ambitions for zero carbon emissions and full circularity by 2030[1]. This has also an implication for the pavement engineering community which has to proactively look for sustainable ways to support the growing traffic demand[1].

Widening of existing pavements (henceforth referred to as "pavement widening") is a commonly adopted practice by road agencies to support more traffic [2]. Hence, there is a demand from various road agencies around the globe to widen the pavements more sustainably [1]. These ambitions can be achieved as sustainability in pavement widening involves optimizing designs to require less material. Therefore, reducing emissions, implementing recyclable materials, and ensuring a longer lifespan of road infrastructure to avoid frequent reconstruction[3].

For example, in the Netherlands, the arterial road network reached a mature state many years ago, and since then, traffic intensities continued to grow, causing significant congestion [1]. Therefore, the most practical solution in many cases has been to widen the pavement on existing embankments to create additional lanes for vehicles [4].

Previous research literature [3] concluded that as the road is widened, non-uniform settlements between the old and new sections of the embankment may arise. These non-uniform settlements may cause differences in layer thicknesses [5]. These variations can lead to stress concentrations at the longitudinal widening joint, which are prone to cracking and ravelling [6]. The high-stress areas are common at the joint interface where the new pavement connects with the old [7].

Using EVP material model is considered important according to the literature[2] for AC as the behaviour of asphalt pavements under traffic loads and environmental conditions is time-dependent and complex. Such behaviour involves various physical phenomena like viscoelasticity, viscoplasticity, and cracking [8].

Another popular material choice used in research [9] is viscoplastic material model. These materials can undergo permanent deformation under cyclic loads beyond their elastic limit [10]. Both viscoelastic and viscoplastic types of materials show dependencies on temperature and loading conditions, but their long-term behaviours are notably different, with viscoelasticity being associated with recoverable deformations and viscoplasticity with permanent changes[11].

Past research studies [12] introduced a combined elasto-visco-plastic (EVP) material model which integrates the generalized Maxwell model to represent viscoelastic behaviour and the Drucker-Prager model for plasticity. The comparison between elastic and EVP-material models showed that EVP models give a more accurate numerical interpretation of the creep recovery response of hot mix asphalt concrete[9].

Also, accurate modelling of the interface in pavement widening is technologically challenging due to the complex behaviour of materials. Additionally, the computational demands of such models are high, and obtaining adequate field data for validation adds to the challenge [6]. The past research study [13], used an interfacial cohesive zone model (CZM) to characterize the properties of interlayer bonding materials. Such method allows evaluation of shear strength along with other associated properties such as the adhesive's ductility, cohesion, and internal friction angles [14].

1.1 Problem Statement

The widening of existing pavements, a commonly adopted practice to accommodate growing traffic demands, presents significant challenges in terms of sustainability, structural integrity, and performance. As countries like the Netherlands strive towards zero carbon emissions and full circularity by 2030, there is a pressing need for pavement engineering solutions that align with these ambitious goals. However, existing research predominantly focuses on individual aspects such as material models or pavement widening, overlooking the integrated influence of geometrical sensitivity, material behaviour, and interface modelling.

The necessity for an improved understanding of stress concentrations in widened pavement structures is underscored due to the implications for sustainable and resilient pavement design. An examination of the effects of material properties, joint placement, and load distribution on stress concentration is critical for maintaining or enhancing pavement performance and longevity while reducing carbon emissions. The knowledge gap regarding these effects is addressed by the implementation of advanced material models into Finite Element Method simulations to optimize pavement design practices effectively. The challenge is to guide decision-making in pavement design towards attaining environmental sustainability while fulfilling the functional requirements of transportation infrastructure. Enhanced understanding of related factors is pursued to aid in advancing pavement design and promoting sustainable transportation systems.

1.2 Research Motivation

The motivation behind the current research stems from the need to improve the understanding of critical locations in widened pavements to develop more sustainable and resilient pavement designs. By implementing material models and conducting in-depth analyses, the study aims to contribute to reducing carbon emissions while maintaining or enhancing the performance and durability of pavements. Additionally, the findings will assist pavement engineers and designers in making informed decisions regarding material selection, joint placement, and load distribution, ultimately leading to safer and more efficient transportation infrastructure.

1.3 Research Scope

The research will focus on Finite Element Method (FEM) models in pavement widening, specifically addressing the elasto-visco-plastic (EVP) behaviour of asphalt surfaces. The study investigates the impact of variations in base layer thickness, base layer material stiffness, and load location on stress concentrations. Additionally, the effectiveness of reduced base layers in new pavement and the implications of reducing the recessing length of old pavement into the new pavement is explored. The research will also delve into the interface between pavement layers using cohesive zone modelling and compare it with a full bond model and a sensitivity analysis. A comparative analysis between 2D and 3D models will be conducted.

1.4 Research Questions

In order to resolve the research problem explained in Section 1.1 and based on the motivation and scope from Section 1.2 and Section 1.3, the main research questions will be formulated. To answer the research questions, it will be further sub-divided into sub-research questions which will be studied chronologically. The main research questions are:

- 1. How can an elasto-visco-plastic material model be developed for the surface asphalt layer in finite element method simulations?
 - Sub-questions:
 - a) What are the key parameters required to define the elasto-visco-plastic behaviour of asphalt materials?
 - b) How does the newly developed EVP model compare with existing material models in terms of accuracy and reliability?
- 2. Where are the critical stress concentrations located in pavements due to widening, and how can they be identified?
 - Sub-questions:
 - a) What simulation techniques can be used to accurately identify these critical locations?
 - b) How does widening of pavement influence the distribution and magnitude of stress concentrations?
- 3. In what ways does the variation of load location, base layer thickness, and base layer material stiffness effect stress concentration in pavement widening scenarios?
 - Sub-questions:
 - a) Which of these factors has the greatest impact on stress concentration, and to what degree?
 - b) How does the interaction between these factors influence the overall stress distribution in the widened pavement?
- 4. How do reduced recessing lengths and reduced base layers in new pavement designs perform compared to standard designs?
 - Sub-questions:
 - a) What trade-offs exist between reducing recessing length/base layer thickness and maintaining pavement integrity?
- 5. How does modelling the interface between pavement layers using cohesive zone modelling compare with a full bond model in terms of predicting pavement performance?
 - Sub-questions:
 - a) How do the results of cohesive zone model impact the design recommendations for pavement interfaces?

In summary, the research seeks to investigate the implementation of developed material models into Finite Element Method based software to determine critical locations within pavements. By addressing specific research questions related to material models, joint behaviour, and stress concentrations, the study aims to enhance the understanding of pavement performance. The following chapters will delve into the methodologies, analyses, and findings that contribute to addressing the research objectives. Through this research, valuable insights will be gained, paving the way for improved pavement designs and sustainable transportation infrastructure.

1.5 Research Outline

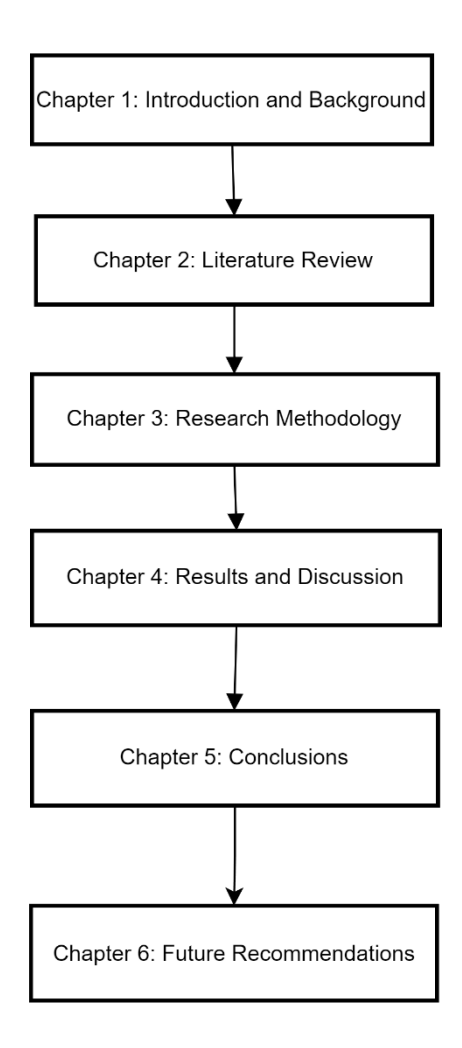


Figure 1 Research Framework

The thesis is structured to progressively introduce, explore, and conclude an investigation into the challenges and solutions involved in pavement widening. Each chapter is designed to present a logical progression of research activities and findings:

Chapter 1: Introduction - This chapter sets the stage for the entire thesis by introducing the topic of pavement widening. It establishes the background by highlighting the importance and the context within which the research is conducted. The chapter also clearly defines the aim of the research, the scope within which the research questions will be addressed, and the specific objectives that the research intends to achieve.

Chapter 2: Literature Review - In this chapter, a detailed review of existing literature relevant to pavement widening is provided. Here, the focus is on outlining the challenges specifically related to widening joints and summarizing the body of research that has already been conducted in this area. The literature review serves to identify where there are gaps in current knowledge that this thesis will attempt to fill.

Chapter 3: Methodology - The third chapter describes the research methods used to carry out the study. It explains the material modelling techniques that were employed and provides details of the numerical simulations that were conducted.

Chapter 4: Results - Here, the outcomes of the numerical simulations and analyses are presented. The chapter dives into the specifics of the stress distribution found within the pavement structure due to widening, and highlights areas that may be problematic. These findings are crucial as they provide evidence-based insights that could influence pavement design practices.

Chapter 5: Conclusions - The concluding chapter wraps up the study by summarizing the key findings. It shows the importance of the study in advancing the field of pavement engineering and discusses the implications of the research results. The conclusions drawn from the research are intended to contribute to knowledge and suggest potential areas for future research.

2 Literature Review

In the current chapter, a literature review is performed to identify the parameters that effect pavement widening and to determine the type of material models (including viscoelastic and elasto-visco-plastic etc.) used in the modelling of pavement materials. Also, the interface material in widened pavements joints from previous research is discussed. The literature is divided into three sections as follows, Section 2.1 presents the materials and common material models that are available currently to implement into pavement models. Section 2.2 contains the description of the possible effects that can arise due to widening of pavements and Section 2.3 describes the computational modelling details of the interface with cohesive zone modelling.

2.1 Pavement Widening

The current section initially describes the types of pavements widening and the techniques involved in their construction from previous studies. Later the common effects within the pavement due to widening according to past researchers were also discussed.

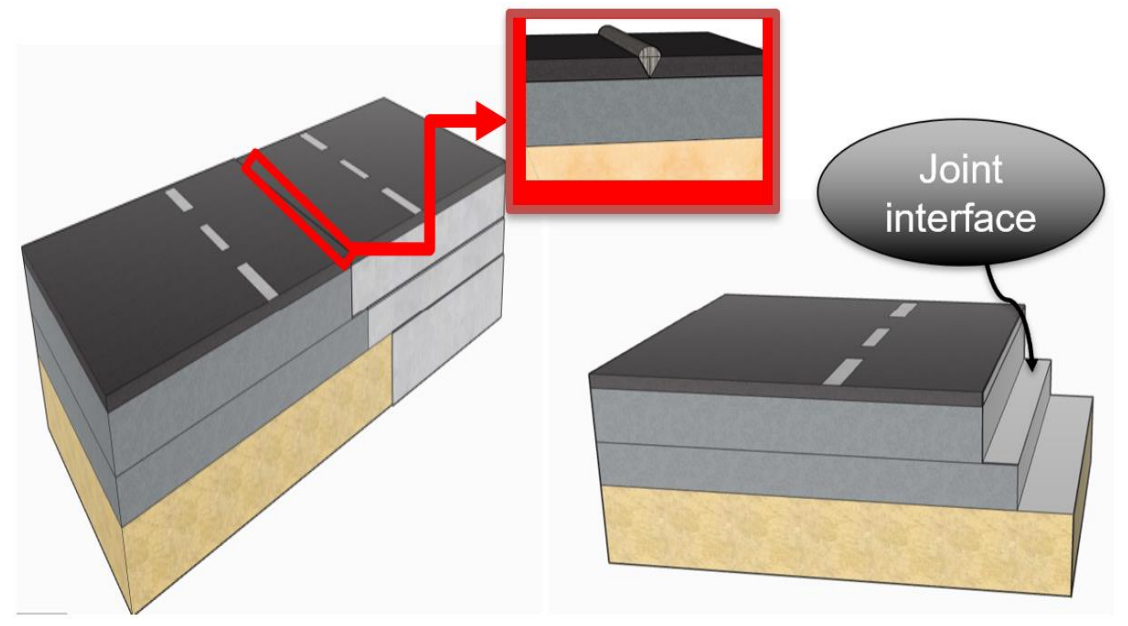


Figure 2 Widened Pavement section and the joint interface along widened section.

2.1.1 Types of Pavements widening

Smooth and well-maintained roads are essential for ensuring the smooth flow of traffic and providing a safe and comfortable driving experience [3]. Some of the benefits and considerations associated with pavement and widening projects include increased road capacity, improved safety for motorists, enhanced accessibility for pedestrians and cyclists, reduced travel times, and improved overall infrastructure quality [15]. Moreover, the concept of pavement widening with respect to sustainability involves optimizing designs to require less material and thus reducing emissions, while implementing recyclable materials and ensuring longer lifespan of the road infrastructure[16]. This approach aligns with global sustainability goals and is highlighted as a necessary consideration for pavement engineering to support the growing traffic demand in a responsible manner.[3]

However, as identified by the researchers [4], the Netherlands' arterial road network reached a mature state of coverage throughout the country, and since then, traffic volumes increased steadily, and each workday now sees an intolerable number of hours of delays due to congestion. In this condition, when the current road width cannot handle the traffic, a road widening project (considered the quickest and most affordable solution to this mobility and environmental issue [4]) is typically used.

The choice of pavement type and widening technique is crucial in ensuring the durability and long-term performance of the road infrastructure [15]. Factors such as traffic volume, climate conditions, and available budget are supposed to be considered while selecting the appropriate pavement type and widening technique, as suggested by the study [3].

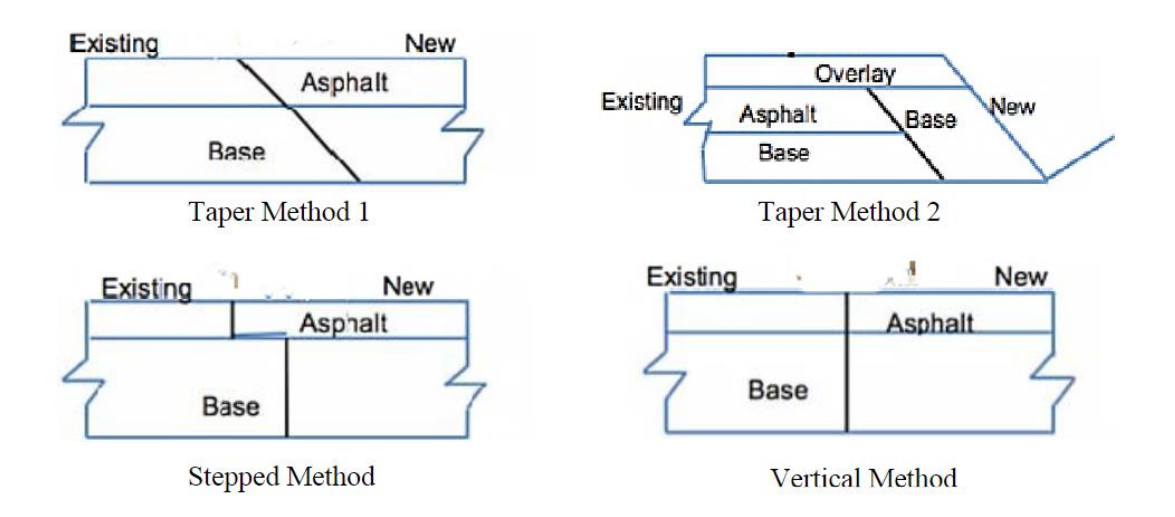


Figure 3 Different types of joint configurations in pavement widening from the study[3]

According to the research [3], Common pavement widening techniques included:

- 1. Constructing new lanes adjacent to existing ones: Additional lanes parallel to the existing ones, effectively increasing the road's capacity are constructed.
- 2. Adding shoulder lanes: Widening the road by adding extra lanes specifically designated as shoulders, for emergency vehicle access or as a space for cyclists and pedestrians.
- 3. Reconstructing the entire pavement: For this process, the existing pavement was removed and replaced with a wider and more durable pavement structure that can accommodate increased traffic volumes.

The current research deals with the addition of parallel lanes to the existing ones. However, there are numerous critical issues in road widening, and if the widening is done incorrectly, several problems can arise during its lifetime, such as non-uniform settlements between the old and new parts of the embankment and stability issues at the longitudinal joints causing reflective cracking [16]. Hence, such effects within the pavement due to widening are discussed in the following section.

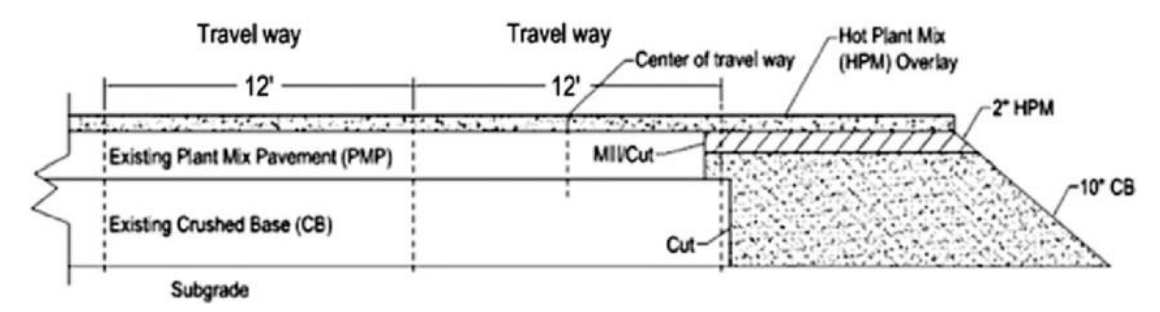


Figure 4 Widened pavement section with stepped lap configuration between the old and new pavement[3]

2.1.2 Current Failure mechanisms of Pavement Widening

The current section provides an overview of the prevailing failure mechanisms in pavement widening projects, including cracking due to stress concentrations, settlements, and construction failures. Recent research findings elucidate strategies to mitigate these issues, such as optimizing loading positions, surface thickness, and material properties, as well as implementing geosynthetic reinforcement and comprehensive maintenance plans. Additionally, the utilization of Finite Element Method (FEM) modelling techniques to analyse pavement widening scenarios is discussed, highlighting the value of these approaches in informing design decisions and enhancing pavement performance. Future research directions focus on identifying load distribution patterns and optimizing critical parameters at joint locations in widened pavement models, aiming to address existing gaps in understanding and improve the long-term sustainability of transportation infrastructure.

2.1.2.1 Cracking due to stress concentrations

An inevitable issue due to the joint widening between the new and the old pavement sections, were found to be longitudinal surface cracking and ravelling along the joint line [15]. To prevent such cracking issues, it is advised that the choice of loading position that significantly affects the pavement's response, should be factored into the design. The study from [17] concluded that deterioration is more critical when the location of the joint is in the vehicle wheel path. In practice, keeping a sufficient gap between the joint's location and the position of the vehicle's wheels is advised. Under repeated traffic loading, cracks develop at the joints and propagate in an upward direction[17]. To avoid such cracks methods like increasing the surface thickness and having the modulus values of existing and new pavement close to each other were adopted[5]. Another interesting finding from the research [17] showed that, as the modulus for hot mix asphalt is increased, the reflective cracking of asphalt in widened pavement section increases. For finding an optimal stiffness difference between the asphalt material in new and old pavement. A parametric analysis with respect to base stiffness was performed.

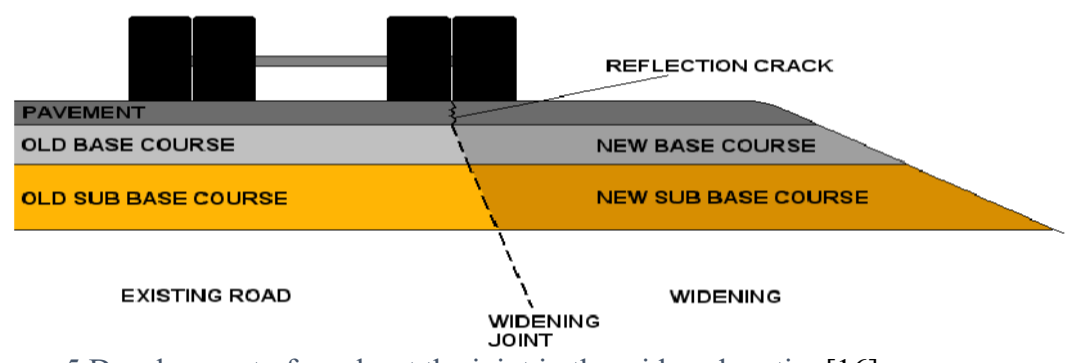


Figure 5 Development of cracks at the joint in the widened section[16]

Also, another study [18] shows highlighted that increasing the thickness of hot-mix asphalt surfacing and decreasing surface modulus can mitigate reflective cracking. Moreover, uniform modulus across new and existing pavement bases significantly reduces the potential for crack propagation.[18] Geosynthetic reinforcement was also shown to effectively decrease stress centralization, thereby delaying the reflective cracking process.[18]

2.1.2.2 Cracking due to settlements

The studies [7] and [4] concluded that the process of widening and raising an existing roadway on a soft soil foundation resulted in significant differential settlement between the old and new sections of the roadbed. In a comparative analysis conducted over a period of fifteen years post-construction, research [7] has revealed that roadbeds subjected to raising and widening processes demonstrate significantly greater settlement than those constructed without modification. Specifically, central measurements of the roadbeds indicated that the total settlement of modified roadbeds reached 297.05 mm, whereas directly constructed roadbeds exhibited a lesser total settlement of 234.85 mm. According to another study [5], due to such settlements in the foundation, it is the subbase that first reaches the failure strength due to the tensile stress experienced from the differential settlement, which serves as the critical location to further investigate.

2.1.2.3 Construction Failures

The study [19] identifies several factors contributing to these structural failures, including inadequate design considerations, improper construction techniques, and insufficient soil stabilization measures. It also highlights the impact of increased traffic loads and environmental factors on the performance of widened roads.

The paper [20] outlines remedial measures, which include retrofitting road sections with additional reinforcements, improving drainage systems to prevent water accumulation, and implementing proper soil stabilization techniques. The study emphasizes the importance of enhanced quality control during construction and a comprehensive maintenance plan to ensure the durability and safety of widened road sections.

2.1.2.4 Previous Studies of FEM Modelling in Pavement Widening

The research [17] incorporated linear elastic fracture mechanics to analyse the influence factors of crack propagation and utilized the computer code ABAQUS for the finite element analysis. The results demonstrate that certain improvements in construction quality, pavement design, and the use of crack insulating products like geogrid can prevent or delay the onset of such reflective cracking in asphalt pavement widening [17].

The study [18] harnesses FEM to delve into the propagation mechanisms of reflective cracks in asphalt pavements through a sophisticated three-dimensional layered model. Utilizing the ABAQUS software, the research [18] integrates fracture mechanics theory alongside the extended finite element method, investigating into the dynamic mechanical responses of pavements subjected to various external loads and internal properties.

By integrating full structural modelling within the finite element analysis, the research [4] identifies the distribution of stress and strain, mapping areas prone to potential damage. This approach facilitates a nuanced understanding of how widened pavements respond under varying traffic loads, revealing the importance of detailed modelling in anticipating the performance of widened sections and informing strategies to prevent cracking and deformation.

The study [19] simulates various loading and temperature conditions to understand the stresses and the potential for cracking in the concrete pavement slabs. The stress distributions in widened slabs were compared with skewed and rectangular joints under different loading scenarios, applying temperature loads and mechanical loads separately and combined. From the research conducted previously using Finite Element Modelling (FEM), it has proved to be a valuable approach to simulate real world scenarios and hence FEM also plays an important role in the current research.

2.1.2.5 Current Research Focus

The current research identifies load distribution patterns that affect joint performance by simulating different loading positions along and away from the joint path, offering insights into optimizing the load response of widened pavements. Moreover, although numerous researchers studied the settlement and cracking related issues in pavement widening, the effects at the critical location developed due to widening have not been discussed. The current research focused on the development of multiple widened pavement models to understand the effect of variation in parameters (such as the stiffness, layer thickness, load location etc) at the critical location.

2.2 Pavement Materials and Material Models

A standard structure for a flexible pavement consists of layers of materials that are specifically designed to withstand the stresses and strains caused by vehicular traffic[21]. The layers are Surface layer, Base layer, subbase layer and a subgrade layer[21]. The surface layer is usually the topmost layer of the pavement, directly exposed to traffic with a primary function providing a smooth and durable riding surface for vehicles[22]. The base layer, located beneath the surface layer, helps to distribute the load from traffic evenly and provide additional support[22]. The subbase layer, positioned beneath the base layer, further enhances the structural integrity of the pavement by providing additional load-bearing capacity and drainage capabilities. The subgrade layer, located at the bottom of the pavement structure, serves as the foundation, and transfers the load from the upper layers into the underlying soil [7]. These layers work together to ensure the long-term performance and durability of the pavement[21]. To achieve maximum effectiveness and longevity, it is crucial that these layers are constructed using appropriate materials.

2.2.1 Pavement Materials

In pavement construction, the various layers contribute unique properties to the overall performance of the roadway[21]. Typically, the surface layer and the base layer consist of asphalt, a material chosen for its durability and ability to withstand traffic wear[22]. The subbase layer is usually composed of granular materials, serving as a foundation for the asphalt layers above and providing drainage, while the subgrade is the bottommost layer composed of compacted natural soil or engineered fill material, imparting structural support to the entire pavement system[22].

Previous research into the material models for asphalt has set a strong foundation for the current study. By reviewing and discussing these established material models, the current research can build upon them, potentially offering insights into the behaviour of asphalt, especially in the context of widened pavements, that present their own unique set of challenges and stress conditions.

2.2.2 Visco-Elastic Generalized Maxwell Material Model

In the above-mentioned materials, asphalt is a viscoelastic material. Viscoelastic materials are materials that exhibit a combination of elastic and viscous behaviour during deformation [23]. The elastic behaviour allows these materials to store energy when a force deforms them, like a spring, and this deformation is recoverable. The viscous behaviour, on the other hand, enables the material to dissipate energy during deformation, like honey or syrup, and the deformation might not be recoverable [24]. The unique characteristic of viscoelastic materials is that their response to load includes an immediate elastic response and a time-dependent viscous response[2]. Hence, upon the application of a load, the material will instantly deform to some extent (elastic response), and then continue to deform slowly over time (viscous response). When the load is removed, the material will recover its shape partially but might not return to its original form completely due to the energy dissipated during the viscous flow[24]. The behaviour can be mathematically described through forms like the Prony series to express the relaxation modulus in terms of time [8].

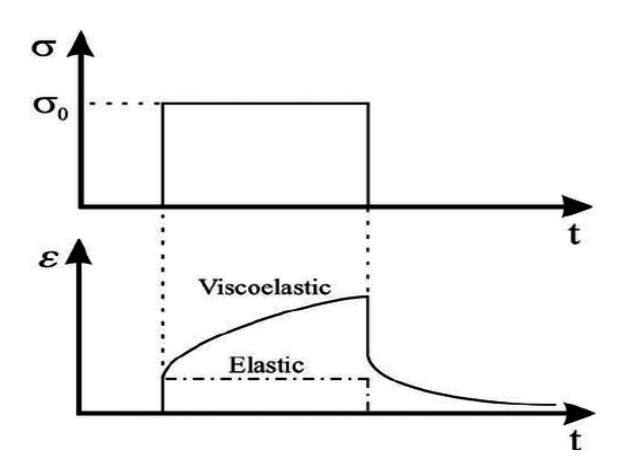


Figure 6 Stress and Strain response of Viscoelastic material over time.

The Generalized Maxwell (GM) material model is commonly used to represent the viscoelastic (VE) behaviour of asphalt pavements [24]. The model considers the asphalt layer as a series of Maxwell elements, each consisting of a spring and dashpot in parallel. The spring represents the elastic response of the asphalt, while the dashpot represents its viscous behaviour[25]. The combination of these elements' accounts for both the immediate elastic response and the delayed viscous response of the asphalt pavement [24]. According to the authors [8], the generalized Maxwell material model enables more accurate modelling of asphalt surface layers. The authors [26], also concluded that the viscoelastic model predicted larger displacements than the linear-elastic model, emphasizing the importance of using a viscoelastic constitutive model for a more accurate analysis. However, none of the mentioned studies considered the plastic deformation experienced by the pavement surface due to long term repetitive loads. The current research adopts the criteria that the VE displacements or strains being higher than the elastic strains, according to researchers [26], to validate the VE nature of the developed Elasto-Visco-Plastic (EVP) material model. Moreover, the material model developed also considered the plastic behaviour to predict permanent deformations occurring in the pavement surface. Few studies that also discuss the implementation of EVP material model into pavement surface layer were reviewed in the following section.

2.2.3 Elasto-Visco-Plastic Material Model

Asphalt pavements experience both recoverable deformations (viscoelastic behaviour) and permanent deformations (plastic behaviour). According to a study by [12], an EVP model addressed the shortcomings of simpler models that were unable to capture the combined effects of viscoelastic behaviour, plastic deformation, and damage under environmental loading conditions. By analysing the numerical results in [12], it was possible to identify the mechanisms of failure, such as the loss of cohesion proved as a dominant failure mechanism in porous asphalt mixtures, that cannot be understood with simpler material models. Another study from [2] concluded that the EVP model presented more accurate predictions of both the maximum strain during loading and the residual strain after unloading compared to elastic models. Moreover, [2] also concluded that the stress-strain curves generated from EVP models displaying both the initial elastic response and the subsequent viscoelastic flow, presented a more complete picture of the material's mechanical behaviour under various loading conditions. Also, a study from [11], concluded that the accumulation of tensile viscoplastic strain at the pavement surface due to repeated loading can be associated with the onset of pavement cracking on the surface. However, in contrast to the above findings, on study by [9] concluded that because of its over-prediction of yield stresses, the EVP material model could lead to an underprediction of permanent deformation, which is critical for understanding and preventing rutting in asphalt pavements.

While the studies employing EVP material models have significantly advanced the understanding of asphalt pavement behaviour under various loading conditions, they do not extend their analysis to the specific context of pavement widening. Although the models offer valuable insights into general pavement performance and potential failure mechanisms, the unique considerations associated with widened pavements—such as the impact of joints, the differential behaviour of adjoining sections, and the altered stress distribution due to widening—were not covered within these studies. Therefore, there remains a research gap in applying EVP material models to simulate the distinct conditions inherent to pavement widening, that the current research has dealt with. The next section explains the literature on modelling the joint interface in pavement widening.

2.3 Cohesive Zone Modelling

Interface in pavement structure refers to the zone where two different pavement layers meet each other[27]. In pavement widening, the cross-section of the joint along the length of a pavement at which the existing (old) and new pavement meet is known to be an interface. The interface behaves as a critical transition zone between the existing pavement structure and the new pavement section added during the widening process[1]. The interface is a key focal point in pavement widening projects because of the potential for differential behaviour between the old and new pavements due to differences in materials, construction methods, aging, and environmental exposure[28]. This is typically where an adhesive material is applied to bond the pavement layers together[13]. The adhesive material used in pavement engineering between the layers is known as tack coat[29]. The purpose of using asphalt tack coat in these pavement interlayers is to ensure a strong bond between the asphalt overlay and the semi-rigid base[14]. The bond is crucial for the mechanical response of the asphalt pavement during traffic and temperature loading[14]. Asphalt tack coat plays a significant role in the mechanics response of asphalt pavement, especially in terms of reflective crack propagation[29].

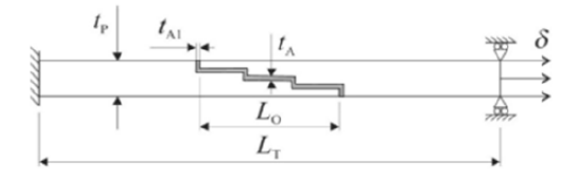


Figure 7 Adhesive bond testing in a Stepped lap joint configuration from research [27]

The study [30], concluded that the CZM is an effective modelling technique for predicting the mechanical performance of adhesively bonded stepped-lap joints. Moreover, it was also found that the geometry of the joint plays a significant role on the maximum load supported by the adhesive joint. Within pavement engineering, a study from researchers [31], concluded that the cohesive zone modelling is capable of accurately simulating the fracture behaviour of asphalt concrete, as demonstrated by close agreement with laboratory experiments. Conclusions from another research[13], suggested to underscore the importance of considering the influence of the interlayer adhesive material as an actual layer rather than simply as a coefficient in pavement structure design and performance analysis. Moreover, according to the research [32], lower adhesive strengths were suggestive of more damage initiations at the pavement surface, potentially indicating that adhesive damage is a significant factor in "top-down" cracking initiations.

CZM requires defining a traction-separation relationship that describes the stress across the potential crack surfaces as a function of the separation distance. The law reflects the material's ability to transfer stress across a crack before it fully propagates [14].

The researchers in the study [13] used an interfacial cohesive zone model to characterize the properties of interlayer bonding materials. This approach included experimental tests like a pull-out test and an oblique-shear test to determine the optimal dosage of adhesive material.

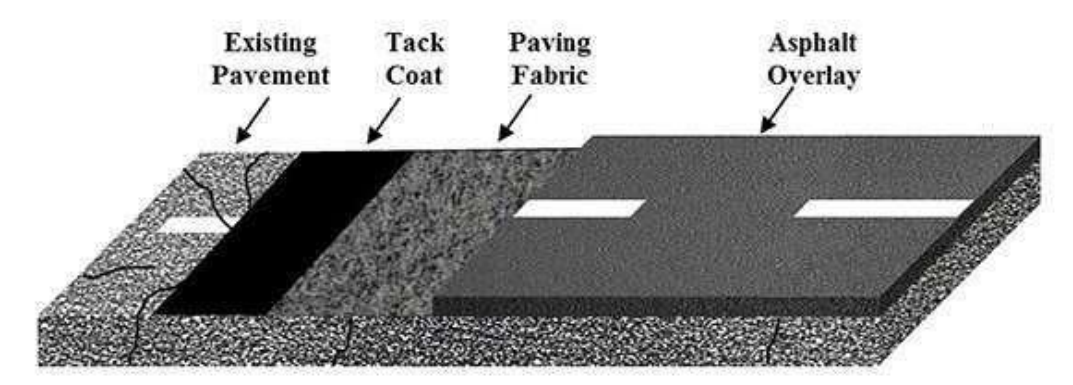


Figure 8 Tack coat material between the layers of pavement for interlayer bonding.

The literature extensively explores Cohesive Zone Modelling as a valuable method for predicting the mechanical performance of adhesive joints, demonstrating its effectiveness in various materials engineering contexts, including its ability to simulate fracture behaviour in asphalt concrete closely. Despite these advancements, there remains a noticeable gap in the current body of knowledge, the application of CZM within the specific scope of pavement widening. None of the studies have investigated the potential of integrating CZM with an elasto-visco-plastic material model in the context of pavement widening. Furthermore, the combination of CZM and EVP models have not been explored to examine the interfacial effects between the old and new pavement sections, which is a critical aspect of widened pavement structures. The current research intends to bridge this gap by developing an integrated CZM and EVP approach, aiming to provide a more comprehensive understanding of the interface behaviour in widened pavements. In doing so, this study will contribute novel insights into the

design and maintenance of durable, expanded roadway infrastructure, addressing a crucial need in the field of pavement engineering.

2.4 Conclusion

In conclusion, the literature review was structured to explore crucial aspects of pavement widening, significant design factors, and material models used in computational simulations. Three main sections divided the review: Pavement Widening, Pavement Materials and Material Models, and Cohesive Zone Modelling.

The Pavement Widening section discussed the crucial role of such projects in easing traffic congestion and enhancing road infrastructure. Various methods of widening were examined, including an assessment of their advantages and the technical challenges encountered. Notable issues such as non-uniform settling and the stability of longitudinal joints indicated the need for rigorous design and precise construction techniques.

In the section concerning Pavement Materials and Material Models, the behaviour of pavement materials, with a focus on asphalt under stress, was detailed. The discussion centred on viscoelastic and elasto-visco-plastic models, highlighting their capability to effectively capture asphalt responses to various conditions. Nonetheless, the frequency of applying these models to pavement widening scenarios was noted as relatively rare.

Cohesive Zone Modelling, in the final section, was presented as a significant approach for examining interactions at interfaces where different pavement layers merge during widening projects. While Cohesive Zone Modelling ability to predict joint performance was recognized, its combined use with material models in the context of widened pavements was seen as an under-investigated area.

3 Research Methodology

To make the research process more efficient, a research framework was developed as the first task. As described in Figure 12, at the beginning of research, the study parameters, cross-section of geometry and material models are outlined. With the obtained parameters, the next step is to develop a representative Finite Element Method (FEM) based model with appropriate material choice. Considering permanent deformation as an important aspect for the widened pavements, an elasto-visco-plastic (EVP) material model was implemented. The implementation of EVP was done to achieve a more realistic simulation of widened pavement model behaviour under different conditions as the required models are not commonly available in the commercially available FE programs.

After implementation of the material model, at first the material model is validated. The validated material model is then used to implement into widened pavement FEM model, prepared to identify critical locations due to the addition of widened sections. Parametric analyses of load locations, base layer thickness and material stiffness are then carried out to investigate their effects at the identified critical locations. Moreover, two different widened pavement models with "reduced recessing length" (see Section 3.4) and reduced base layers (see Section 3.4) were also developed to study the effect at the critical locations. Finally, the interface between widened pavement layers is modelled using cohesive zone modelling, comparing the results with a full bond interface model. The comparative assessment is designed to understand the role of interlayer bonding in enhancing the performance of the widened pavement structures.

3.1 Cross Sectional geometry of widened pavements

The cross-sectional geometry of the widened pavement model analysed in the current research is presented in Figure 10. Elastic material parameters and thicknesses use for the different layers are listed in Table-1. As mentioned in the methodology framework, a 2D geometry of the widened pavement structure was developed initially to implement the study parameters and developed material model into the pavement layers. All the layers expect the surface layer (SL) are assumed to be elastic and fully bonded with its nearing layers. Since the SL is one of the most important layers of the structure, more realistic EVP material parameters are used (see Table 2-3). The reinforcement was embedded into the New Base Layer 2 (NBL-2) as shown in Figure 10, and the reinforcement details used in the model are mentioned in Table-1. The boundary conditions, load and mesh are discussed in detail under the Finite Element Model (FEM) chapter.

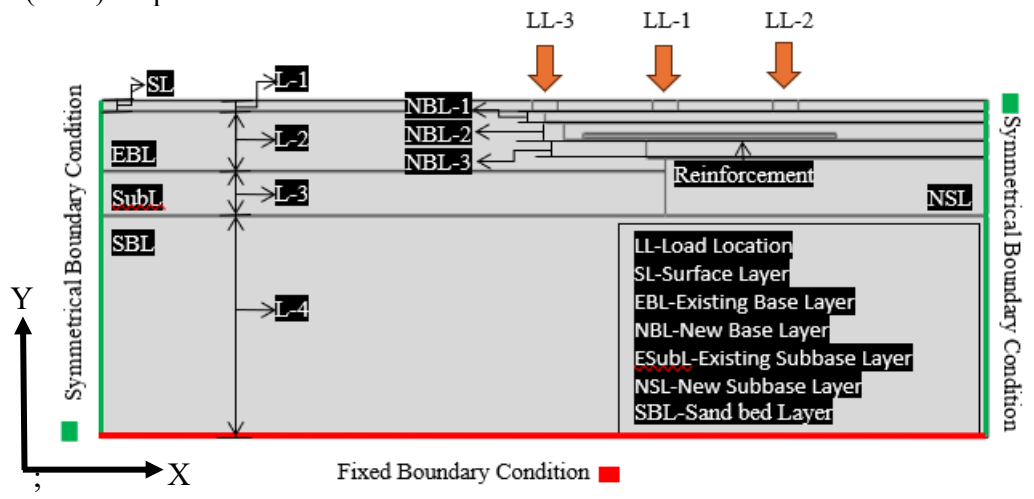


Figure 9 Cross-Section of Widened pavement model analysed in the current research.

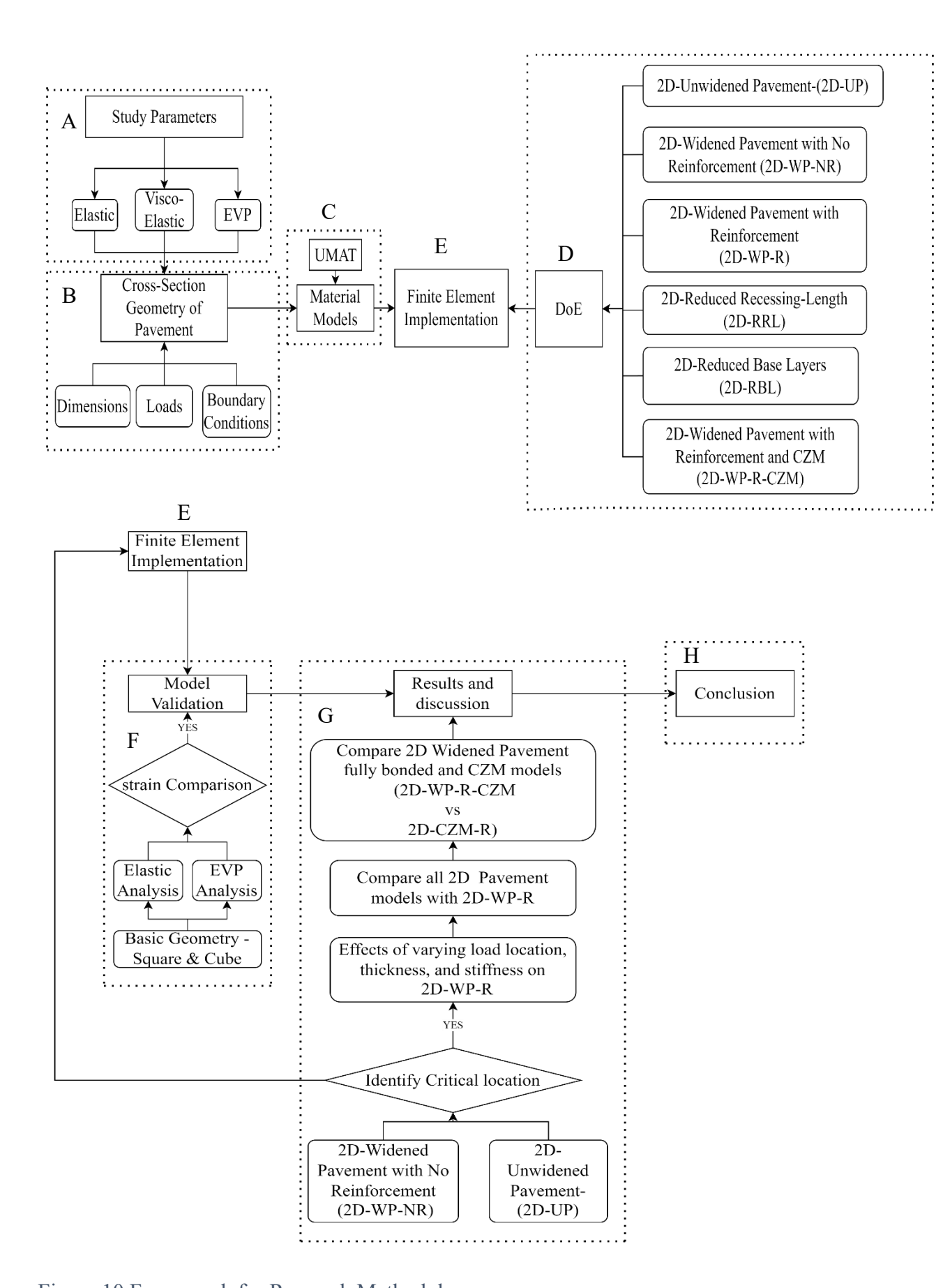


Figure 10 Framework for Research Methodology

3.2 Study Parameters

The section describes different parameters that were consider in this study. These include material parameters for elastic, viscoelastic and plastic materials, pavement layer thicknesses and parameters for modelling the interface of joint in pavement widening.

3.2.1 Elastic Parameters

Elastic parameters such as stiffness and Poisson ratio of the material used in this research are presented in Table-1. The elastic material parameters are based on current design standards adopted in Netherlands [1].

Table 1 Elastic Parameters of material in each pavement layer in a widened pavement model based on current design standards adopted in Netherlands[22]

Material	Existing	Surface	Existing	New	New	Sand	Reinforcement
Properties	Subbase	Layer	asphalt	asphalt	Subbase	bed	Glasfalt
	(EsubL)	(SL)	Base	Base	(NSL)	(SBL)	
			(EBL)	(NBL)			
Stiffness	600	2500	5000	7500	600	150	73000
(MPa)							
Poisson ratio	0.3	0.3	0.3	0.3	0.3	0.2	0.2
Thickness	200 mm	50 mm	270 mm	210 mm	260 mm	1000	4 mm
	(L-3)	(L-1)	(L-2)	(LN-2)	(LN-3)	mm	
						(L-4)	

3.2.2 Viscoelastic Material Parameters

As proposed by several past studies [33][24][25], asphalt mix layers can be modelled as a viscoelastic (VE) material to effectively capture the pavement responses in several cases. This is because, asphalt mixes are found to recover the original shape to some extent when the stress is removed[25], which is a typical characteristic of VE material [33]. According to the past research [33], for VE materials, the generalized Maxwell (GM) model, as shown in Figure 12, allows to capture a wide range of VE responses to loading conditions that asphalt pavements experience in the real world. Moreover, when comparing GM model with single Maxwell or Kelvin-Voigt researchers [22] concluded that GM model is more accurate in representing the material behaviour in the context of Asphalt pavements. Hence, in the current research, two components-based GM model was used.

The VE parameters for the GM model characterized by elastic moduli and dynamic viscosities adopted from the previous research [24] as mentioned in Table-2. The top component of the GM model (E_{∞}) , as shown in Figure 12, represents an infinite elastic spring to capture the long-term elastic response of the asphalt material, whereas the middle and last components in Figure 12 utilize elastic modulus (E_i) , and dynamic viscosity (η_i) , to capture the material behaviour under sustained loading.

Table 2 Viscoelastic Parameters for EVP material in widened pavement model

Material behaviour	Number of Component	Modulus-E MPa	Dynamic viscosity-η (MPa.s)	Infinite Elastic Spring Modulus- Einf (MPa)
Viscoelastic	1	750	24.607044	50
	2	1700	10.094521	50

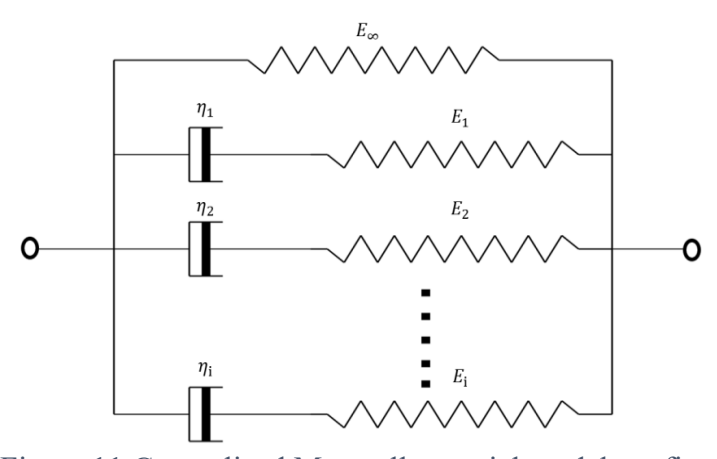


Figure 11 Generalized Maxwell material model configuration.

3.2.3 Plastic Material Parameters

Plastic materials are crucial in pavement engineering as materials can undergo permanent deformation without fracturing[34]. This deformation, often caused by repetitive traffic loads, can lead to rutting, a common pavement distress [16]. To describe this behaviour, a plastic material model widely used in pavement engineering, such as the Drucker-Prager (DP) model, is employed [24]. This model considers pressure-dependent yielding, making it suitable for materials experiencing varying stresses [13]. Capturing appropriate plastic material properties is important in this research because it enables more realistic behaviour of the material and determines the response of the pavement to repeated traffic under long-term loading conditions.

Table-3 presents the DP plasticity model's material parameters, such as cohesion, friction angle, and hardening parameters adopted from the previous research [9]. The parameters represent internal strength, resistance to sliding, and the material's ability to strengthen under repeated loading, respectively. The selection of these parameters ensures a realistic simulation of the material's response to various stresses and deformation conditions.

Table 3 Plastic Material parameters for EVP material model based on Drucker-Prager yield criteria.

Material behaviour	Cohesion	Friction Angle	Hardening-A	Hardening-B
Plastic	0.8	0.087	1	1

3.2.4 Cohesive Material Parameters

Tack coat material is utilised in pavement widening, facilitating bonding between existing and widened pavement layers [24]. The type of tack coat material selection significantly impacts bonding effectiveness [20]. The tack coat at the joint in pavement widening in this research is modelled using Cohesive Zone Modelling (CZM), a widely used method for accurately simulating joint interface behaviour [25, 26].

Table 4 outlines the material parameters used in CZM for the current research. These parameters include Young's Modulus, Nominal stress, and fracture energy, providing insights into the initial bonding strength and crack propagation within the tack coat material. Modelling the interface in pavement widening allows for comparison with a fully bonded widened pavement model, assessing the interface's influence at critical locations.

Table 4 Material parameters for Cohesive Zone Modelling material at the joint in pavement widening.

Cohesive	Young's	Nominal	Fracture
Material	Modulus (E)	Stress	Energy (mJ)
Tack Coat	8500 MPa	2 MPa	1.5

3.3 Material Model

In the current chapter, the focus is on the study of material models, essential for the prediction of material behavior in asphalt. The foundational concepts of material models, specifically targeting the elasto-plastic and viscoelastic-plastic models, are explained.

Attention is given to the theoretical frameworks that dictate material responses and the consequential ramifications for their use in practical environments. A basic elastic material followed by Generalized Maxwell model based Viscoelastic (VE) material and the Drucker-Prager criterion for plasticity, are described for their applications in structural and geotechnical engineering. The subsequent development and analysis of an elasto-visco-plastic material model underscores the chapter's dedication to presenting accurate descriptions of material behaviors, particularly in the case of asphalt.

3.3.1 Basic Material Models

Understanding the mechanical behaviour of materials is fundamental in various engineering disciplines, from structural design to materials science. This part of the current chapter explores three basic material models: Elastic, Viscous, and Plastic, each capturing distinct aspects of material response under different loading conditions.

3.3.1.1 Elastic Material Model

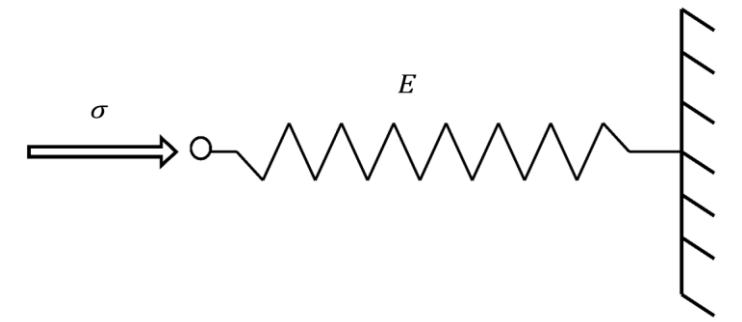


Figure 12 Elastic Single Spring Mechanical Model

Elasticity refers to the ability of a material to undergo deformation and then return to its original shape and size when the deforming force is removed. It is characterized by the linear relationship between stress (force per unit area) and strain (deformation) in the material. Elasticity is often defined with an example of a spring component which can store energy under stress.

Hooke's Law is a fundamental principle that describes the relationship of stress in the context of elastic deformation. For a single spring system as shown in Figure 13, consider a linear spring subjected to a stress (σ) with an elastic modulus (E), Hooke's Law for this system is expressed as:

The equation describes the linear relationship between stress (σ) and strain (ε), reflecting the elastic behaviour of the material. Stress is defined as force per unit area, and strain is the ratio of deformation to the original dimension. The equation describes the linear relationship between stress and strain, reflecting the elastic behaviour of the material.

To simulate the elastic behaviour of a material, multiple spring components are placed in parallel configuration as shown in Figure 14. Depending on the situation a series configuration can also be used. Parallel configuration of components emphasizes on stresses being divided into each individual component and for springs in series the stresses are equal in all the components. The strain experienced by all the spring components in Figure 14 is equal.

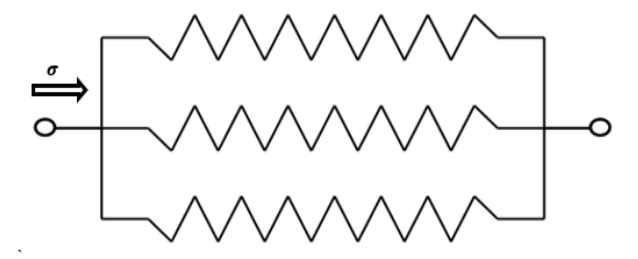


Figure 13 Elastic Spring in Parallel Configuration `

3.3.1.2 Viscous Material Model

Viscosity is a property of a material that measures its resistance to flow or deformation under the influence of an applied force. In the context of a simple viscous system, the relationship between stress and strain rate is often described by Newton's law of viscosity. For a simple fluid flow scenario, Newton's Law of Viscosity is given by:

 $\sigma = \eta \cdot \dot{\varepsilon}$

where:

 σ – Stress,

 η – Viscosity,

ė –Strain rate.

The above equation expresses the linear relationship between stress and strain rate in a viscous material. The dynamic viscosity (η) is a measure of the internal friction or resistance to flow. Generally, viscosity is represented with dashpot mechanical model element, to simulate the material behaviour.

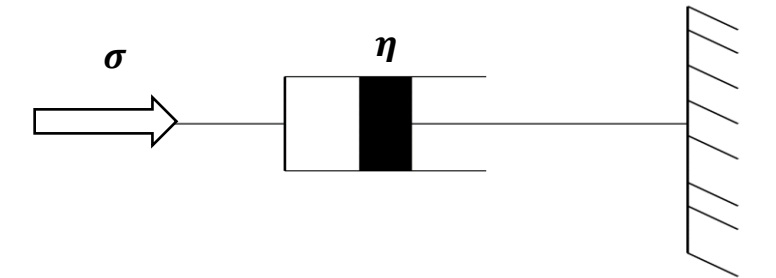


Figure 14 Viscous Single Dashpot Mechanical Model

3.3.1.3 Plastic Material Model

The behaviour of plastic materials is characterized by their ability to undergo permanent deformation or plastic deformation under applied stress. Unlike elastic materials that return to their original shape after deformation, plastic materials undergo permanent changes in shape. The stress-strain relationship for plastic deformation is typically described by the flow rule. For a simple one-dimensional plastic deformation scenario, the stress-strain relationship can be expressed as follows:

$$\sigma = \sigma_{v} - q$$

The equation defines the stress (σ) in the material as the difference between the yield stress (σ_y) and the overstress (-q). The yield stress is the stress level at which the material begins to deform plastically. Overstress (-q) is a concept used in plasticity models that accounts for stress that is exceeding the yield stress, and is defined as:

$$- q = \frac{\partial \psi}{\partial \xi}$$

The overstress (-q) is related to the plastic potential function (ψ) through its derivative with respect to equivalent plastic strain (ξ). This relationship suggests that the overstress changes based on how the plastic potential function changes with respect to the equivalent plastic strain.

The plastic flow function is represented by f, which defines the condition under which plastic deformation occurs. The function involves stress and overstress, or alternatively, stress and the change in the equivalent plastic strain $(\Delta \xi)$

$$f(\sigma,q) \to f(\sigma,\Delta\xi) \to 0$$

The plasticity condition is met when this function approaches zero.

Finally, the plastic strain rate $(\Delta \dot{\varepsilon}_p)$ is defined as the rate at which the material continues to deform plastically. It is given by the product of the change in the internal variable $(\Delta \xi)$ and the partial derivative of the plastic flow function (f) with respect to the stress (σ)

$$\Delta \dot{\varepsilon}_p = \Delta \xi \frac{\partial \mathbf{f}}{\partial \sigma}$$

These equations collectively describe a model in which a material begins to deform plastically after reaching a certain yield stress level, and it continues to deform at a rate governed by its internal state and the stress applied. A reduction needs to be caused in the overstress for stresses to reach back to yield surface. This type of model is essential for predicting the behaviour of materials under loads that result in permanent deformation.

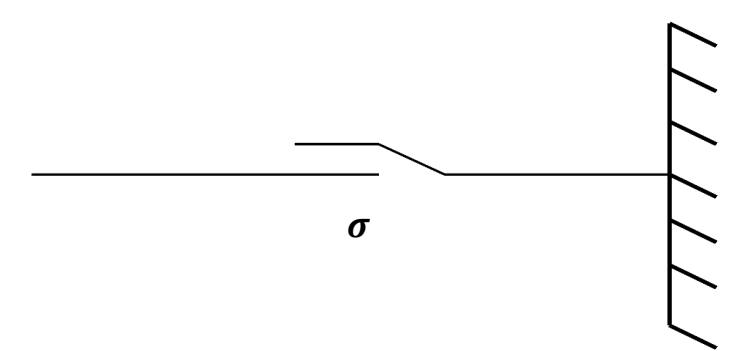


Figure 15 Single Plastic Slider Mechanical Model

3.3.2 Combination of basic material models

The current section explores the integration of fundamental material models to capture the behaviour of materials subjected to mechanical loading and environmental factors. Specifically, focusing on the combination of viscoelastic and elasto-plastic material models, essential for accurately simulating the mechanical response of asphalt under varying conditions.

3.3.2.1 Viscoelastic Material Models

Asphalt material, which is of primary interest for the current research, is both viscous and elastic in nature. Such a material is called viscoelastic material [8]. The behaviour of asphalt pavements under traffic loads and environmental conditions is time dependent. A previous study [26] found that the deflection values predicted by the viscoelastic model were slightly larger than those predicted by the linear-elastic model. This is because the viscoelastic model accounts for the time-dependent behaviour of the asphalt material, which is more representative of real-world conditions.

For accurate modelling of asphalt behaviour, various configurations of spring and dashpot elements exist. Few examples of such configurations are Maxwell, Kelvin-Voigt, and Burgers model. In a simple Maxwell model, the spring and dashpot are arranged in series and for the Kelvin-Voigt model, spring and dashpot are arranged in parallel configuration. An example for a basic Maxwell element in presented in Figure 17.

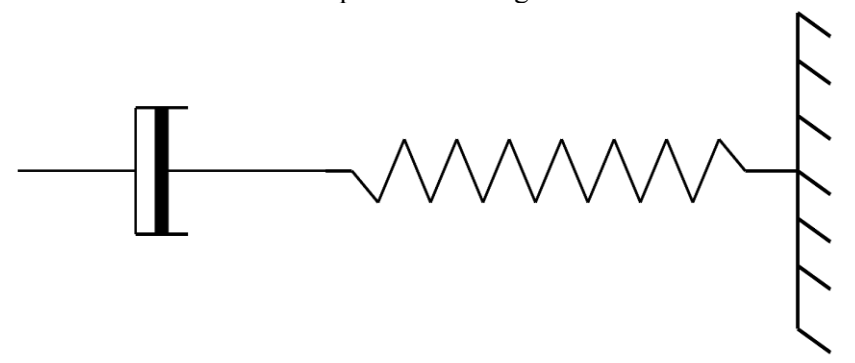


Figure 16 Viscoelastic Maxwell Element

For a series combination, the total stress ($\sigma_{total}(t)$) is equal to the stress in each component:

$$\sigma_{total}(t) = \sigma_{Elastic}(t) = \sigma_{Viscous}(t)$$

For a simple Maxwell element, one of the basic components of a viscoelastic model, the stress-strain relationship is given by:

$$\sigma(t) = E. \varepsilon(t) + \eta \cdot \dot{\varepsilon}(t)$$

where:

 $\sigma(t)$ is the stress at time t, E is the elastic modulus, $\varepsilon(t)$ is the instantaneous strain at time t, η is the viscosity of the material, $\dot{\varepsilon}(t)$ is the strain rate.

The above equation combines both elastic and viscous components, illustrating how the material responds to both instantaneous deformation and time-dependent deformation.

For the current research, a Generalized Maxwell (GM) model is adopted to simulate the required viscoelastic material behaviour. GM model is generally used when the material model comprises of multiple elements as it helps in capturing broad range of material behaviour compared to a single element [24]. The GM Model is a viscoelastic model that extends the simple Maxwell model to incorporate multiple Maxwell elements in parallel, each contributing to the overall material response. GM model is used to capture more complex viscoelastic behaviour with a distribution of relaxation times. Basic GM model configuration is presented in Figure 18.

The overall stress in the GM model, considering the contributions from different Maxwell elements is given by,

$$\sigma = \sigma_{\infty} + \sum_{i=1}^{N} \sigma_{i}$$

where:

 σ is the stress,

 σ_{∞} is the stress single spring, $\sigma_{\rm i}$ is the stress in i^{th} Maxwell component of the GM model,

N is the total number of components.

The equations to arrive at the above equation for the stresses in GM model is given in detail in the next section of this chapter.

The Generalized Maxwell (GM) model and Prony series are related concepts in the context of viscoelasticity. The Prony series is a mathematical representation used to approximate the relaxation behaviour of a viscoelastic material, while the Generalized Maxwell model is a physical model that describes the viscoelastic behaviour based on multiple Maxwell elements in parallel [25].

For the Generalized Maxwell model with Prony series, the relaxation times and Prony coefficients are needed as input for the material model along with the number of components in the model. The function below is represented in terms of Prony series, which assumes that,

$$E = E_{\infty} + \sum_{i=1}^{N} E_{i} \exp\left(-\frac{t}{\tau_{i}^{E}}\right)$$

where E_{∞} , E_i - elastic moduli of infinite spring and the i^{th} component of the GM model and τ_i^E – relaxation times for each Prony component.

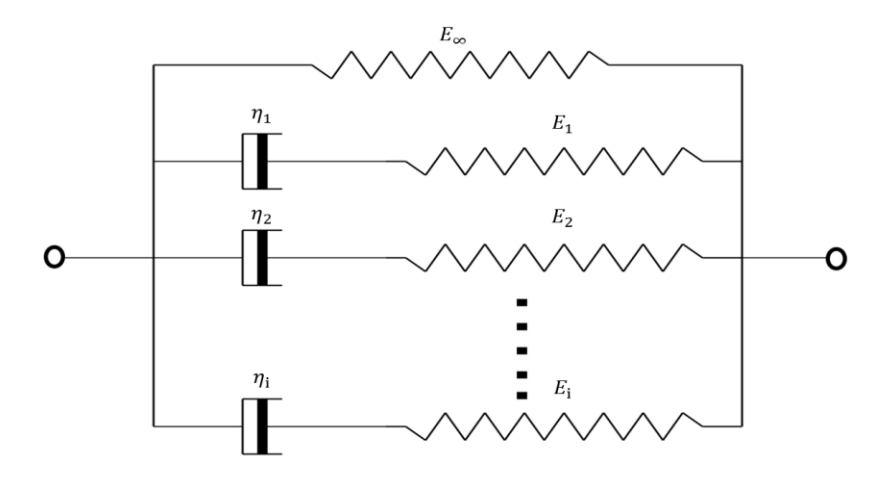


Figure 17 GM material model configuration.

3.3.2.2 Elasto-Plastic Material Model

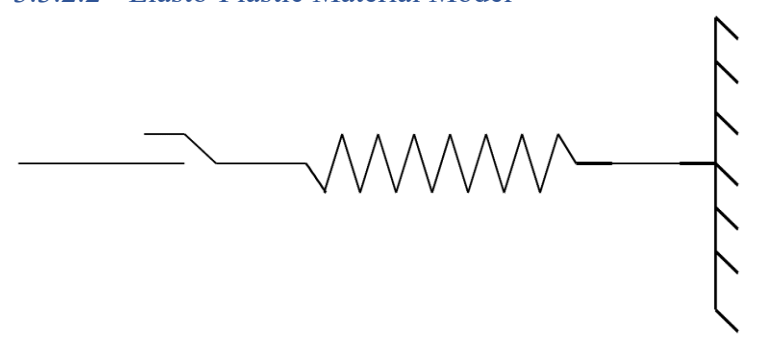


Figure 18 Elasto-Plastic material model component.

The elasto-plastic model combines the concepts of linear elasticity and plasticity, particularly in the context of materials that undergo both elastic and plastic deformation. The Drucker-Prager (DP) criterion is a widely used criterion for modelling the yield condition of plastic materials. Generally, the DP criterion is applied in geotechnical purposes and the sign convention in the equations with respect to compression and tension are different in structural applications. Also, DP yield surface is an ultimate Desai surface (another widely used plastic yield criterion) with the Hardening parameter $\alpha[9]$. Desai surface (shown in Figure 20) incorporates the ideas from the Drucker-Prager approach but extends them to address material behaviours, including anisotropy, tension-compression non-symmetry, and the influence of different stress paths[35]. Hence, the DP model used in structural applications and the further modified version used in current research are mentioned below.

Standard Drucker-Prager yield criterion in structural engineering is expressed as:

$$f = \sqrt{J_2} + A. I_1 + B = hard$$

The modified Drucker-Prager yield criterion used in current research is expressed as:

$$f = \sqrt{J_2} + (1 + \text{hard}) \cdot (A \cdot I_1 + B)$$

where:

f is the yield function,

 J_2 is the second invariant of the deviatoric stress tensor,

hard is hardening factor,

 I_1 is the first invariant stress tensor, which is also the mean of stresses in principle direction, A, B are the plastic coefficients.

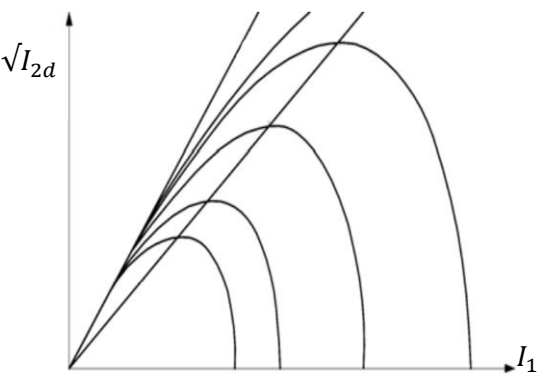


Figure 19 Yield function HISS (Desai,1986): (a) in space I_1 - $\sqrt{I_{2d}}$ [35]

The Drucker-Prager yield surface is typically defined in terms of stress invariants, such as the first invariant of stress (I_1) and the second invariant of deviatoric stress (J_2) . This graphical representation is a way to visualize the Drucker-Prager yield surface, which represents the boundary beyond which plastic deformation occurs in materials subjected to stress. The slope angle (ϕ) is typically known as the friction angle and is a key parameter in plasticity models like Drucker-Prager. The specific parameters (hard and A) determine the characteristics of the slope angle and hence the shape of the yield surface in this graphical representation.

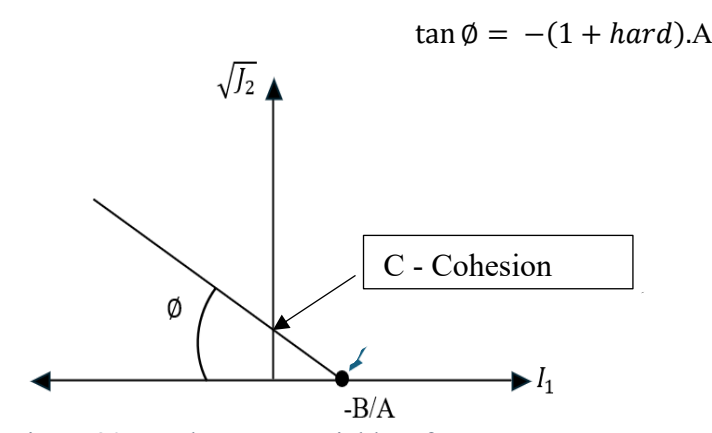


Figure 20 Drucker-Prager yield surface.

3.3.2.3 Replacing Elastic Spring with Viscoelastic Configuration

To capture the viscoelastic nature along with plastic behaviour in material model, the elastic spring in Figure 19 is replaced by a Generalized-Maxwell (GM) model from Figure 10 as shown in Figure 18. The GM spring and dashpot system allow to calculate the stresses until yield. Once the yield stress is reached, the plastic slider activates, causing a reduction in stresses according to the modified Drucker-Prager yield criterion.

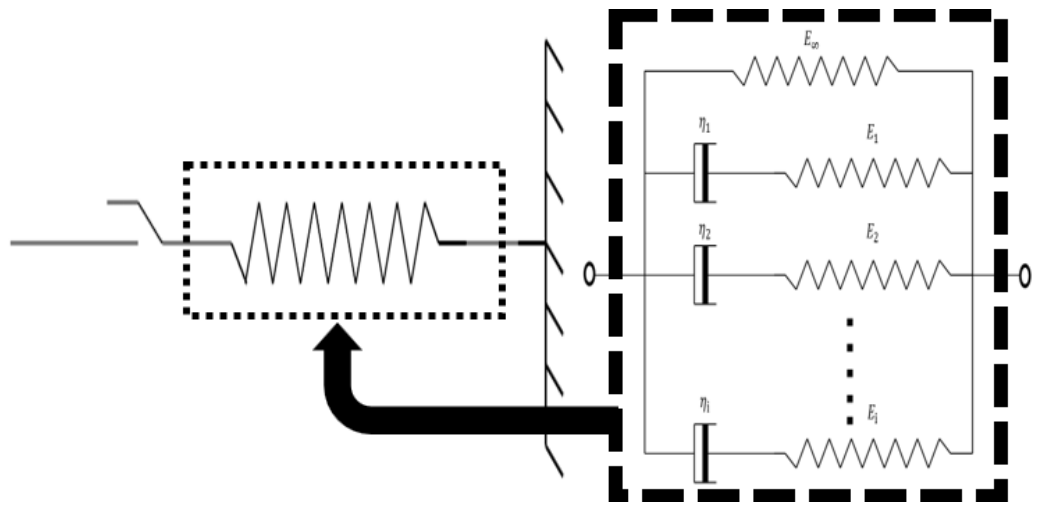


Figure 21 Replacing the elastic spring in Elasto-Plastic model with GM Model

In the plastic state, plastic strains are accumulated. The plastic flow rule determines how the material deforms plastically under certain conditions. The evolution of plastic strain is also governed by an isotropic hardening rule, which modifies the yield surface based on accumulated plastic strain. The derivation behind the Drucker Prager yield criteria and the hardening phenomenon is presented in the next subsection of the current chapter.

3.3.3 Elasto-Visco-Plastic Material Model

The paper [12] introduces a viscoelastic–plastic damage model which integrates the generalized Maxwell model to represent viscoelastic behaviour and the Drucker–Prager model for plasticity. The comparison results between elastic and viscoelastic-plastic (EVP) damage mode shows that EVP models give a more accurate numerical interpretation of the creep recovery response of hot mix asphalt concrete[9]. They better predict the maximum and permanent strains.

Based on previous studies, development of an EVP material model proved necessary to capture accurate material response of asphalt material in pavements. Hence, the theory and equations behind the developed EVP material model for the current research is presented in this section. The EVP model is a combination of GM material model and Drucker-Prager material model. The GM material model to simulate the viscoelastic material behaviour is first described followed by the plastic material model.

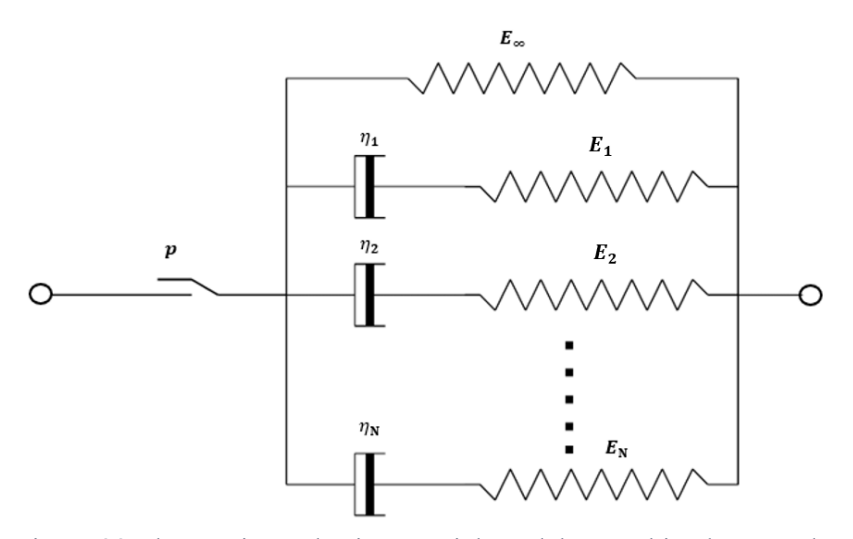


Figure 22 Elasto-Visco-Plastic Material Model - Combined GM and Drucker-Prager

The provided information describes a comprehensive material model, starting with a viscoelastic model incorporating Maxwell elements, where stress-strain relations, evolution equations, and constitutive relations are detailed. This model is then integrated into an elastovisco-plastic material model, utilizing a Drucker-Prager yield criterion, hardening function, and Newton-Raphson iterations for force equilibrium. The material model considers hardening, consistency conditions, and evolves viscoelastic and plastic strains over time. The resulting equations capture the behaviour of materials under various loading conditions, combining viscoelastic, and plastic responses in a systematic manner.

3.3.3.1 Viscoelastic material model Equations

The equations (1) & (2) describe the stress-strain relationship for the GM viscoelastic material, where σ_i is stress, ε is strain, ε_{vi} is the viscoelastic strain, E_i is the elastic modulus, and η_i is the viscosity of the i^{th} component. The constitutive equations for a single spring (σ_{∞}) and a single Maxwell viscoelastic component (σ_i) are as follows,

$$\sigma_{\infty} = E_{\infty} \varepsilon \tag{1}$$

$$\sigma_{i} = E_{i}(\varepsilon - \varepsilon_{vi}) = \eta_{i}\dot{\varepsilon}_{vi} \tag{2}$$

The differential equation (3) governs the behaviour of the Maxwell viscoelastic material which involve the rates of change of viscoelastic strain ($\dot{\varepsilon}_{vi}$) and viscoelastic strain (ε_{vi})

$$\eta_{i}\dot{\varepsilon}_{vi} + E_{i}\varepsilon_{i} = E_{i}\varepsilon \tag{3}$$

$$\dot{\varepsilon}_{vi} + \frac{E_{i}}{\eta_{i}} \varepsilon_{vi} = \frac{E_{i}}{\eta_{i}} \varepsilon \tag{4}$$

From solving equation (4) for all Maxwell components (i), the homogeneous and particular solutions are calculated. The homogeneous solution to the differential equation, where $\varepsilon_{Vi_{hom}}$ represents the homogeneous part of the viscoelastic strain, and C_1 is a constant.

Homogeneous solution:
$$\dot{\varepsilon}_{vi} + \frac{E_i}{\eta_i} \varepsilon_{vi} = 0 \rightarrow \varepsilon_{Vi,hom} = C_1 e^{-\frac{E_i}{\eta_i} t}$$

The particular solution to the differential equation involves a convolution integral over time. It determines the behaviour of the material based on the external influences.

Particular solution:

$$\varepsilon_{\nu i, \text{ part}} = \int_0^t e^{-\frac{E_i}{\eta_i}(t-s)} \cdot \frac{E_i}{\eta_i} \varepsilon(s) ds$$
 (5)

Taking out the terms dependent on variable (t) from the integral, further solving the equation (5),

$$\int_0^t e^{-\frac{E_i}{\eta_i}(t-s)} \cdot \frac{E_i}{\eta_i} \varepsilon(s) ds = \frac{E_i}{\eta_i} e^{-\frac{E_i}{\eta_i}t} \cdot \int_0^t e^{\frac{E_i}{\eta_i}s} \varepsilon(s) ds \tag{6}$$

Using integration by parts on the integral in equation (6),

$$\int_{0}^{t} e^{\frac{E_{i}s}{\eta_{i}}} \varepsilon(s) ds = \frac{\eta_{i}}{E_{i}} e^{\frac{E_{i}}{\eta_{i}}s} \varepsilon(s) \Big|_{0}^{t} - \int_{0}^{t} \frac{\eta_{i}}{E_{i}} e^{\frac{E_{i}}{\eta_{i}}s} \dot{\varepsilon}(s) ds = \frac{\eta_{i}}{E_{i}} \Big[e^{\frac{E_{i}}{\eta_{i}}t} \varepsilon(t) - \varepsilon(0) - \int_{0}^{t} e^{\frac{E_{i}}{\eta_{i}}s} \dot{\varepsilon}(s) ds \Big]$$

$$\int_{0}^{t} e^{-\frac{E_{i}}{\eta_{i}}(t-s)} \cdot \frac{E_{i}}{\eta_{i}} \varepsilon(s) ds = \frac{E_{i}}{\eta_{i}} e^{-\frac{E_{i}}{\eta_{i}}t} \cdot \frac{\eta_{i}}{E_{i}} \Big[e^{\frac{E_{i}}{\eta_{i}}t} \varepsilon(t) - \varepsilon(0) - \int_{0}^{t} e^{\frac{E_{i}}{\eta_{i}}s} \dot{\varepsilon}(s) ds \Big] =$$

$$= \varepsilon(t) - \varepsilon(0) e^{-\frac{E_{i}}{\eta_{i}}t} - \int_{0}^{t} e^{-\frac{E_{i}}{\eta_{i}}(t-s)} \dot{\varepsilon}(s) ds$$

$$(7)$$

Equation (7) represent the evolution of strain over time in terms of the material parameters, incorporating viscoelastic behaviour. The stress in terms of the strain and viscoelastic strain, implementing the parameters of different Maxwell elements in the model from the 1^{st} to the N^{th} component is given below,

$$\sigma_{i}(t) = E_{i}(\varepsilon(t) - \varepsilon_{vi}(t)) \tag{8}$$

The overall stress in the Generalized Maxwell Model, considering the contributions from different Maxwell elements,

$$\sigma = \sigma_{\infty} + \sum_{i=1}^{N} \sigma_{i}$$

The incremental stress in the next time step, considering elastic responses and changes in the Maxwell element properties, is calculated using the equations below depending on the dimension of the model.

 E_{i} - is an elastic modulus representing the instantaneous or infinite-time response in 1D. D_{i} - is a stiffness tensor associated with the infinite-time response in 2D or 3D space.

The equation to describe the incremental stress in the next time step ($^{t+\Delta t}\sigma$) in terms of the total strain (ϵ) and the historic viscoelastic strains (H_i) associated with different Maxwell elements is as follows,

1D:
$$^{t+\Delta t}\sigma = E_{\infty}^{t+\Delta t}\varepsilon + \sum_{i=1}^{N} E_{i}^{t+\Delta t}H_{i}$$

Similar to the 1D case, this equation extends to 2D/3D space.

2D/3D:
$$^{t+\Delta t}\sigma = D_{\infty}$$
: $^{t+\Delta t}\varepsilon + \sum_{i=1}^{N} D_i^{t+\Delta t} H_i$

 D_{∞} represents the stiffness tensor associated with the infinite-time response in 2D or 3D space corresponds to the long-term stiffness of the material.

The equation (9) describes the evolution of the historic viscoelastic strain (H_i) associated with the i-th Maxwell element over time.

$$t^{t+\Delta t}H_{i} = e^{-\frac{\Delta t}{k_{i}}t}H_{i} + e^{-\frac{\Delta t}{2k_{i}}t}\Delta\varepsilon$$

$$e^{-\frac{\Delta t}{2k_{i}}t+\Delta t}H_{i} = e^{-\frac{\Delta t}{2k_{i}}t}H_{i} + t\Delta\varepsilon$$

$$t^{t+\Delta t}\bar{H}_{i} = t\bar{H}_{i} + t\Delta\varepsilon$$
(9)

 ${}^t\bar{H}_i = e^{-\frac{\Delta t}{2k_i}} {}^tH_i$ represents the memory of past viscoelastic strain in the i-th Maxwell element.

Viscoelastic stress (${}^t\sigma_{ve}$) at time t as a function of total strain (ϵ), historic viscoelastic strain (H), and changes in total strain over time ($\Delta\epsilon$) is,

$${}^{t}\sigma_{ve} = D_{\infty}: {}^{t-\Delta t}\varepsilon + D_{\infty}: {}^{t}\Delta\varepsilon + \sum_{i=1}^{N} D_{i}e^{-\frac{\Delta t}{2k_{i}}}: ({}^{t-\Delta t}\bar{H}_{i} + {}^{t}\Delta\varepsilon)$$
 (10)

Expressing the viscoelastic stress of the next time step in terms of the viscoelastic stress in the current time step,

$$with \ ^{t}\sigma_{ve} = \ ^{t}\sigma_{ve} + \sum_{i=1}^{t+\Delta t} \Delta \sigma_{ve}$$

$$with \ ^{t}\sigma_{ve} = D_{\infty} : \ ^{t}\varepsilon + \sum_{i=1}^{N} D_{i}e^{-\frac{\Delta t}{2k_{i}}} : \ ^{t}\bar{H}$$

$$and \ ^{t+\Delta t}\Delta \sigma_{ve} = \left(D_{\infty} + \sum_{i=1}^{N} D_{i}e^{-\Delta t/2k_{i}}\right) : \ ^{t+\Delta t}\Delta \varepsilon$$

$$(11)$$

It also holds that,

$${}^{t}\sigma_{ve} = D_{\infty}: \ {}^{t-\Delta t}\varepsilon + \sum_{i=1}^{N} D_{i}e^{-\frac{\Delta t}{2k_{i}}}: \ {}^{t-\Delta t}\bar{H} + \left(D_{\infty} + \sum_{i=1}^{N} D_{i}e^{-\frac{\Delta t}{2k_{i}}}\right): \ {}^{t}\Delta\varepsilon \tag{12}$$

Combining the last two equations (10) and (11) for ${}^t\sigma_{ve}$ results in,

$$D_{\infty} : {}^{t}\varepsilon + \sum_{i=1}^{N} D_{i}e^{-\frac{\Delta t}{2k_{i}}} : {}^{t}\bar{H}_{i}$$

$$= D_{\infty} : {}^{t-\Delta t}\varepsilon + \sum_{i=1}^{N} D_{i}e^{-\frac{\Delta t}{2k_{i}}} : {}^{t-\Delta t}\bar{H}_{i} + \left(D_{\infty} + \sum_{i=1}^{N} D_{i}e^{-\frac{\Delta t}{2k_{i}}}\right) : {}^{t}\Delta\varepsilon$$

$$D_{\infty} : \left({}^{t}\varepsilon - {}^{t-\Delta t}\varepsilon\right) + \sum_{i=1}^{N} D_{i}e^{-\frac{\Delta t}{2k_{i}}} : {}^{t}\bar{H}_{i}$$

$$= \sum_{i=1}^{N} D_{i}e^{-\frac{\Delta t}{2k_{i}}} : {}^{t-\Delta t}\bar{H}_{i} + D_{\infty} : {}^{t}\Delta\varepsilon + \left(\sum_{i=1}^{N} D_{i}e^{-\frac{\Delta t}{2k_{i}}}\right) : {}^{t}\Delta\varepsilon$$

$$D_{\infty} : {}^{t}\Delta\varepsilon - D_{\infty} : {}^{t}\Delta\varepsilon + \sum_{i=1}^{N} D_{i}e^{-\frac{\Delta t}{2k_{i}}} : {}^{t}\bar{H}_{i} = \sum_{i=1}^{N} D_{i}e^{-\frac{\Delta t}{2k_{i}}} : {}^{t-\Delta t}\bar{H}_{i} + \left(\sum_{i=1}^{N} D_{i}e^{-\frac{\Delta t}{2k_{i}}}\right) : {}^{t}\Delta\varepsilon$$

$$\sum_{i=1}^{N} D_{i}e^{-\frac{\Delta t}{2k_{i}}} : {}^{t}\bar{H}_{i} = \sum_{i=1}^{N} D_{i}e^{-\frac{\Delta t}{2k_{i}}} : {}^{t-\Delta t}\bar{H}_{i} + \left(\sum_{i=1}^{N} D_{i}e^{-\frac{\Delta t}{2k_{i}}}\right) : {}^{t}\Delta\varepsilon$$

$$(13)$$

Equation (14) describes the time-dependent viscoelastic stress $^{t+\Delta t}\sigma_{ve}$ in terms of total strain, viscoelastic strain, and their time derivatives,

$$t + \Delta t \sigma_{ve} = D_{\infty} : t + D_{\infty} : t + \Delta t \Delta \varepsilon + \sum_{i=1}^{N} D_{i} e^{-\frac{\Delta t}{2k_{i}}} : (t \bar{H}_{i} + t + \Delta t \Delta \varepsilon)$$

$$= D_{\infty} : t + D_{\infty} : t + \Delta t \Delta \varepsilon + \sum_{i=1}^{N} D_{i} e^{-\Delta t/2k_{i}} : (t + t + \Delta t \Delta \varepsilon)$$

$$= \left(D_{\infty} + \sum_{i=1}^{N} D_{i} e^{-\frac{\Delta t}{2k_{i}}} \right) : \left({}^{t} \varepsilon + {}^{t+\Delta t} \Delta \varepsilon \right) = \mathbb{C}_{ve} : {}^{t+\Delta t} \varepsilon$$
 (14)

 \mathbb{C}_{ve} - is the viscoelastic stiffness tensor that combines the contributions from the instantaneous elastic response D_{∞} and the viscoelastic contributions from each Maxwell element.

The transformation between stress and strain using the inverse of stiffness is defined as:

$$\varepsilon_{GM} = \mathbb{C}_{ve}^{-1} : \sigma \to \dot{\varepsilon}_{GM} = \mathbb{C}_{ve}^{-1} : \dot{\sigma}$$

The strains obtained from the Generalized Maxwell viscoelastic model are used to calculate the stresses. These stresses are used as trial stress for the plastic material model of the elastoviscoplastic material model. Once these stresses cross the yield stress, reduction of stresses occurs to simulate the plastic nature.

3.3.3.2 Newton-Raphson Iteration

The Newton-Raphson method is a numerical method used to find successively better approximations to the roots (or zeroes) of a real-valued function. In the context of material modelling and finite element analysis, it is used to solve the nonlinear equations that characterize the material behaviour under certain conditions. The process starts by initializing the stress variable σ_{∞} with a trial value and setting the plastic strain increment $\Delta \xi$ to zero. The iterative procedure then begins, forming the Jacobian matrix and the residual vector based on the current state and solving the resulting linear system to update σ_{∞} and $\Delta \xi$. This loop continues, with updates applied at each iteration, until a convergence criterion - a small, predefined tolerance - is satisfied, indicating that the solution has been found. Upon convergence, the equivalent plastic strain is updated to reflect the new deformation state, completing the iteration process.

First σ_{∞} is initialized as the "trial" value and $\Delta \xi$ is initialized to zero.

$$\sigma_{\infty} \leftarrow {}^{\text{trial}} \sigma_{\infty}$$
; $\Delta \xi = 0$; converged = .false.

Inside the loop:

- The Jacobian matrix and residual vector are formed using partial derivatives from the previous code segment.
- A system of linear equations is solved for $\partial \sigma_{\infty}$ and $\partial \Delta \xi$ using matrix inversion.
- σ_{∞} and $\Delta \xi$ are updated.
- Residual functions R1 and R2 approach zero after several iterations.
- The "converged" variable is updated based on a convergence criterion, comparing the square of the changes to a predefined tolerance (ε^2) .
- After convergence, the equivalent plastic strain ξ is updated.

The loop continues until the "converged" condition is satisfied.

####CODE###
do while not converged

$$\begin{bmatrix} \frac{\partial \mathbf{R}_1}{\partial \sigma_{\infty}} & \frac{\partial \mathbf{R}_1}{\partial \Delta \xi} \\ \frac{\partial \mathbf{R}_2}{\partial \sigma_{\infty}} & \frac{\partial \mathbf{R}_2}{\partial \Delta \xi} \end{bmatrix} \begin{bmatrix} \delta \sigma_{\infty} \\ \delta \Delta \xi \end{bmatrix} = \begin{bmatrix} -\mathbf{R}_1 \\ -\mathbf{R}_2 \end{bmatrix}$$

$$\sigma_{\infty} \leftarrow \sigma_{\infty} + \delta \sigma_{\infty}$$
; $\Delta \xi \leftarrow \Delta \xi + \delta \Delta \xi$

converged =
$$(\delta \sigma_{\infty} : \delta \sigma_{\infty} + (\delta \Delta \xi)^2) \leq \varepsilon^2$$

enddo

$$\xi \leftarrow {}^{t}\xi + \Delta\xi$$

3.3.3.3 Plastic material model of Equations

The equations below describe the behaviour of materials under plastic conditions, incorporating plasticity criteria, consistency conditions, hardening, and constitutive relations. The Drucker-Prager model is a specific instance of such models, providing a yield criterion for plasticity. The hardening function introduces hardening effects in the plasticity model. Constitutive equations relate stress, plastic strain, internal variables, and consistency conditions to ensure that the model remains physically consistent. The Lagrangian formulation, which is based on the principle of maximum plastic dissipation, helps to setup equilibrium conditions and evolution equations for the internal variables.

$$g = -(\sigma: \dot{\varepsilon}_{p} + q.\dot{\xi}) \tag{15}$$

subjected to
$$f(\sigma, q) \le 0$$
 (16)

'f' represents the plasticity criterion where σ is stress, $\dot{\epsilon}_p$ is plastic strain rate, $\dot{\xi}$ is equivalent plastic strain rate, and q is the overstress. The equation (15) mentioned above needs to minimize under the conditions that inequality (16) holds. This minimization problem can be solved via the mathematical technique, called constrained minimization. The Lagrangian is defined as,

$$\mathcal{L} = g + \dot{\lambda} \cdot f$$

Applying constrained minimization technique on our model together with the Kuhn-Tucker conditions gives,

$$\frac{\partial \mathcal{L}}{\partial \sigma} = \frac{\partial g}{\partial \sigma} + \dot{\lambda} \frac{\partial f}{\partial \sigma} = 0 \tag{17}$$

$$\frac{\partial \mathcal{L}}{\partial \mathbf{q}} = \frac{\partial g}{\partial \mathbf{q}} + \dot{\lambda} \frac{\partial f}{\partial \mathbf{q}} = 0 \tag{18}$$

$$\dot{\lambda}$$
. $f = 0, \dot{\lambda} \ge 0$

Substituting equations (15) and (16) in equations (17) and (18),

$$\frac{\partial \mathcal{L}}{\partial \sigma} = \frac{\partial (-(\sigma; \dot{\varepsilon}_{p} + q, \dot{\xi}))}{\partial \sigma} + \dot{\lambda} \frac{\partial f}{\partial \sigma} = 0$$
$$-\dot{\varepsilon}_{p} + \dot{\lambda} \frac{\partial f}{\partial \sigma} = 0 \tag{19}$$

$$\frac{\partial \mathcal{L}}{\partial \mathbf{q}} = \frac{\partial (-(\sigma; \dot{\varepsilon}_{\mathbf{p}} + q, \dot{\xi}))}{\partial \mathbf{q}} + \dot{\lambda} \frac{\partial f}{\partial \mathbf{q}} = 0$$
$$-\dot{\xi} + \dot{\lambda} \frac{\partial f}{\partial \mathbf{q}} = 0 \tag{20}$$

From equation (19) and (20), the rates of plastic strain and equivalent plastic strain can be calculated as follows,

$$\dot{\epsilon}_{p} = \dot{\lambda} \frac{\partial f}{\partial \sigma}$$

$$\dot{\xi} = \dot{\lambda} \frac{\partial f}{\partial q}$$

For the Drucker-Prager criteria it holds that $\frac{\partial g}{\partial q} = 1$ and therefore,

$$\dot{\xi} = \dot{\lambda} \ or \ \Delta \xi = \Delta \lambda$$

And hence,

$$\Delta \varepsilon_{\rm p} = \Delta \xi \frac{\partial f}{\partial \sigma} \tag{21}$$

The residual functions are initially calculated due to the crucial role in time integration schemes. The residual functions are used to compute the changes in stress and strain over time while ensuring that the system remains in equilibrium. If the residual functions are close to zero, it indicates that the numerical solution is approaching equilibrium.

The equation (22) represents residual function R_1 that should approach zero. It involves the stress (σ), the viscoplastic strain (${}^t\epsilon_{GM}$), and the change in viscoplastic strain ($\Delta\epsilon_{GM}$). The material is in equilibrium when R_1 is zero.

$$R_1 = {}^{t+\Delta t}\sigma - \mathbb{C}_{ve}: ({}^{t}\varepsilon_{GM} + \Delta\varepsilon_{GM}) \to 0$$
 (22)

Similar to R_1 , equation (23) represents another residual function R_2 , which should approach zero. It involves the plasticity criterion f, stress (σ), the equivalent plastic strain (ξ), and the change in the equivalent plastic strain ($\Delta \xi$).

$$R_2 = f(t^{t+\Delta t}\sigma, t^{\xi}, \Delta \xi) \to 0$$
 (23)

The change in strain vector of the GM model is the total strain increment minus the plastic strain increment,

$$\Delta \varepsilon_{\text{GM}} = \Delta \varepsilon - \Delta \varepsilon_{\text{p}} \tag{24}$$

From the substitution of equation (21) into (24)

$$\Delta \varepsilon_{\rm GM} = \Delta \varepsilon - \Delta \xi \frac{\partial f}{\partial \sigma}$$

$$\begin{bmatrix} \frac{\partial R_1}{\partial \sigma} & \frac{\partial R_1}{\partial \Delta \xi} \\ \frac{\partial R_2}{\partial \sigma} & \frac{\partial R_2}{\partial \Delta \xi} \end{bmatrix} \begin{bmatrix} \delta \sigma \\ \delta \Delta \xi \end{bmatrix} = -\begin{bmatrix} R_1 \\ R_2 \end{bmatrix}$$

The change in residual function R_1 equation (22) with respect to stress and the change in the equivalent plastic strain,

$$\frac{\partial R_1}{\partial \sigma} = \mathbb{I} - \frac{\partial \bar{f}}{\partial \Delta \epsilon_{GM}} : \frac{\partial \Delta \epsilon_{GM}}{\partial \sigma}$$
 (25)

$$\frac{\partial R_1}{\partial \Delta \xi} = -\frac{\partial \overline{f}}{\partial \Delta \varepsilon_{GM}} : \frac{\partial \Delta \varepsilon_{GM}}{\partial \Delta \xi}$$
 (26)

The equations (27) and (28) involve the change of the residual function R_2 with respect to stress and the change in the internal variable,

$$\frac{\partial R_2}{\partial \sigma} = \frac{\partial f}{\partial \sigma} \tag{27}$$

$$\frac{\partial R_2}{\partial \Delta \xi} = \frac{\partial f}{\partial \Delta \xi} \tag{28}$$

Equations (29) and (30) describe the partial derivatives of the viscoplastic strain ($\Delta \epsilon_{GM}$) with respect to stress and the change in equivalent plastic strain,

$$\frac{\partial \Delta \varepsilon_{\text{GM}}}{\partial \sigma} = -\Delta \xi \frac{\partial^2 f}{\partial \sigma \partial \sigma} \tag{29}$$

$$\frac{\partial \Delta \varepsilon_{\text{GM}}}{\partial \Delta \xi} = -\frac{\partial f}{\partial \sigma} \tag{30}$$

The equation (31) defines a constant \mathbb{C}_{ve} (Material tensor) related to the material properties,

$$\frac{\partial \bar{f}}{\partial \Delta \varepsilon_{GM}} = \mathbb{D}_{\infty} + \sum_{i=1}^{N} \mathbb{D}_{i} e^{-\frac{\Delta t}{2k_{i}}} = \mathbb{C}_{ve}$$
 (31)

From equations (25), (26), (27) and (28), the change of R₁ and R₂ with respect to stress and the equivalent plastic strain, considering the second derivatives of the plasticity criterion g,

$$\frac{\partial R_1}{\partial \sigma} = \mathbb{I} - \mathbb{C}_{ve} : \left(-\Delta \xi \frac{\partial^2 g}{\partial \sigma \partial \sigma} \right) = \mathbb{I} + \Delta \xi \mathbb{C}_{ve} : \frac{\partial^2 f \partial \sigma}{\partial \sigma \sigma}$$
(32)

$$\frac{\partial \mathbf{R}_{1}}{\partial \Delta \xi} = -\mathbb{C}_{ve} : \left(-\frac{\partial \mathbf{g}}{\partial \sigma} \right) = \mathbb{C}_{ve} : \frac{\partial \mathbf{f}}{\partial \sigma}$$
 (33)

$$\frac{\partial R_2}{\partial \sigma} = \frac{\partial f}{\partial \sigma} \tag{34}$$

$$\frac{\partial R_2}{\partial \Delta \xi} = \frac{\partial f}{\partial \Delta \xi} \tag{35}$$

Jacobian matrix J that relates changes in stress and the change in equivalent plastic strain to changes in the residual functions is presented. It involves the derivatives of R₁ and R₂ with respect to stress and the change in equivalent plastic strain.

$$J = \begin{bmatrix} \mathbb{I} + \Delta \xi \mathbb{C}_{ve} : \frac{\partial^2 f}{\partial \sigma \partial \sigma} & \mathbb{C}_{ve} : \frac{\partial f}{\partial \sigma} \\ \frac{\partial f}{\partial \sigma} & \frac{\partial f}{\partial \Delta \xi} \end{bmatrix}$$
(36)

These equations describe a viscoplastic material model with a specific plasticity surface, residual functions R1 and R2, sensitivity to changes in stress, internal variables, and viscoplastic strain. The model involves Generalized Maxwell elements and considers the evolution of the material's behaviour over time.

For the Drucker Prager Yield criteria, the yield function is defined in terms of the second invariant of the deviatoric stress (J2), the hardening variable ("hard"), and material constants A, B, h_A, and h_b.

$$f = \sqrt{J_2} + (1 + \text{hard})(AI_1 + B)$$
 (37)

The hardening variable depends on time and an additional variable $\Delta \xi$,

hard =
$$h_A(1 - e^{-h_b t(\xi + \Delta \xi)}\xi)$$
 (38)

The Prager consistency condition should hold which is defined as:

$$\frac{Df}{Dt} = \left(\frac{\partial f}{\partial t}\right)^{\mathsf{T}} \cdot \dot{\sigma} + \frac{\partial f}{\partial \xi} \cdot \dot{\xi} = 0 \tag{39}$$

with

$$\frac{\partial f}{\partial \xi} = \frac{\partial f}{\partial \text{ hard}} \cdot \frac{\partial \text{ hard}}{\partial \xi} = (AI_1 + B) \cdot \left(\frac{\partial \text{ hard}}{\partial \xi}\right) \tag{40}$$

The evolution of stress in terms of strain rate, viscoelastic equivalent strain rate ($\dot{\xi}$), and the plasticity direction $\frac{\partial f}{\partial \sigma}$ is defined as:

$$\dot{\sigma} = D_{e} \left(\dot{\varepsilon} - \dot{\xi} \frac{\partial f}{\partial \sigma} \right) \tag{41}$$

The evolution of strain rate in terms of stress rate is now written as:

$$\dot{\varepsilon} = D_{e}^{-1}\dot{\sigma} + \dot{\xi}\frac{\partial f}{\partial \sigma} \tag{42}$$

Solving the Prager consistency condition for equivalent plastic strain gives:

$$\dot{\xi} = \frac{\left(\frac{\partial f}{\partial \sigma}\right)^{\mathsf{T}} \dot{\sigma}}{\frac{\partial f}{\partial \xi}} \tag{43}$$

Substituting equation (43) in equation (42) results in:

$$\dot{\varepsilon} = D_{e}^{-1}\dot{\sigma} + \frac{\partial f}{\partial \sigma} \frac{\left(\frac{\partial f}{\partial \sigma}\right)^{T} \cdot \dot{\sigma}}{\frac{\partial f}{\partial \xi}} = \left[D_{e}^{-1} + \frac{1}{\left(\frac{\partial f}{\partial \xi}\right)} \frac{\partial f}{\partial \sigma} \left(\frac{\partial f}{\partial \sigma}\right)^{T} \right] \dot{\sigma}$$
(44)

To express the stress rate in terms of the strain rate the Sherman-Morrison formula is used. The strain equation above can then be rewritten as:

$$\dot{\sigma} = \left[D_{e} - \frac{D_{e} \frac{\partial f}{\partial \sigma} \left(\frac{\partial f}{\partial \sigma} \right)^{\mathsf{T}} D_{e}}{\frac{\partial f}{\partial \xi} + \left(\frac{\partial f}{\partial \sigma} \right)^{\mathsf{T}} D_{e} \frac{\partial f}{\partial \sigma}} \right] \cdot \dot{\varepsilon}$$
(45)

3.3.4 Summary

In the current chapter, material models were thoroughly explored, and the foundation was laid for further experimental validation. The principles of the elasto-plastic and viscoelastic-plastic models, particularly in relation to the Drucker-Prager criterion, were presented in a detailed manner. The interrelation between these models and the generalized Maxwell model was systematically examined, providing an advanced elasto-visco-plastic model that enhances the accuracy in predicting asphalt behaviour. It was shown that a deep comprehension of material models is vital for the advancement and innovation in materials engineering.

With the theoretical aspects of material models addressed, the focus of the thesis now moves to the subsequent section, which delves into the Design of Experiment. The next part will seek to illustrate the real-world utility of the material models discussed, aiming to confirm the predictive accuracy and applicability in engineering contexts.

3.4 Design of Experiment

The Design of Experiment mentioned in the current research is utilized to systematically investigate the effects of various parameters such material stiffness, load location etc on the behaviour of widened pavement models. Table 5 presents different combination of models that were studied and compared. As explained in the methodology framework, initially, the critical locations were identified by comparing unwidened pavement (2D-UP) with widened pavement without reinforcement (2D-WP-NR). Subsequent analyses were done to measure the impact of embedded reinforcement (2D-WP-R). Furthermore, the effect of variation in material stiffness, base layer thickness, and load location at the critical location in pavement widening were analysed.

As explained in the Introduction chapter, one of the major goals of the research was to look at the possibility of reducing the utilization of natural material which will ultimately lead to reduction in Carbon-footprint from the pavement sector models with reduced recessing/overlapping length (2D-RRL-R) and with reduced number of base layers (2D-RBL-R) were analysed (see Figure 24).

Finally, the joint interface is a critical location that can dictate the performance and longevity of the widened pavement, as it is often the weakest link due to potential debonding or differential settlement. The joint interface behaviour in widened pavement is modelled using cohesive zone modelling (CZM). By implementing CZM, it is possible to capture the behaviour of the interface, including the peak stress that can be carried by the joint. Results from the model incorporating CZM (2D-WP-R-CZM) was compared to those of the widened pavement model, providing insights into joint interface behaviour.

Pavement Model	Pavement Model Name
Acronym	
Model: 2D-UP	2D-Unwidened Pavement Model
Model: 2D-WP-NR	2D-Widened Pavement Model based on Current
	Design Requirements No Reinforcement
Model: 2D-WP-R	2D-Widened Pavement Model based on Current
	Design Requirements with Reinforcement
Model: 2D-RRL-R	2D-Widened Pavement Model – Reduced
	Recessing/Overlapping length with Reinforcement
Model: 2D-RBL-R	2D-Widened Pavement Model – Reduced base layers
	with Reinforcement
Model: 2D-EBT-R	2D-Widened Pavement Model – Equal Base
	Thickness with Reinforcement
Model: 2D-WP-R-CZM	2D-Widened Pavement Model – Current Design
	Requirements with Reinforcement and Cohesive Zone
	Modelling

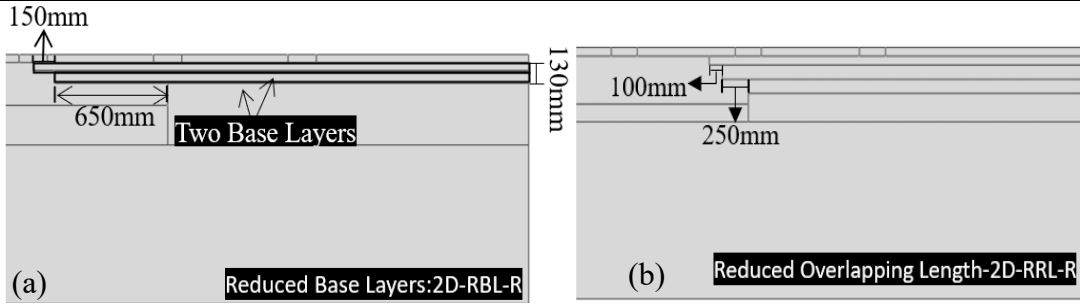


Figure 23 2D-widened pavement FEM models with (a) Reduced number of Base layers and (b) Reduced Recessing/overlapping length in base layer.

3.5 Finite Element Implementation

The current section presents a brief description of the development and implementation of material model in Finite elements.

3.5.1 User Material Subroutine

User-MATerial (UMAT) allows users to define custom material models that are not available in the standard material library[36]. By writing a material subroutine, users can incorporate desired material behaviour into the numerical simulations that better reflect real-world conditions[33]. Such implementations are particularly useful in cases where materials exhibit nonlinear, anisotropic, or rate-dependent properties that standard models cannot accurately capture[36].

3.5.2 Finite Element Model

In the widened pavement model as shown in Figure 25, side edges were considered as symmetrical vertical edges. This is justified because in field condition the stresses can travel through side bodies such as (soil etc.) [36]. The bottom edge was considered to fixed, assuming full stability in the underlying layers[36]. This is justified considering perpetual pavement concepts in the Netherlands. After setting the boundary conditions, the load representing tire pressure was-applied at three different locations separately (see Figure 10), with a tire pressure of 0.8MPa.

Standard quadratic CPS8 elements are used to mesh different layers of the widened pavement. These elements were used because, the 8-node biquadratic plane stress quadrilateral elements provide a higher level of precision in capturing the stress and strain distribution, due to the ability to model the curvature and stress more accurately than the linear counterparts [37].

To model the joint, cohesive elements were inserted between the existing and new pavement base layers. The interface at the joints were designed using COH2D4: A 4-node two-dimensional cohesive elements. The cohesive elements simulate the behaviour of the jointed interfaces by allowing for separation and sliding between adjacent pavement layers, thus capturing the effect of interlayer shear and debonding[38].

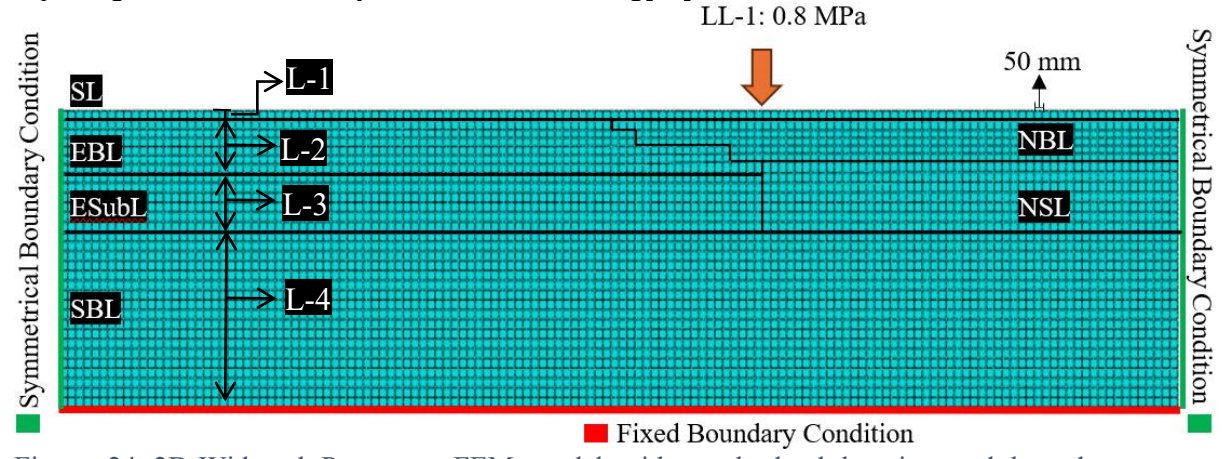


Figure 24 2D-Widened Pavement FEM model with mesh, load location and boundary condition.

3.6 Validation of material models

As stated in the research objective, an elasto-visco-plastic (EVP) material model is developed to predict stresses in pavement widening. Before using the models for further analysis, the developed EVP model was validated by comparing the results with the well-known elastic material model. Simplified geometry in 2D and 3D were utilized for this purpose to eliminate other geometrical effect as shown in Figure 26.

3.6.1 Viscoelastic Material Model Validation

According to the past researchers [24] the VE strains are higher in comparison to elastic strains and such a comparison was used for the material model validation. To capture the material response a time dependent load of 0.8MPa was applied. As shown in Figure 27, the maximum magnitude of load is reached at 2.5 seconds and then the load is removed by 5 seconds. The total analysis time for basic 2D-Geometry model was 10s as the materials relaxation effects can

only be captured over long period of time. Further moving on to the pavement models, the time of the analysis is changed back to 1s.

3.6.1.1 2D- & 3D – Geometry

The geometrical dimension of both the 2D and 3D model are presented in the Figure 26a-26b. To have a correct comparison, the same geometrical dimensions were used to study-both elastic and EVP models. To observe more impact of the plastic behaviour within the EVP material model, the applied load is increased from 0.8MPa to 4MPa. The remaining parameters such as the boundary conditions, load location and mesh, are same as 2D- model shown in Figure 26(a).

The obtained strain ε_{xx} for the analysis of the basic 2D- Elastic and EVP material models, and 3D-models with EVP material model is illustrated in Figure 28(a) and (b). The material response to applied load is divided into 3 zones as shown in Figure 28 (b). Zone I is the region where the load is applied till it reaches the maximum as shown in Figure 27. In Zone II the unloading starts, and the zone region ends by the time the unloading is complete. Finally, Zone III represents the region in which the relaxation effects of the material can be observed. It is noteworthy that even though the elastic model promptly returns to its original shape upon removal of the load as shown in Figure 28(a). The EVP material takes approximately eight seconds for the material to reach the same state, this clearly shows that the EVP material is showing a time effect as comparison of the elastic material.

The strain ε_{xx} for the 2D model from Figure 28(a) shows how the EVP material model experiences 5.4% higher strains compared to the elastic material model due to the time-dependant behaviour of the EVP material. Additionally, it is observed from Figure 28(b) that the strain ε_{yy} in the EVP model is approximately 10.5% higher than that of the strain in the elastic material model for the 2D-Geometry. Similarly, for the 3D- EVP material model, the strain ε_{yy} is observed to be approximately 11.3% higher compared to the strain in the elastic material model. The observed trend of increase in strains for EVP material model prove that the elastic model results are conservative.

Figure 28(b) also illustrates a comparison between the strains ε_{yy} of 2D- and 3D- models, specifically at the node positioned directly beneath the load location (see Figure 26). The strains ε_{yy} in the 2D model are higher by 22.8% compared to the strain in the 3D model. The 3D model considers the deformation that occurs not just vertically and horizontally, but also in the depth. Also, the difference mesh elements used in both the models explain the differences observed in the models. Given that the 3D FEM model yields more conservative results, the subsequent focus of the current research is directed towards the utilization of 2D models in pavement widening analysis.

When the load applied on 2D- model in Figure 26(a) is increased to validate the plastic nature of the EVP material model, as shown in Figure 29, a permanent micro strain of approximately 5820.9 becomes evident in the material after the complete removal of the load. This shows that the developed material model is able to capture permanent deformation in the material.

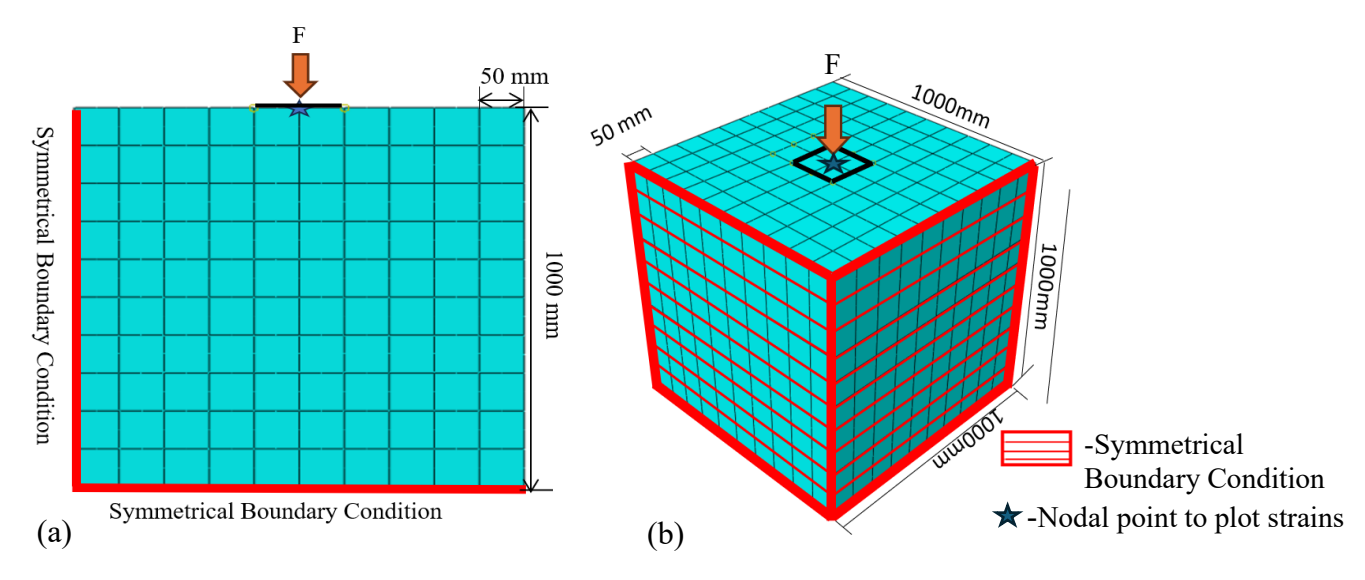


Figure 25 Mesh, Load and Boundary Condition of (a) 2D- & (b) 3D- Geometries used for material model validation.

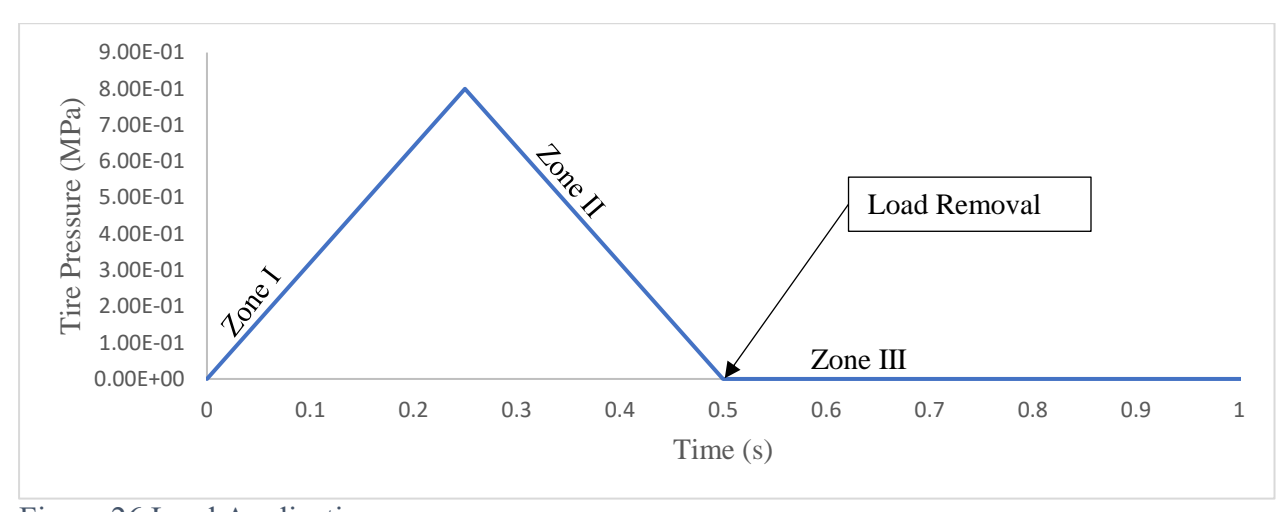
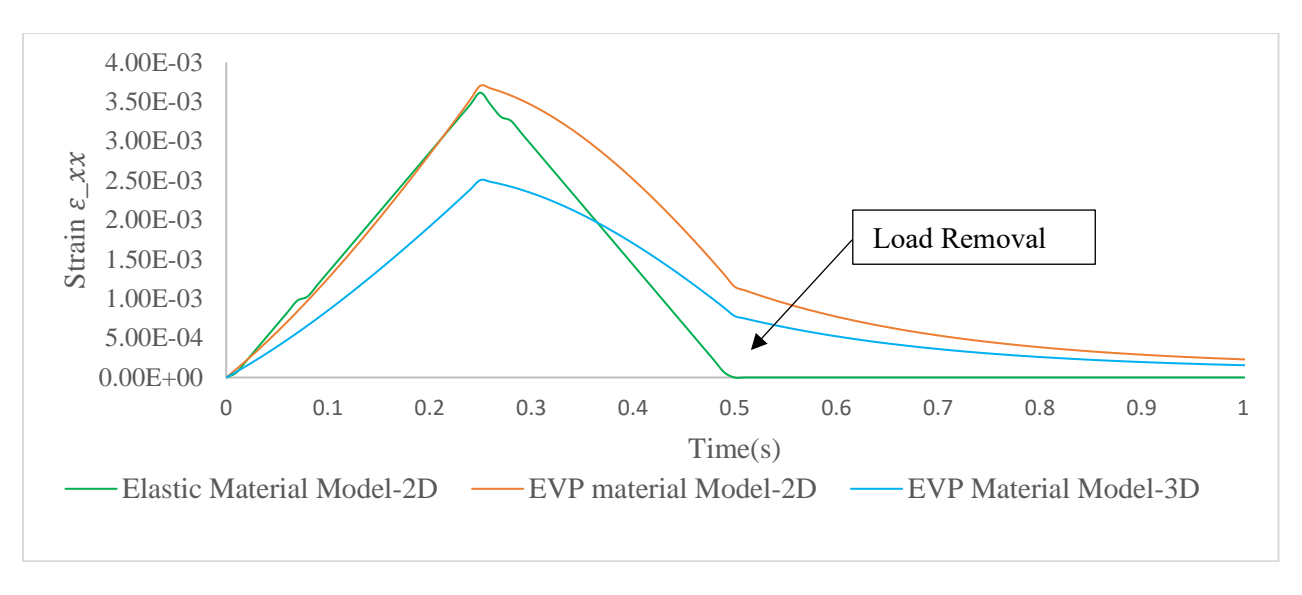


Figure 26 Load Application



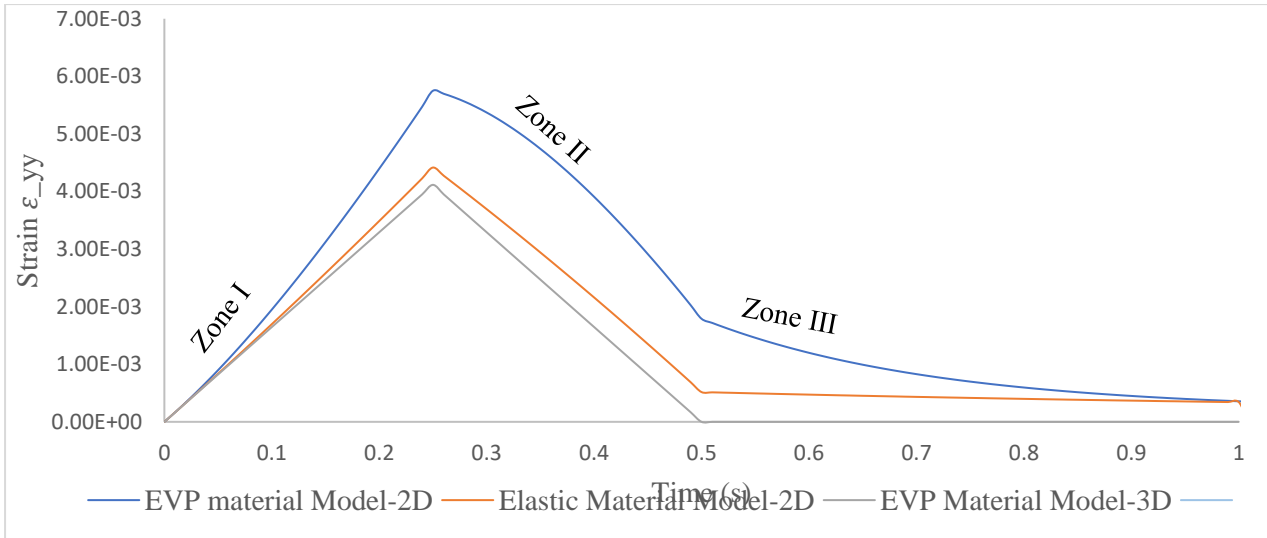


Figure 27 (a) Strain ε_{xx} and (b) Strain ε_{yy} over time for Elastic and EVP Material Models at the node under applied load in 2D-and 3D- models

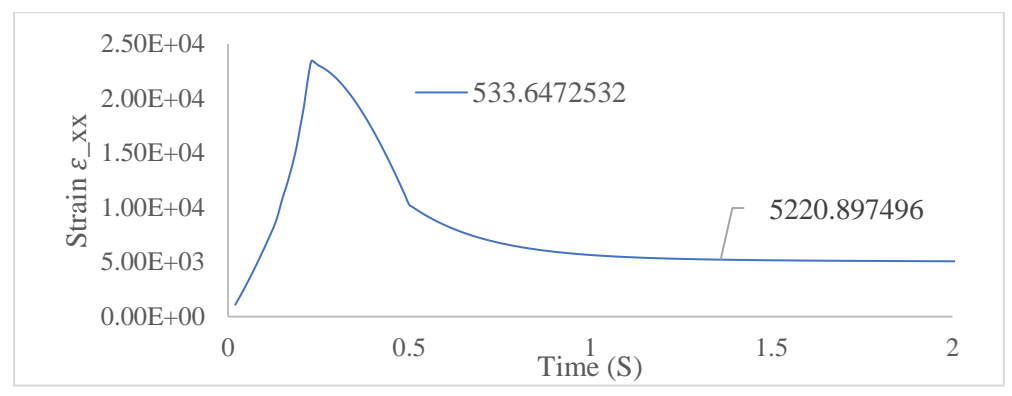


Figure 28 Plastic Strains ε_{xx} in 2D-geometry validating the material model plastic behaviour.

4 Results & Discussion

The results obtained from the FEM analysis of the pavement models given in Table-5 are discussed in the current chapter. The main research objective was to develop an EVP material model to better capture the behaviour surface asphalt layer in pavements. With the development of an EVP material model, it is incorporated as a subroutine in the FEM software to further progress into the research with respect to pavement widening. In line with the research objective, identifying the critical location in widened pavement model without reinforcement was done by comparison with an unwidened pavement. Additionally, reinforcement was added to the widened pavement model to understand the influence of reinforcement at the earlier identified critical location. Moreover, the effect of the parameters such as material stiffness, base layer thickness and load location at the critical location was investigated. To evaluate the performance of standard pavement widening design, the widened pavement model with reinforcement is analysed with reduced recessing/overlapping length and reduced number of base layers. Finally, to investigate the joint interface in widened pavement model, as sensitivity analysis was conducted by implementing a material with a high and low stiffness into the interface. The results from the different stiffness CZM models are then compared to the results from the widened pavement model. This is done by mainly plotting the stress and strains at the critical location for the pavement models.

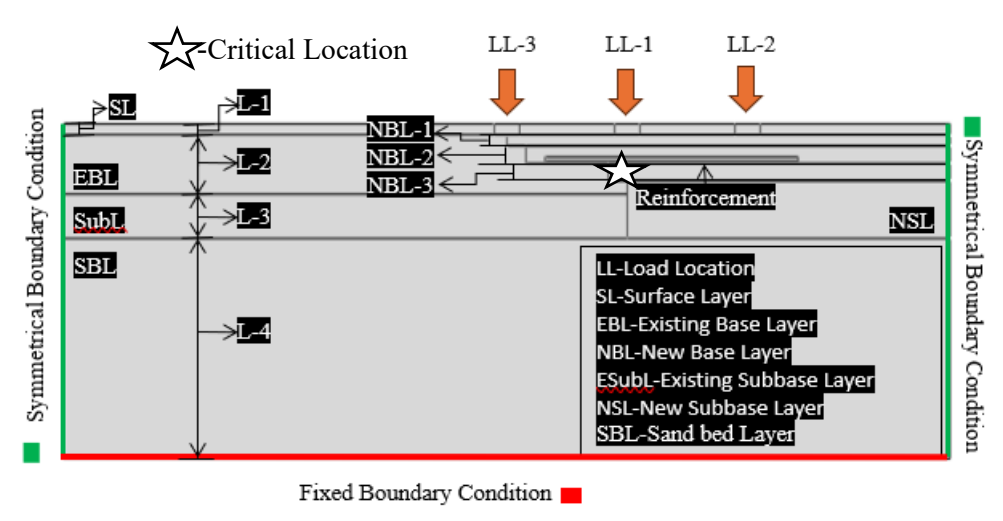


Figure 29 Critical location in widened pavement.

4.1 Effect of Pavement Widening

Pavement widening can often lead to several distresses, including longitudinal cracking, non-uniform settlement, and reflection cracking[15]. These issues develop stress concentrations in a pavement widening situation often at the longitudinal joint, where the new pavement meets the old[3]. Hence in accordance with the research objective, to identify the critical location with such stress concentrations in a widened pavement model, an unwidened pavement is designed and analysed along with a widened pavement model. By comparing the stress and strain values at the critical location in both the models, the effect of widening in pavements was analysed.

From the analysis of the unwidened and widened pavement models, the critical location was observed at intersection between subbase and subgrade in the widened pavement section (see Figure 30). The stresses and strains were hence plotted between the two models at the height of the critical location, to study the differences due to widening. The stresses along the width (σ_{xx}) and along the depth (σ_{yy}) of pavement models, at the height of critical location for both unwidened and widened pavement models are plotted as shown in Figure 31 (a). Following the stresses, the strains ε_{xx} and ε_{yy} along the width and depth of the pavement at the height of

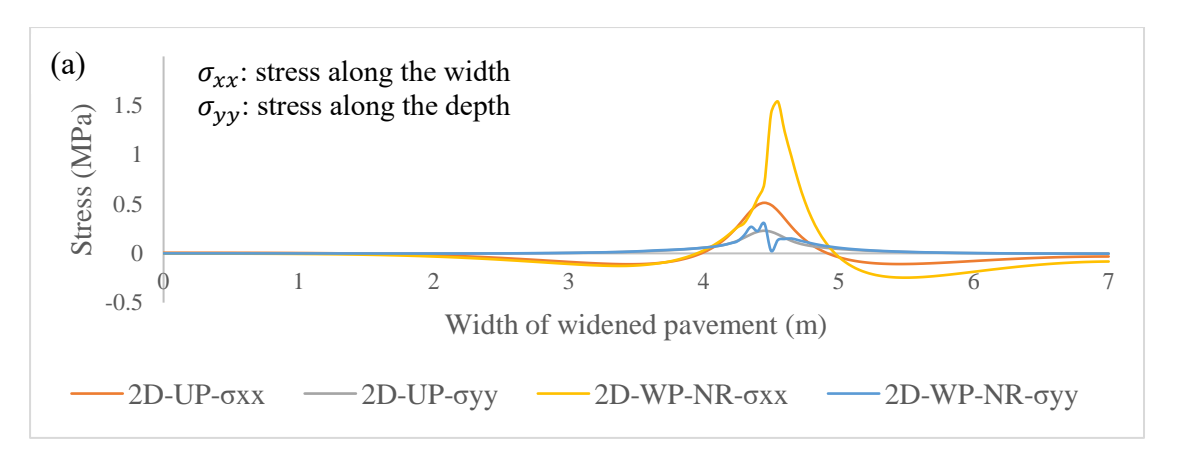
critical location are plotted in Figure 31(b). Also, the stresses and strains at the critical location in unwidened and widened pavement were described in Table-2.

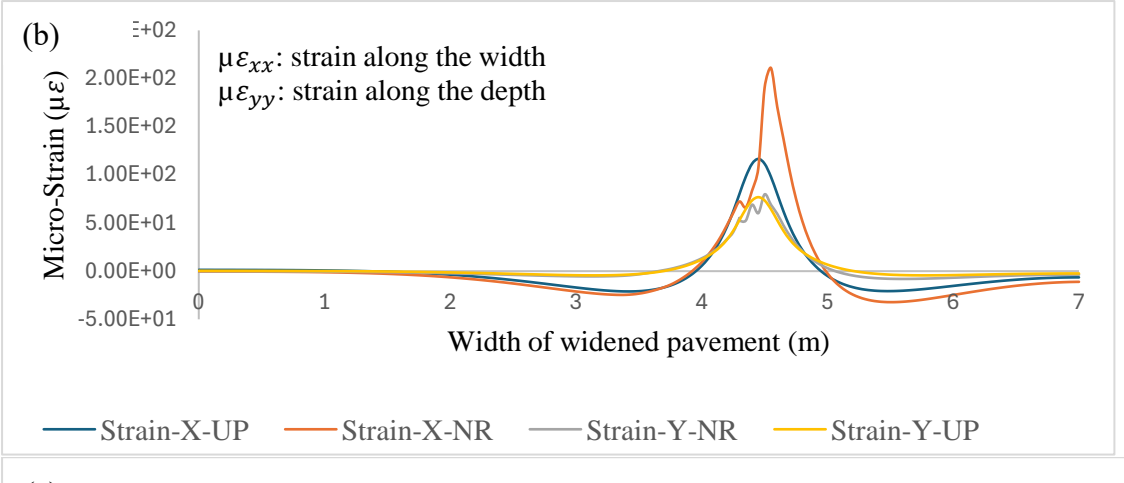
The stress σ_{xx} in the widened pavement model was the highest stresses (see Figure 31(a)). σ_{xx} in the widened pavement model was 2 times higher than the unwidened model. This difference is mainly due to change in material stiffness along the width of widened pavement. A similar trend of increase in stress is also observed in stresses σ_{yy} and σ_{xy} for the widened pavement, with an increase of 29% and 2.29% compared to the unwidened pavement at the critical location (see Table-6). Also, the micro-strains in the widened and unwidened pavement model at the critical location were compared. The micro-strains $\mu \varepsilon_{xx}$ and $\mu \varepsilon_{yy}$ in widened pavement model at the critical location were higher by 97.2% and 4.92% respectively, as compared to the unwidened pavement. However, the micro-strains $\mu \varepsilon_{xy}$ was reduced by 27.51% in the widened pavement model in contrast to unwidened pavement.

The remarkable increase in stress σ_{xx} highlights the considerable impact of material stiffness changes and the resulting stress concentrations post-widening. Similarly, the stresses σ_{yy} and σ_{xy} also exhibit noticeable increases. Furthermore, the corresponding micro-strains $\mu\varepsilon_{xx}$ have surged significantly in the widened model. However, the micro-strain $\mu\varepsilon_{xy}$ diverges from this trend, showing a reduction. These findings underscore the necessity for enhanced design and material selection considerations when widening pavements to mitigate the development of stress concentrations that could lead to premature failure.

Table 6 Stress and Micro-Strains at the critical location in Unwidened and widened pavement models

Models	$\sigma_{\chi\chi}$ (MPa)	σ_{yy} (MPa)	σ_{xy} (MPa)	$\mu arepsilon_{\chi\chi}$	$\mu \varepsilon_{yy}$	μ $ε_{xy}$
2D-UP	0.51150	0.25590	0.19696	107	73.2	93.1
2D-WP-NR	1.55054	0.33177	0.20146	211	76.8	67.5
Percentage Increase or Decrease (%)	+203%	+29%	+2.29%	+97.2%	+4.92%	-27.51%





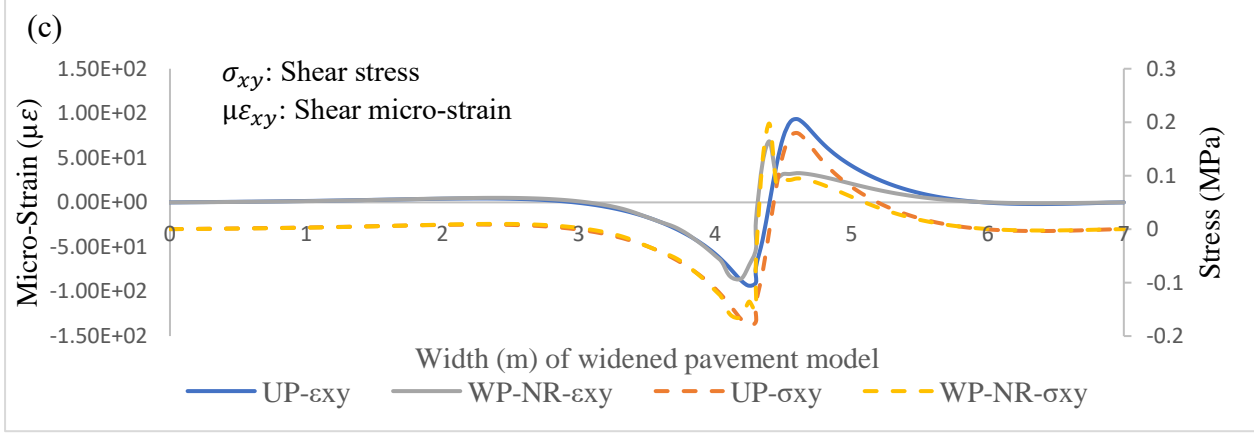


Figure 30 (a) Stress (σ_{xx}) and (σ_{yy}) , (b) micro-strain $(\mu \varepsilon_{xx})$ and $(\mu \varepsilon_{yy})$ and (c) Stress (σ_{xy}) and micro-strain $\mu \varepsilon_{xy}$ in both unwidened (2D-UP) and widened pavement without reinforcement (2D-WP-NR) models.

4.2 Effect of Reinforcement in Pavement Widening

The addition of reinforcement to the widened pavement model was investigated to assess its influence on stress and strain at the critical location. Reinforcement was investigated for its potential to alleviate the previously identified stress concentrations and strain values in the widened pavement model. The reinforcement was embedded into the new base layer 2 (NBL-2) to provide a constraint similar to real life conditions, as shown in Figure 32. Results are tabulated, contrasting the stress and strain responses for both models (See table 7). Specifically, the measurements of stress and strain along the width (σ_{xx} and $\mu \varepsilon_{xx}$), the depth (σ_{yy} and $\mu \varepsilon_{yy}$),

and in-plane shear (σ_{xy} and $\mu \varepsilon_{xy}$) were analyzed at the critical location, also shown in Figure 32 (a) and (b).

The embedment of reinforcement in the 2D-WP-R model resulted in a slight decrease in the stress σ_{xx} by 1.2%. This suggests a subtle improvement along the width due to the reinforcement. Conversely, a small increase in the vertical stress σ_{yy} by 2.7%, and the in-plane shear stress σ_{xy} by 3.56% was observed, indicating a slight improvement in the material's resistance to both vertical and lateral shifts. Furthermore, strain measurements exhibited minor but noticeable differences; a decrease in the strain $\mu \varepsilon_{xx}$ and $\mu \varepsilon_{yy}$ by 1.4% and 5.2% was observed while shear strain $\mu \varepsilon_{xy}$ increases by 3.6%.

In the results, it is evident that the stress σ_{xx} is significantly higher than both σ_{yy} and σ_{xy} (see Figure 32(a)). The comparatively lower values of σ_{yy} and σ_{xy} suggest that the stresses along the depth and the shear stress within the plane of the pavement are less critical under the same loading conditions. The slight differences in stress and strain values indicate that the impact of reinforcement on the critical location is relatively minimal. Despite the limited effect, the reinforcement's role in redistributing stresses and its potential in improving the performance of widened pavements should not be disregarded. It is noted that reinforcement contributes to the stress transfer across the interface between the existing and new pavement bases, thereby influencing the stress distribution along the width of the pavement. However, the study related to the reinforcement is out of the scope for current research and hence, further research may explore how the design and material of the reinforcement can be optimized for more significant impact on the widened pavement's structural response.

Table 7 Stresses and Strains at the critical stress location for widened pavement models with and without reinforcement

Models	$\sigma_{\chi\chi}$	σ_{yy}	$\sigma_{\chi y}$	$\mu \varepsilon_{xx}$	$\mu \varepsilon_{yy}$	$\mu \varepsilon_{xy}$
	(MPa)	(MPa)	(MPa)			
2D-WP-NR	1.55054	0.04590	0.24033	0.000205	-5.7e-05	8.33e-05
2D-WP-R	1.53179	0.04714	0.248883	0.000202	-5.4e-05	8.62e-05
Percentage	-1.2%	+2.7%	+3.56%	-1.4%	-5.2%	+3.60%
Increase or						
Decrease (%)						

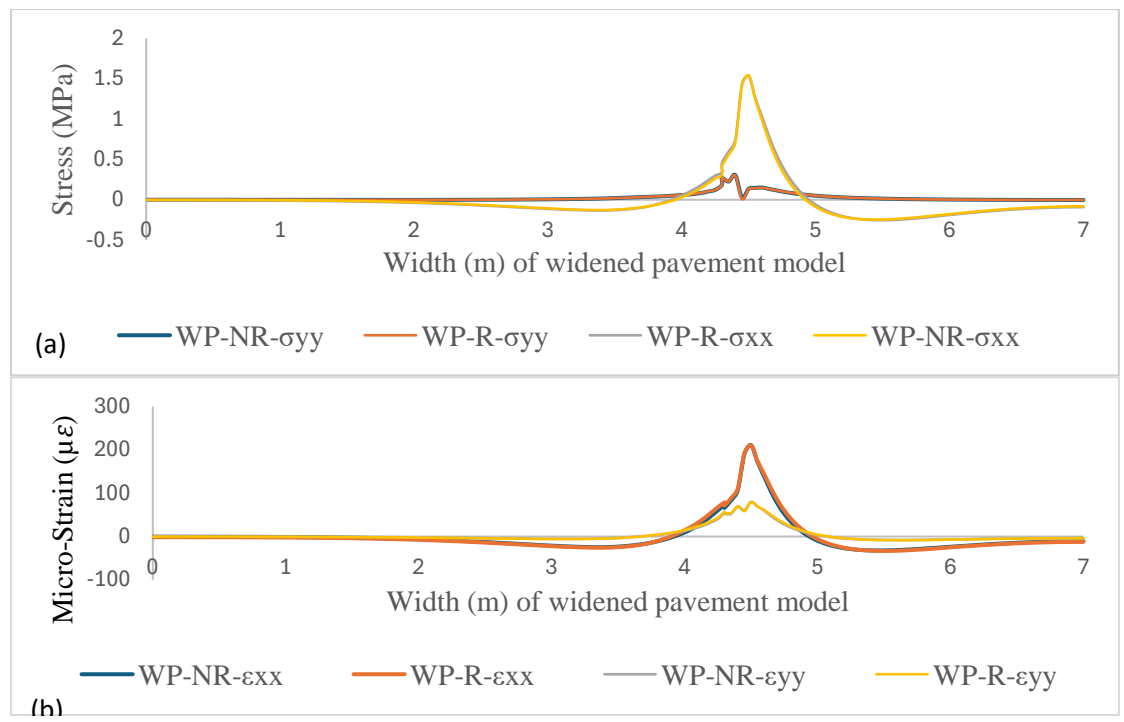


Figure 31 (a) Stresses σ_{yy} and σ_{xx} and (b) Micro-strains $\mu \varepsilon_{xx}$ and $\mu \varepsilon_{yy}$ along the width of the pavement in widened pavement models with and without reinforcement.

4.3 Effect of Load Location

In pavement engineering, it's well understood that different points on or within a pavement structure will respond differently to loads applied on the surface due to variations in the supporting material, the presence of joints or interfaces, and changes in the geometrical layout of the pavement layers. The purpose of subjecting the widened pavement model with reinforcement to varying load locations is to understand how the placement of the load affects the stress and strain at the critical points within the pavement structure. This critical location is typically prone to the highest potential for damage exists and where stress concentrations are most likely to occur.

The widened pavement model with reinforcement is subjected to varying location of load, to understand the effect of load location at the critical location. The pavement model is analysed under three loading locations, load location 1 (LL-1) being applied above the joint of subbase layers. The load location 2 (LL-2) and location 3 (LL-3) are situated \pm 0.75m away from LL-1 (see Figure 10). The stress concentrations developed in the critical location are of interest for the current research and hence the stress and strain results at the critical location are mentioned in Table-8.

The stress σ_{xx} experiences the highest stresses under LL-1 compared to LL-2 and LL-3. σ_{xx} under LL-1 experienced an increase of 75 % and 89.5% as compared to stress under LL-2 and LL-3. A similar trend of increase in stresses is also observed in σ_{yy} and σ_{xy} as well (see Figure 33 (a) and (b)). The corresponding strains ($\mu\varepsilon_{xx}$, $\mu\varepsilon_{yy}$ and $\mu\varepsilon_{xy}$) were also highest under the LL-1. LL-3, however, induces the least stresses at the critical location in the pavement structure, potentially making it more desirable in terms of minimizing the risk of stress-related damage such as cracks or deformation when compared to LL-2. LL-2, while experiencing higher stress and strain than LL-3, still experiences stress lower than LL-1. Lower stresses and strains are generally preferable, as they suggest a reduced likelihood of overstressing the pavement, which could lead to premature failure[3].

The significant increase in stress σ_{xx} and strain ε_{xx} observed at Load Location-1, situated directly above the joint of the subbase layers, can be attributed to the vulnerability and sensitivity of this position within the pavement structure. As the joint represents a point of material discontinuity and potential weakness, it is less capable of dispersing the load, resulting in a higher concentration of stress and an associated increase in strain. In contrast, Load Locations-2 and -3, being further from the critical location, distribute the load over a wider area, lessening the stress and strain before reaching the critical location. The direct path of stress transfer across the joint at LL-1 and critical location enhances the effects, leading to significantly higher stress and strain. The understanding of the effect of load location emphasizes the importance of wheel path in pavement design to minimize the occurrence of high stress concentrations that can lead to accelerated pavement deterioration. It is safe to say that a minimum distance between the wheel path and joint location is required for reducing the effects at the interface in widened pavements.

Table 8 Stresses and Strains at the critical stress location for widened pavement model subjected to variation in load location.

Models	$\sigma_{\chi\chi}$ (MPa)	σ_{yy} (MPa)	σ_{xy} (MPa)	$\mu \varepsilon_{xx}$	$\mu \varepsilon_{yy}$	$\mu \varepsilon_{xy}$
2D-WP-R	1.53179	0.14714	0.24888	202.3	54.6	86.2
Load Location-1						
2D-WP-R	0.3881	0.11527	0.12082	47.1	45.3	41.0
Load Location-2						
2D-WP-R	0.1670	0.01946	0.00689	21.4	40.9	23.9
Load Location-3						

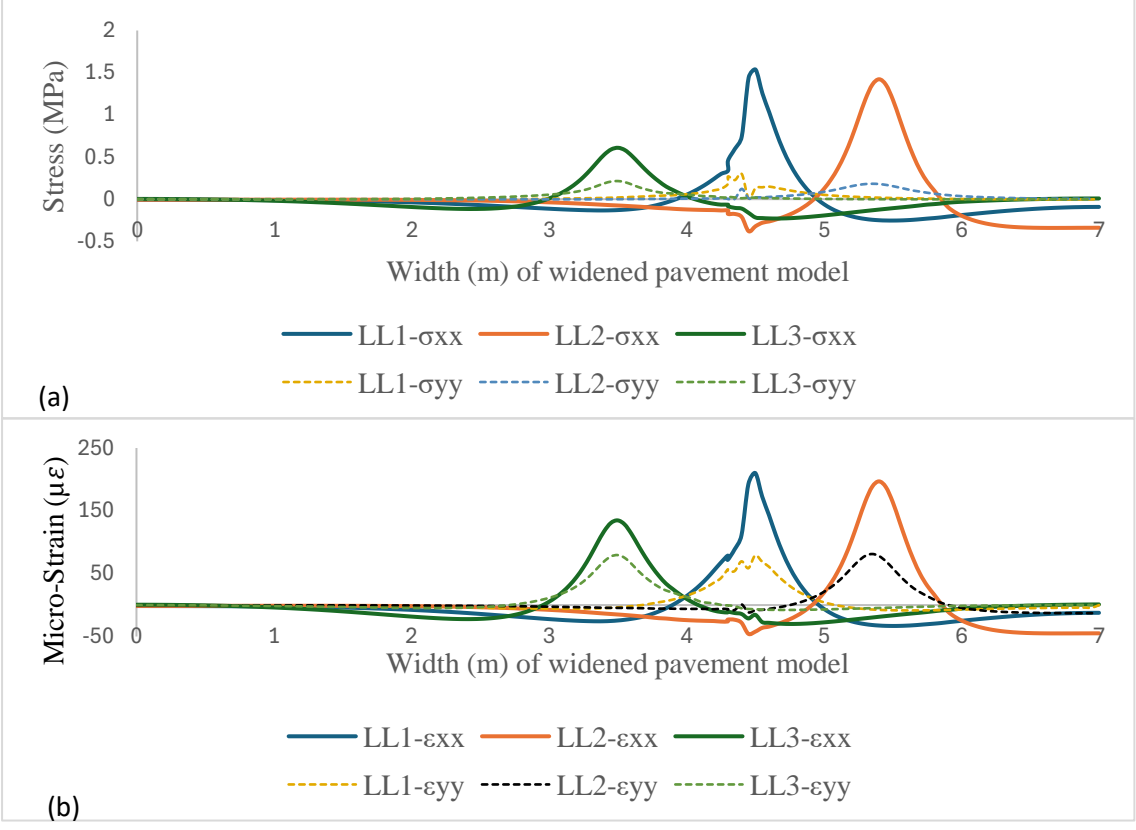


Figure 32 (a) Stresses σ_{yy} and σ_{xx} and (b) Micro-strains $\mu \varepsilon_{xx}$ and $\mu \varepsilon_{yy}$ along the width of the pavement in widened pavement models with varying load location.

4.4 Effect of varying material stiffness of base layer in widened pavement

Variations in the stiffness between the old and new base layers in widened pavements result in differential settlement and load transfer, which are major contributors to longitudinal cracking[5]. If the new layer is significantly stiffer, it may attract more load, increasing stress at points where the new and old pavements meet[5]. If the new layer is significantly less stiff, the interface may still experience high stress due to inadequate load distribution[5]. Either of the mentioned scenarios create a potential for pavement cracking and reduced performance.

Hence the performance of current standards in pavement widening was evaluated with increasing and decreasing material stiffness of the base layer in the widened part of the pavement. From Table-3, according to the current standards the difference between the stiffness of the existing base layer (EBL) and new base layer (NBL) is 2500MPa. The difference in stiffness is increased and decreased by 1500MPa and 3000MPa to conduct parametric analysis and the results from the analyses were recorded as shown in Table-9.

A 1500MPa increase in stiffness resulted in stress increments of 10% for σ_{xx} , 31.8% for σ_{yy} , and 3.11% for σ_{xy} , suggesting that the material's rigidity may contribute to higher stress concentrations. Correspondingly, strains $\mu \varepsilon_{xx}$, $\mu \varepsilon_{yy}$, and $\mu \varepsilon_{xy}$ decreased by 10%, 9.2%, and 14.8%. Greater stiffness implies that the material will exhibit less immediate deformation under load; however, excessive rigidity can translate to increased stress within the material, potentially exceeding its failure point over time.

Meanwhile, enhanced stiffness by 3000MPa intensified the previous trend, with stress increases of 19% for σ_{xx} , 47.7% for σ_{yy} , and 5.3% for σ_{xy} , and decreases in strains $\mu \varepsilon_{xx}$, $\mu \varepsilon_{yy}$, and $\mu \varepsilon_{xy}$ by 15%, 20.3%, and 28% respectively. The heightened stiffness seems to aggravate stress concentrations significantly and further reduce material deformation.

Conversely, reducing the base layer's stiffness by 1500MPa led to decreased stresses σ_{xx} by 13%, σ_{yy} by 65%, and σ_{xy} by 4.1% and increased strains $\mu \varepsilon_{xx}$ by 9%, $\mu \varepsilon_{yy}$ by 14.2%, and $\mu \varepsilon_{xy}$ by 13.8%, implying a less stiff material might absorb and distribute stresses more efficiently, but with an increase in deformation. A further reduction in stiffness by 3000MPa dramatically decreased stresses σ_{xx} by 23.5%, σ_{yy} by 75%, and σ_{xy} by 12.5% while increasing strains.

In conclusion, the variation in material stiffness of the base layer in widened pavements has a profound impact on the distribution of stresses and strains at the critical location, influencing the likelihood of premature pavement failure. An increase in stiffness tends to increase stresses which could lead to cracking, while a decrease in stiffness may result in higher strains and potential deformation. These findings underscore the importance of carefully considering and selecting the stiffness of base layer materials during the pavement widening process to ensure a balance between load distribution and structural integrity, ultimately extending the lifespan and sustainability of the pavement structure.

Table 9 Stresses and Strains at the critical stress location for widened pavement model subjected to variation in base layer material stiffness.

Models	$\sigma_{\chi\chi}$ (MPa)	σ_{yy} (MPa)	σ_{xy} (MPa)	$\mu \varepsilon_{xx}$	$\mu \varepsilon_{yy}$	$\mu \varepsilon_{xy}$
2D-WP-R	1.5317	0.04714	0.24888	0.0002023	-5.4e-05	8.62e-05
Increased Stiffness by 1500MPa	1.7034	0.06893	0.25753	0.0001869	-4.9e-05	7.43e-05
Increased Stiffness by 3000MPa	1.89987	0.08916	0.26326	0.0001702	-4.3e-05	6.22e-05
Decreased Stiffness by 1500MPa	1.33133	0.01663	0.23417	0.0002210	-6.3e-05	0.00010
Decreased Stiffness by 3000MPa	1.17624	-0.0107	0.21926	0.0002358	-0.00064	0.00011

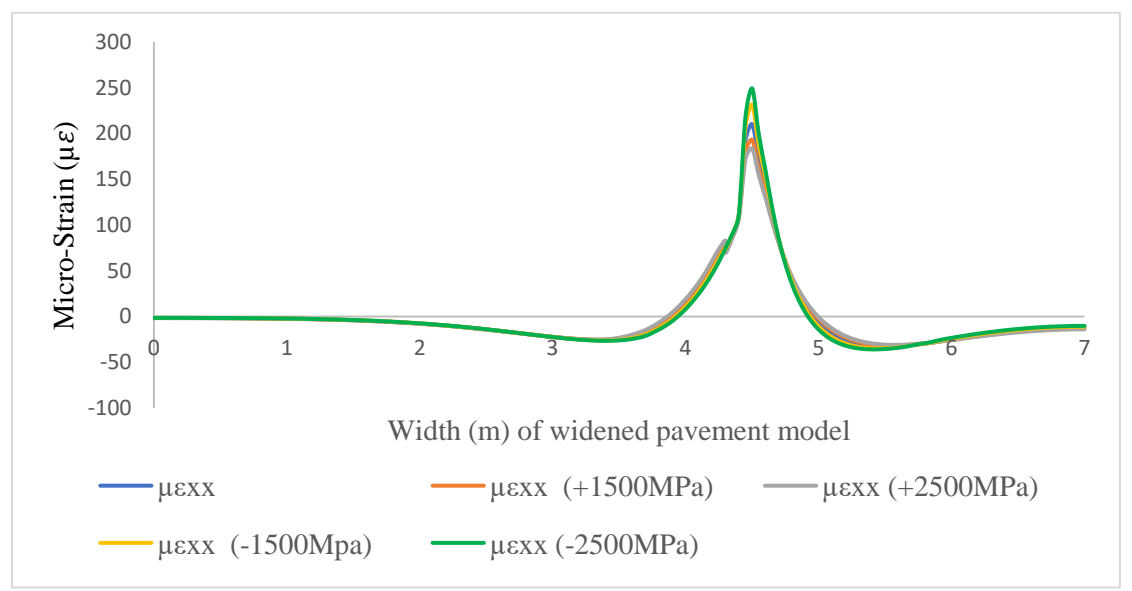


Figure 33 Micro-Strain $\mu \varepsilon_{xx}$ along the width of the pavement in widened pavement models with varying material stiffness.

4.5 Effect of varying base layer thickness in widened pavement

The impact of varying base layer thickness in the widened section of the pavement model at the critical location was investigated. By investigating the effects of base layer thickness variations, engineers and researchers aim to optimize pavement design for durability, safety, and cost-effectiveness, ensuring that infrastructure can adequately serve its intended purpose throughout its design life. It has been indicated by previous studies that significant deviations in base layer thickness between existing and widened pavements may lead to settlement issues at the subgrade level[5]. Consequently, the current research evaluated the existing pavement widening standards by altering the thickness of the base layer in the widened section. The standard design for a widened pavement model (see Figure 10) consists of a base layer thickness of 210 mm (see Table-3). In this section, the base layer thickness was alternately increased and decreased, each by 25 mm and 50 mm. Table 10 offers a detailed account of the stresses and strains at the critical location for the widened pavement model subjected to variations in base layer thickness.

In scenarios with the thickness increased by 25 mm, stresses σ_{xx} and σ_{xy} were observed to decrease by 3.8% and 4.1% respectively, whereas stress σ_{yy} increased by 30%. Strains $\mu \varepsilon_{xx}$, $\mu \varepsilon_{yy}$, and $\mu \varepsilon_{xy}$ experienced decreases of 50%, 9.2%, and 4.6% respectively.

An increase in thickness by 50 mm led to further reductions in stresses σ_{xx} and σ_{xy} , by 5.8% and 12.5% respectively. Conversely, stress σ_{yy} increased by 14.5%. Strain responses also followed a decreasing trend, with $\mu \varepsilon_{xx}$, $\mu \varepsilon_{yy}$, and $\mu \varepsilon_{xy}$ reducing by 70%, 9.2%, and 4.6% respectively.

When the thickness was reduced by 25 mm, increases in stresses σ_{yy} , σ_{yy} , and σ_{xy} by 5.5%, 29.8%, and 12.9% respectively were observed. Also, Strains $\mu \varepsilon_{xx}$, $\mu \varepsilon_{yy}$, and $\mu \varepsilon_{xy}$ increased by 4.7%, 1.8%, and 13.8% respectively. A more significant thickness reduction of 50 mm increases the stresses σ_{xx} , σ_{yy} , and σ_{xy} by 10%, 42.8%, and 17.2%, respectively, with corresponding increases in strains $\mu \varepsilon_{xx}$, $\mu \varepsilon_{yy}$, and $\mu \varepsilon_{xy}$ of 20%, 5.2%, and 10.8%.

Table 10 Stresses and Strains at the critical stress location for widened pavement model subjected to variation in base layer thickness.

Models	$\sigma_{\chi\chi}$ (MPa)	σ_{yy} (MPa)	σ_{xy} (MPa)	$\mu \varepsilon_{xx}$	$\mu \varepsilon_{yy}$	$\mu \varepsilon_{xy}$
2D-WP-R	1.53179	0.04714	0.248883	0.0002023	-5.4e-05	8.62e-05
Thickness 25mm+	1.47005	0.06626	0.237686	0.0001007	-4.9e-05	8.23e-05
Thickness 25mm-	1.62436	0.06769	0.285939	0.0002138	-5.5e-05	9.91e-05
Thickness 50mm+	1.44074	0.05549	0.216917	0.0000898	-5.0e-05	7.51e-05
Thickness 50mm-	1.70801	0.07105	0.292673	0.0002581	-5.7e-05	9.67e-05

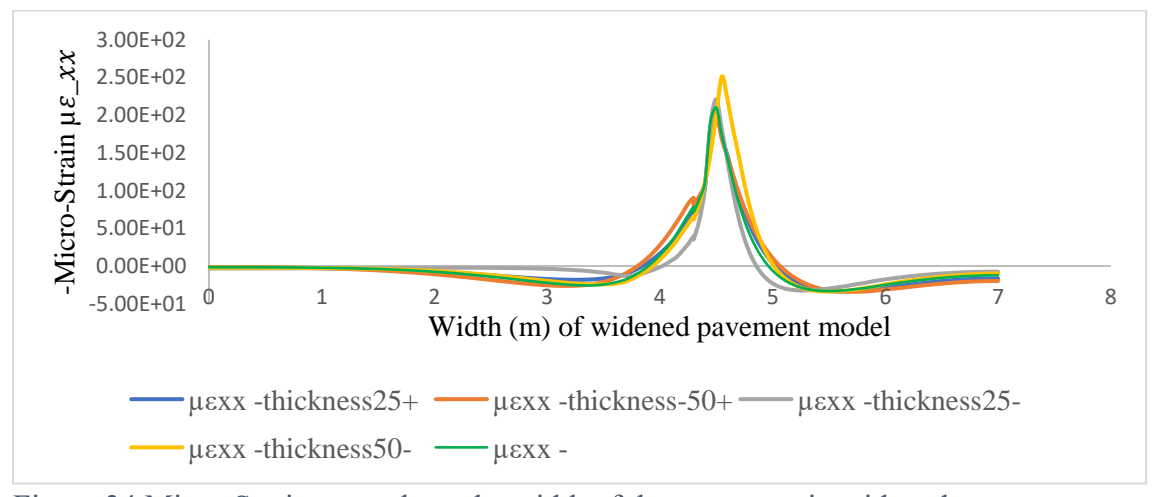


Figure 34 Micro-Strain $\mu \varepsilon_{xx}$ along the width of the pavement in widened pavement models with varying material stiffness.

4.6 Effect of varying Recessing/Overlapping length in base layer

The partitioning of the new base layer into multiple segments—NBL-1, NBL-2, and NBL-3, as depicted in Figure-14—was executed within the widened pavement model to deepen the understanding of different design approaches. The aim of experimenting with varied dimensions of the layered design in two distinct models was to refine the performance of the pavement model based on current design standards (2D-WP-R). In one variant, the model explores the outcome of reducing the recessing or overlapping length where the new base layer interfaces with the existing base layer. The other variant assesses the implications of decreasing the number of base layers from three to two. The modifications are designed to yield comparative data, offering valuable insights for optimizing the widened pavement structure. By scrutinizing these configurations, the analysis intends to identify the most durable and efficient structure under real-world loading conditions.

The current design standard uses the recessing lengths of 150mm, 650mm and 150mm for the layers NBL-1, NBL-2, and NBL-3 into existing base [22]. For the reduced recessing length (2D-RRL-R) model, the recessing length is reduced to 100mm and 200mm for Layers NBL-1 and NBL-3 (see Figure 24(b)). Whereas for NBL-3 the recessing into the existing base layer is removed. To evaluate the performance of the 2D-RRL-R model, the stresses and strains at the critical location are measured as presented in Table-11.

The stress σ_{xx} at the critical location showed an increase of 10.9% in the 2D-RRL-R model compared to the standard design (2D-WP-R). This suggests that the reduction in recessing length causes the pavement to experience higher tensile forces at the critical location. The shear stress σ_{xy} , which relates to the force that tries to cause layers to slide relative to each other, significantly increased by 34.72%. Such a sharp increase indicates that the interface could be under greater strain, increasing the potential for horizontal movement and shearing at the critical location. A 3.25% increase in the stress σ_{yy} suggests a moderate elevation in stress across the width of the pavement. While not as significant as the changes in the other stresses, it still highlights a response to the shortened recessing length. There are substantial increases in strains, with $\mu \varepsilon_{xx}$ rising by 34.72%, $\mu \varepsilon_{yy}$ by 16.67%, and $\mu \varepsilon_{xy}$ by 27.57%.

These higher strain values suggest more significant deformation at the critical location due to the reduced recessing, which could be an indicator of a potential for fatigue and other forms of deformation-induced damage. In summary, the reduction in recessing length influences the structural performance of the widened pavement. It affects the distribution and magnitude of stresses and strains within the pavement, which could lead to premature deterioration if not adequately addressed in the design.

Table 11 Stresses and Micro-Strains at the critical stress location for widened pavement model with reduced base layer recessing length

Models	$\sigma_{\chi\chi}$ (MPa)	σ_{yy} (MPa)	σ_{xy} (MPa)	$\mu \varepsilon_{xx}$	$\mu \varepsilon_{yy}$	$\mu \varepsilon_{xy}$
2D-WP-R	1.53179	0.04714	0.248883	202	54	86.22
2D-RRL-R	1.69952	0.04867	0.33532	272	63	110
Percentage Increase or Decrease (%)	10.96	3.25	34.72	34.65	16.67	27.57

4.7 Effect of Reduction in Number of Base Layers in Widened Pavement

The implementation of a pavement model with a reduced number of base layers, known as the 2D-RBL-R model, serves to explore the balance between cost efficiency and structural performance. By simplifying the layered structure, construction processes may be streamlined, leading to potential reductions in material, labour, and overall project expenditures. Such a model is crucial for assessing the criticality of each layer in meeting design objectives while ensuring sustainability through optimized use of resources. Furthermore, this approach enables an examination of the pavement's ability to withstand traffic demands with a minimized structure, which is particularly relevant for regions with variable traffic patterns or lower traffic loads. Ultimately, the investigation into models like the 2D-RBL-R contributes to the advancement of pavement engineering by challenging existing design and paving the way for cost-effective, and adaptable pavement solutions.

Similar to the 2D-RRL-R model, widened pavement model based on current design standards is compared to the model with reduced base layers (2D-RBL-R). The critical location in the 2D-RBL-R model is shifted upward compared to 2D-WP-R model. The critical location is still however the point of intersection of new base layer (NBL) and new subbase layer (NSL) as seen in previous models. The stress and strain values at the critical location are presented in Table-12.

The model with a reduced number of base layers exhibits a 22.8% decrease in the normal stress σ_{xx} . This reduction implies that the simplified base layer structure could be experiencing lower compressive forces due to the traffic loads. There's a 38.7% increase in the stress σ_{yy} , which suggests a concentrated stress response across the width of the pavement possibly due to the alteration in the base layer structure. An increase of 17% in shear stress σ_{xy} indicates a significant effect in the force that could cause horizontal sliding between the pavement layers at the critical location. All strain values experienced an increase, with $\mu \varepsilon_{xx}$ rising by 40%, $\mu \varepsilon_{yy}$ by almost 3 times and $\mu \varepsilon_{xy}$ by 3.5 times compared to 2D-WP-R model. These heightened strain readings signal an increased deformation at the critical location, which could potentially affect the fatigue life and overall durability of the pavement.

Table 12 Stresses and Micro-Strains at the critical stress location for widened pavement model with reduced number of base layers in widened part

Models	$\sigma_{\chi\chi}$ (MPa)	σ_{yy} (MPa)	σ_{xy} (MPa)	$\mu \varepsilon_{xx}$	μ $ε_{yy}$	$\mu \varepsilon_{xy}$
2D-WP-R	1.53179	0.04714	0.24888	202	54	86.2
2D-RBL-R	1.18404	0.06534	0.2912	339	204	390
Percentage Increase or Decrease (%)	-22.7	38.7	17.2	67.82	277	352.4

When comparing the two models with reduced recessing length and reduced number of layers, two main criteria were considered: the structural integrity of the pavement and the longevity of service life. 2D-WP-R serves as the baseline for performance given that it adheres to current design standards. The model with the reduced number of base layers (2D-RBL-R) shows a mix of decreased compressive and increased deformation responses, which may be beneficial for lower traffic loads but poses concerns for heavy-duty applications. The reduced recessing length model (2D-RRL-R), with increased stresses, suggests a potential for decreased service life due to higher chance of material fatigue and failure in the long term, particularly at

interfaces where layer sliding is more likely. The strain $\mu \varepsilon_{xx}$ is dominant in all three models and was hence plotted as shown in Figure 36.

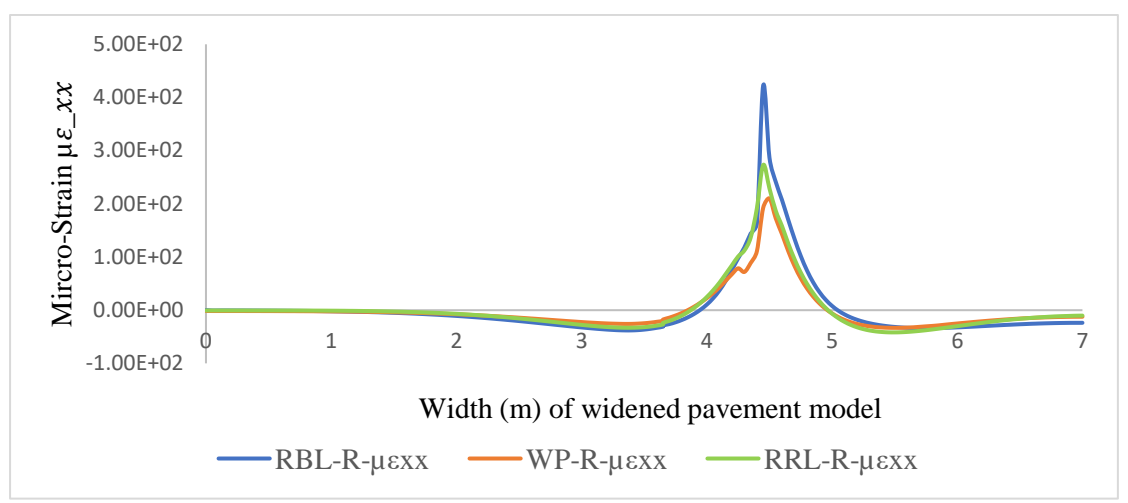


Figure 35 Micro-Strain $\mu \varepsilon_{xx}$ along the width of the pavement in widened pavement models with reduced recessing length and reduced number of base layers.

4.8 Effect of Cohesive Zone Modelling (CZM)

Cohesive zone modelling (CZM) is specifically designed to simulate the behaviour of interfaces or joints with cohesive forces[38]. More realistic representation of the interaction between the existing base layer (EBL) and the new base layers (NBL) in widened pavement across the joint is possible with CZM[39]. In contrast, a full bond model assumes perfect bonding between the layers, neglecting any potential separation or sliding at the interface while cohesive zone modelling is more sensitive to variations in interface conditions[13]. Different parameters within the CZM approach, such as cohesive strength and fracture toughness, can be adjusted to represent the actual behaviour of the joint more accurately [27].

The parameters for the CZM, as outlined in Table-4, were crucial in dictating the behaviour of the interface; these included traction-separation relationships that determine how the interface reacts to stress and how that damage evolves under further loading. The comparison of models with and without CZM (reflected in Figure 37) provide insights into the impact of including interface mechanics in widened pavement models. The critical location's stress and strain behaviours in models with and without cohesive zone modelling were compared, as presented in Table 13 presented in Table-13.

The 2D-CZM-R model shows a 4.49% increase in stress $\sigma_{\chi\chi}$ compared to the 2D-WP-R model, suggesting enhanced tensile forces at the critical location. Notably, there's a 1.29% decrease in the stress σ_{yy} for the 2D-CZM-R model, which could imply that introducing an interface with CZM marginally reduces the stresses acting across the pavement width. The 2D-CZM-R model shows an increase of 4.16% in shear stress $\sigma_{\chi y}$, reflecting a more considerable impact of shear forces at the joint interface. This increment is crucial because it highlights potential interlayer sliding effects that may affect pavement integrity over time. The model with CZM exhibits a 18.32% increase in micro-strain $\mu\varepsilon_{\chi\chi}$ along the length of the pavement. This increase points towards more significant elongation and potential flexibility at the critical location when the joint is modeled with CZM. An increase of 7.04% in micro-strain $\mu\varepsilon_{yy}$ was observed in the 2D-CZM-R model. Although small, this increase could suggest that the interface is experiencing marginally increased compression across the width of the pavement. Lastly,

there's a 4.17% increase in shear micro-strain $\mu \varepsilon_{xy}$ for the 2D-CZM-R model, indicating the potential for additional shear deformation at the pavement joint.

An increase in strains at the interface was observed when the stiffness of the cohesive zone material within the model was reduced. The behaviour was illustrated by the graphs of strain $\mu \varepsilon_{yy}$ (see Figure 37(b)), which compares the model with reduced CZM stiffness against fully bonded layers. This indicates that the interface's capacity to transfer loads and maintain structural integrity is influenced by the stiffness of the CZM material. A lower stiffness correlates to a more significant deformation response under the same loading conditions.

Table 13 Stresses and Micro-Strains at critical location for widened pavement models 2D-WP-R and model with CZM modelling (2D-CZM-R) of the joint

Models	$\sigma_{\chi\chi}$ (MPa)	σ_{yy} (MPa)	σ_{xy} (MPa)	$\mu \varepsilon_{xx}$	μ $ε_{yy}$	$\mu arepsilon_{xy}$
2D-WP-R	1.53179	0.04714	0.24888	202	54	86.2
2D-CZM-R	1.60057	0.04655	0.25923	239	57.8	89.8
Percentage Increase or Decrease (%)	4.49	-1.29	4.16	18.32	7.04	4.17

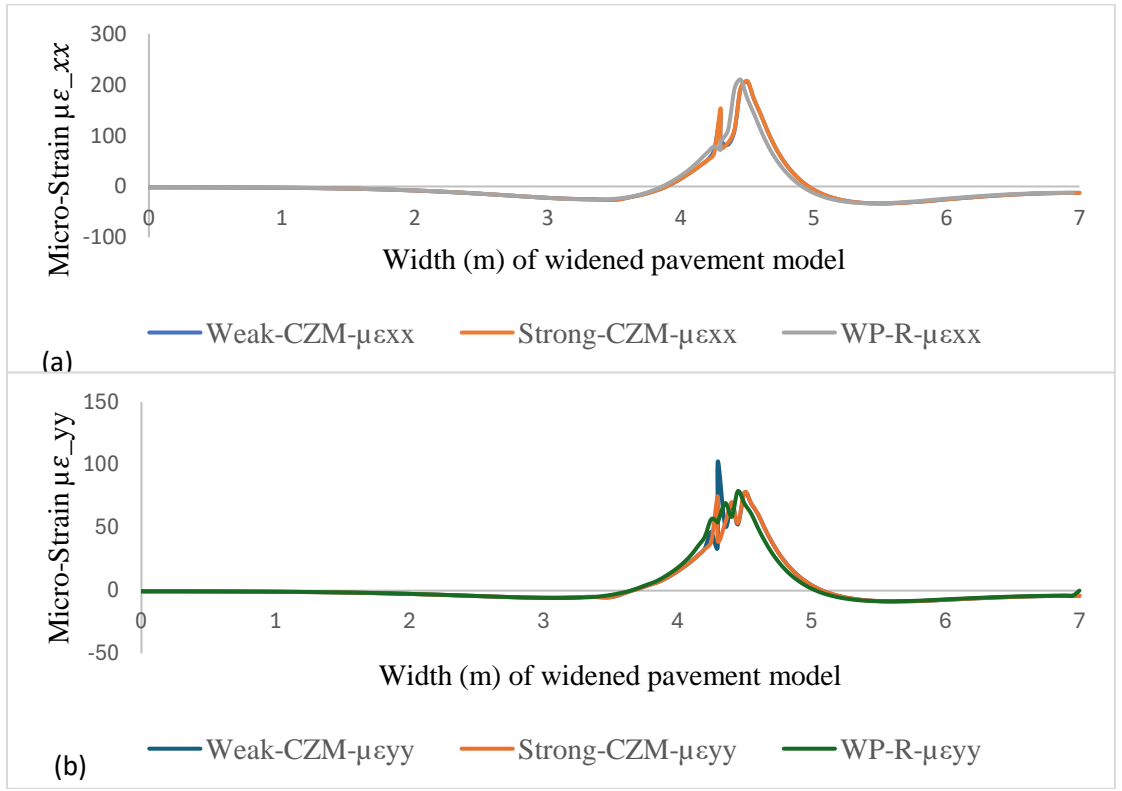


Figure 36 (a) Micro-Strain $\mu \varepsilon_{xx}$ and (b) $\mu \varepsilon_{yy}$ along the width of the pavement in widened pavement models with CZM and current design standards.

4.9 Effect EVP material in Base Layers

The comparison between widened pavement models with surface layer EVP material alone and those with a combination of surface and base layer EVP material provides insights into stress and strain behaviours at critical locations. The stress and microstrains at the critical location are shown in Table14 and the microstrains in X- and Y- direction are shown in Figure 37 (a) and (b).

The 3% increase in stress σ_{xx} suggests a modest increase in tensile forces at the critical location when adding a base layer to the surface layer. The increase in tensile stress may influence pavement performance, particularly in areas prone to cracking or fatigue failure. With a 3.34% increase in stress σ_{yy} , there's a slight rise in stresses acting across the pavement width when the base layer is added. While the increase may contribute to overall structural stability, it also necessitates careful consideration during pavement design and construction to ensure adequate support for traffic loads. The 4% increase in shear stress σ_{xy} highlights the elevated shear forces at the joint interface between the surface and base layers. These increased shear stresses may lead to greater potential for interlayer sliding, which can compromise pavement integrity over time.

The 1.2% increase in micro-strain $\mu \varepsilon_{xx}$ indicates slightly greater elongation and potential flexibility at the critical location when the base layer is added. While increased flexibility can be beneficial in mitigating pavement distress, it also underscores the importance of proper design and construction techniques to maintain pavement performance. The notable 8% increase in micro-strain $\mu \varepsilon_{yy}$ suggests marginally increased compression across the width of the pavement when the base layer is added. The increase in compression underscores the need for proper pavement design to account for the additional loads and stresses imposed on the widened pavement. The 2% increase in shear micro-strain $\mu \varepsilon_{xy}$ indicates the potential for additional shear deformation at the pavement joint. The increased shear deformation highlights the importance of implementing appropriate construction techniques to minimize pavement distress and ensure the longevity of the widened pavement.

Overall, the comparison between widened pavement models with and without a base layer provides valuable insights into the effects of different pavement configurations on stress and strain behaviours. These insights are crucial for informing pavement design and construction practices, ultimately contributing to the successful implementation of pavement widening projects and the long-term sustainability of transportation infrastructure.

Table 14 Stresses and Micro-Strains at critical location for widened pavement models 2D-WP-R with surface layer EVP material and combined surface + base layer with EVP material.

Models	$\sigma_{\chi\chi}$ (MPa)	σ_{yy} (MPa)	σ_{xy} (MPa)	$\mu \varepsilon_{xx}$	$\mu \varepsilon_{yy}$	$\mu arepsilon_{xy}$
2D-WP-R	1.53179	0.04714	0.24888	202	54	86.2
(Surface Layer						
EVP material)						
2D-WP-R	1.5759	0.04924	0.25883	204.24	58.32	87.9
(Surface +Base						
Layer EVP						
material)						
Percentage	3	3.34	4	1.2	8	2
Increase or						
Decrease (%)						

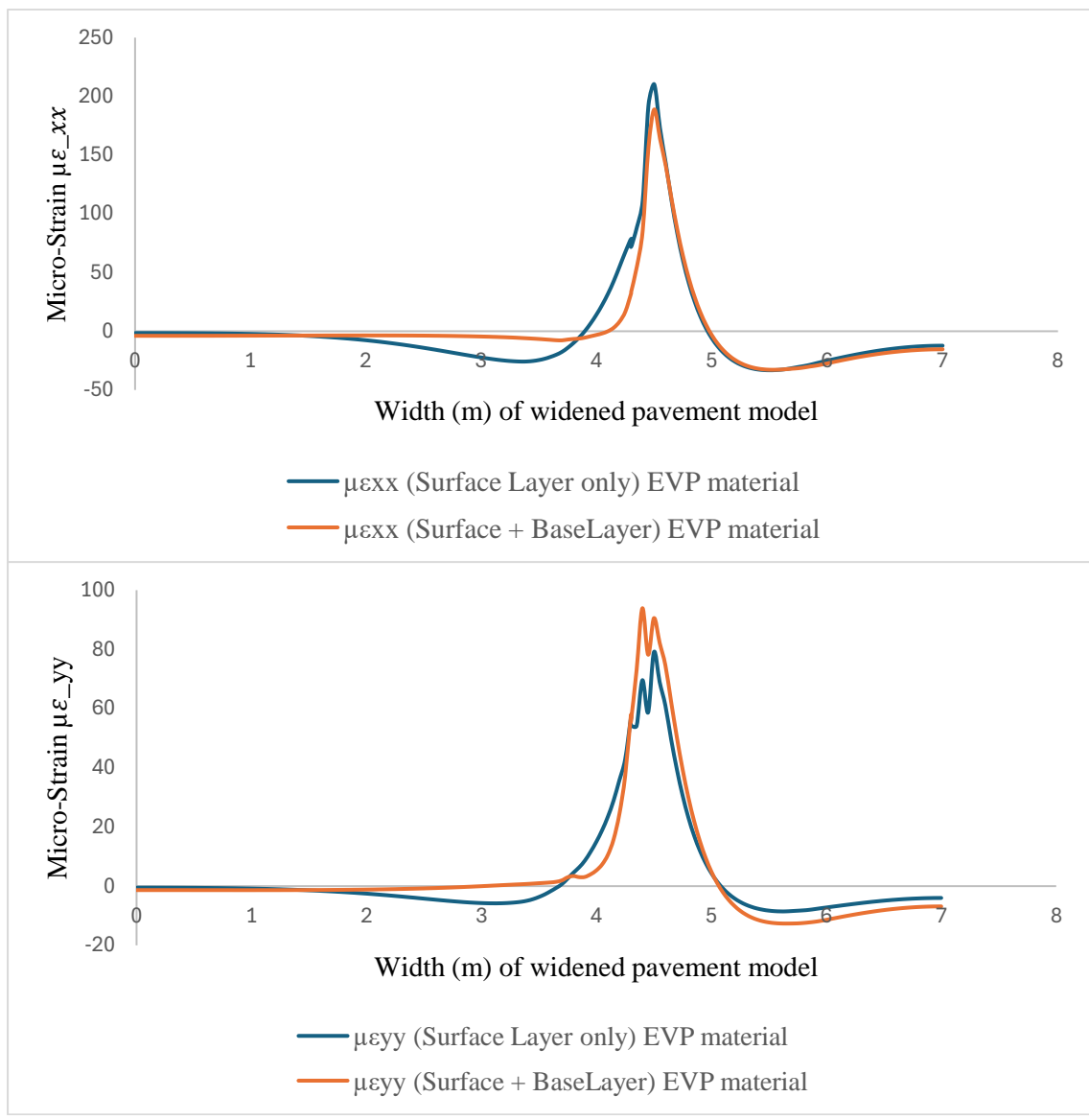


Figure 37 (a) Micro-Strain $\mu \varepsilon_{xx}$ and (b) $\mu \varepsilon_{yy}$ along the width of the pavement in widened pavement models with surface layer EVP material and combined surface and base layer EVP material.

5 Conclusions

In the current chapter, the conclusions based on the research questions mentioned in Chapter 1 are discussed.

1. How can an elasto-visco-plastic material model be developed for the surface asphalt layer in finite element method simulations?

- Sub-questions:

- a) What are the key parameters required to define the elasto-visco-plastic behaviour of asphalt materials?
- b) How does the newly developed EVP model compare with existing material models in terms of accuracy and reliability?

A material model that captures the viscoelastic and plastic characteristics of asphalt was developed for use in simulation studies of pavements using the Finite Element Method (FEM). The material model was tested in both two-dimensional and three-dimensional simulations with uniform geometry for valid comparisons. During the tests, it was evident that the elasto-viscoplastic (EVP) material model displayed a delay in returning to its original shape after the applied load was removed, unlike the elastic model that quickly regains its original shape, emphasizing the time-dependant nature of the asphalt material's response.

The results indicated that the material model was able to experience higher levels of strain than the purely elastic model, pointing to the conservative nature of elastic calculations. The two-dimensional model was particularly sensitive, showing higher strain readings than the three-dimensional model, which considers the full range of deformation across the material depth.

Clearly, the material model revealed the ability to track permanent deformation, as the model was unable to retain its original shape even after the load removal. The material model provides better understanding to elasto-visco-plastic behaviour of the material, useful for more accurate predictions in widened pavements.

2. Where are the critical stress concentrations located in pavements due to widening, and how can they be identified?

- Sub-questions:

- a) What simulation techniques can be used to accurately identify these critical locations?
- b) How does widening of pavement influence the distribution and magnitude of stress concentrations?

In the pursuit to identify critical locations of stress concentrations due to pavement widening, the study compared models of both unwidened and widened pavements. It was found that stress concentrations are particularly significant at the intersection between the base and subbase within the widened pavement section.

The examination of this critical location showed a substantial increase in stresses within the widened pavement model, especially along the width of the pavement, where the stiffness of the material changes. The increase in stress was much higher than that seen in the unwidened pavement model. Similar trends were observed for other stress directions at the same critical location.

Moreover, the study found that strain levels in the widened pavement model increased significantly in comparison with the unwidened model, underscoring the importance of focusing on these areas during the process of widening pavements. However, one form of strain lessened in the widened pavement model, providing an interesting contrast to the other increases. The discussed results highlight the essential need for careful design and material consideration when carrying out pavement widening to prevent the development of stress concentrations that can cause premature deterioration.

- 3. In what ways does the variation of load location, base layer thickness, and base layer material stiffness effect stress concentration in pavement widening scenarios?
 - Sub-questions:
 - a) Which of these factors has the greatest impact on stress concentration, and to what degree?
 - b) How does the interaction between these factors influence the overall stress distribution in the widened pavement?

The objective to understand the influence of varying load locations, base layer thickness, and base layer material stiffness on stress concentration in pavement widening scenarios yielded informative results.

Load placed directly on the joint leads to greater stress and strain compared to locations further from the joint. Conversely, load locations situated farther from the joint displayed lower stress concentrations, suggesting a reduced risk of damage in these areas such as cracks or deformation.

The remarkable increase in stress and strain at the load location above the subbase joint underscores the joint's vulnerability as a point of discontinuity. Load locations away from the joint help to spread out the stresses and thus lessen the overall impact on the pavement.

The findings regarding load location highlight the importance of careful wheel path planning in pavement design to reduce high stress concentrations. Ensuring an adequate distance between the wheel path and the joint location is crucial to minimize the detrimental effects on the interface in widened pavements. Such knowledge is valuable for informing best practices in pavement widening to support the increasing traffic loads while protecting the structural integrity of the pavement.

With respect to the change in material stiffness of the base layer, the research demonstrated that an increase in stiffness led to an increase in stress levels, which may indicate that a more rigid material transfers higher stress within the pavement. Specifically, a moderate increase in stiffness resulted in a noticeable increment in stress, along with a decrease in strains, suggesting that while the material deformed less under load, it incurred more stress which may compromise its long-term integrity.

When the material's stiffness was enhanced even further, the stresses further increased, and the deformation reduced substantially. These findings point to material rigidity being a critical factor in stress amplification within the pavement structure, potentially raising the risk of material failure due to overstress.

On the opposite spectrum, a decrease in base layer stiffness yielded lower stress levels, with corresponding increases in strain, indicating that a less stiff material might endure more deformation but distribute the applied stresses more effectively.

The study concludes that the stiffness variations in the base layer substantially affect stress and strain distribution, thereby influencing the structural health and durability of widened pavements. An optimal balance of base layer stiffness is essential for maintaining the pavement's structural integrity and functionality, which is a pivotal consideration during the pavement widening process to enhance the longevity and performance of the pavement system.

Increasing the base layer thickness leads\ to reduced stresses along the direction of travel and shear stresses, while stress perpendicular to travel direction increases. Strain across all directions decreases, with a significant reduction in the direction parallel to travel.

Further thickness increases result in greater reductions in the directional travel and shear stresses, with the increase in perpendicular stress being less severe. The strains continue to show a decreasing pattern, indicating enhanced resistance to deformation.

In contrast, decreasing the base layer thickness results in higher stresses in the direction of travel, perpendicular to it, and in shear. Strains also rise, reflecting diminished load distribution effectiveness.

A more extensive thickness reduction further amplifies stress and strain increases, highlighting the detrimental effects of a thinner base layer on pavement durability.

A thicker base layer typically improves pavement's ability to manage loads, reducing deformation despite the accompanying rise in perpendicular stress. Conversely, a thinner base layer brings about higher stress and strain, potentially reducing pavement lifespan and necessitating increased maintenance. Selecting an appropriate base layer thickness is crucial for balanced stress distribution and maintaining pavement longevity, especially during widening operations.

- 4. How do reduced recessing lengths and reduced base layers in new pavement designs perform compared to standard designs?
- Sub-questions:
 - a) What trade-offs exist between reducing recessing length/base layer thickness and maintaining pavement integrity?

In the study of reduced recessing length (RRL) in new pavement designs, it was found that both tensile forces at critical locations and shear stresses increased, indicating a higher possibility of horizontal movement and potential shearing. Although the increase in stress across the width was moderate, all types of strain experienced substantial rises, indicative of increased deformation and a heightened risk of fatigue and related damage.

With the reduction in the number of base layers, (RBL) the designs exhibited less normal stress, implying that the pavement could be experiencing lower compressive forces from traffic loads. Nonetheless, the transverse stress and shear stress both increased, which suggested a stress concentration effect and a significant potential for horizontal sliding between pavement layers.

When comparing the models with reduced recessing length and those with a reduced number of layers, both variations present challenges to the structural integrity and service life of pavements. The reduced recessing length model displayed stresses, potentially leading to a shortened service life due to the risk of material fatigue and failure, especially at interfaces where layer sliding might occur. Conversely, the model with fewer base layers showed mixed responses in compressive and deformation reactions, that could offer some benefits for lighter traffic conditions but raises concerns for heavy-duty applications. In summary, the standard

design takes a more conservative approach to ensure durability and minimize maintenance. Models with RBL or RRL carry risks that could lead to a need for more frequent repairs or a shorter overall lifespan of the pavement.

5. How does modelling the interface between pavement layers using cohesive zone modelling compare with a full bond model in terms of predicting pavement performance?

- Sub-questions:

a) How do the results of cohesive zone model impact the design recommendations for pavement interfaces?

Cohesive zone modelling (CZM) offered a more detailed and precise representation of the pavement layer interface compared to a full bond model. CZM simulated the presence of cohesive forces at the interface, offering insights into the interlayer behaviour not accounted for by the assumption of perfect bonding.

Models incorporating CZM with high stiffness adhesion material demonstrated a slight increase in stresses at the critical location, suggesting that these interfaces may experience higher forces. Additionally, the increase in shear stress in models with CZM suggests an increased potential for shear movement at the interface, that needs further consideration in design to prevent failures. The increase in strains along the depth and across the width in the model with CZM showcased that it could contribute to greater deformation under load, implying a need for careful consideration of material and layer interface properties in design to maintain pavement durability.

As stiffness in the cohesive zone material was reduced, models exhibit greater deformation, confirming the influence CZM parameters have on the load-transfer capacity and overall structural behaviour. This illustrates the critical role of accurately capturing the interface properties in the widened pavement design to ensure the pavement system's performance aligns with expectations over its service life.

In conclusion, the findings presented in the current chapter underscore the importance of developing accurate material models and conducting thorough analyses while designing and widening pavements. Through the development of an elasto-visco-plastic material model, identification of stress concentrations, investigation of load variations, base layer thickness, and material stiffness, as well as the evaluation of reduced recessing length and base layers, the study has provided valuable insights into the behaviours of widened pavement structures. Additionally, the comparison between cohesive zone modelling and full bond modelling highlighted the significance of considering interface properties in pavement design. By addressing the objectives, the research contributes to a deeper understanding of the factors influencing widened pavement performance. These insights are crucial for informed decision-making in transportation infrastructure management, ultimately contributing to safer and more resilient road networks.

6 Future Recommendations

The current chapter outlines recommendations for future research, pointing to areas that could benefit from further study and development. The recommendations build on the findings of this research and seek to encourage ongoing advancement in the field of pavement engineering.

1. Advancement of Material Models:

- Continuously refine and enhance elasto-visco-plastic (EVP) material models to better capture the complex behaviour of asphalt materials under varying conditions, including temperature fluctuations, and aging effects.
- Investigate the incorporation of additional parameters into material models to account for factors such as moisture susceptibility and fatigue resistance, which are crucial for accurate pavement performance predictions.

2. Refinement of Stress Concentration Identification Techniques:

- Explore advanced simulation techniques, such as coupled multi-physics simulations, to identify critical stress concentrations more accurately in widened pavements, considering factors like non-linear material behaviour and dynamic loading conditions.
- Develop automated algorithms or machine learning approaches to streamline the process of identifying stress concentration locations and quantifying their severity, facilitating efficient pavement design and maintenance strategies.

3. Comprehensive Analysis of Load Variations:

- Conduct comprehensive studies to assess the effects of various load scenarios, including dynamic loading from heavy vehicles and seasonal fluctuations in traffic volume, on stress distribution and pavement performance.
- Investigate the potential benefits of innovative load management strategies, such as intelligent traffic routing and weight restrictions, in minimizing stress concentrations and extending pavement service life.

4. Optimization of Base Layer Design:

- Explore novel materials and construction techniques for base layers to achieve an optimal balance between stiffness, flexibility, and load-bearing capacity, considering factors such as environmental sustainability and cost-effectiveness.
- Investigate the potential benefits of incorporating reinforcement elements, such as geosynthetics or recycled materials, into base layers to enhance their mechanical properties and mitigate stress concentrations.

5. Integration of Advanced Interface Modelling Techniques:

- Further develop cohesive zone modelling (CZM) approaches to accurately simulate the behaviour of pavement layer interfaces under various loading and environmental conditions.
- Explore the integration of CZM with advanced computational techniques, such as discrete element modelling (DEM) or finite element analysis (FEA), to capture complex interface interactions and facilitate more realistic pavement performance predictions.

6. Long-Term Field Validation Studies:

- Initiate long-term field studies to validate the findings of laboratory-based simulations and numerical models, assessing the actual performance of widened pavements under real-world conditions.
- Collaborate with transportation agencies and industry stakeholders to establish monitoring programs and data collection protocols for ongoing evaluation of widened pavement projects, informing future design improvements and maintenance strategies.

7.Integration of Material, 3D, and Joint Modelling:

- Future research should aim to integrate advanced material modelling, 3D pavement modelling, and joint modelling approaches into a unified framework for comprehensive pavement analysis.
- Develop multi-physics simulation techniques that can capture the interactions between material behaviour, pavement geometry, and joint performance in widened pavements.

8. Integration of Multi-Scale Modelling:

- Integrating multi-scale modelling approaches is crucial for capturing the hierarchical structure and behaviour of pavement materials across different length scales.
- Future research should focus on developing integrated frameworks that seamlessly combine macroscopic, mesoscopic, and microscopic models to simulate the complex interactions between pavement layers.

9. Data-driven Modelling and Machine Learning:

- Harnessing data-driven modelling and machine learning techniques offers great potential for overcoming technical challenges in pavement analysis. Future research should explore the use of big data analytics, artificial intelligence algorithms, and deep learning architectures to extract insights from large-scale pavement datasets.
- Integrating data-driven approaches with physics-based models would enhance the
 accuracy and predictive capabilities of pavement simulations while reducing
 computational costs and modelling uncertainties.

7 References

- [1] "PoA Version Final".
- [2] M. Pasetto and N. Baldo, "Numerical visco-elastoplastic constitutive modelization of creep recovery tests on hot mix asphalt," *Journal of Traffic and Transportation Engineering (English Edition)*, vol. 3, no. 5, pp. 390–397, Oct. 2016, doi: 10.1016/j.jtte.2016.09.009.
- [3] T. Transportation Institute, "Texas Department of Transportation GUIDELINES FOR DESIGN OF FLEXIBLE PAVEMENT WIDENING i," 2006.
- [4] X. Liu, A. Scarpas, C. Van Gurp, and A. Venmans, "Numerical investigation of response of widened pavement system," *Transp Res Rec*, no. 2227, pp. 3–12, Dec. 2011, doi: 10.3141/2227-01.
- [5] Q. Shen, Y. Lu, Y. Yang, and G. Long, "Research on Mechanical Response of Pavement Structure to Differential Settlement of Subgrade on Highway Widening," *Advances in Materials Science and Engineering*, vol. 2021, 2021, doi: 10.1155/2021/4445185.
- [6] X. Weng and W. Wang, "Influence of differential settlement on pavement structure of widened roads based on large-scale model test," *Journal of Rock Mechanics and Geotechnical Engineering*, vol. 3, no. 1, pp. 90–96, Mar. 2011, doi: 10.3724/sp.j.1235.2011.00090.
- [7] K. Li, W. Xu, and L. Yang, "Deformation characteristics of raising, widening of old roadway on soft soil foundation," *Symmetry (Basel)*, vol. 13, no. 11, Nov. 2021, doi: 10.3390/sym13112117.
- [8] W.-L. Huang, H.-Y. Wang, and L.-J. Huang, "Viscoelastic Analysis of Flexible Pavements Embedded with Controlled Low-Strength Material Bases Using Finite Element Method," 2017.
- [9] Y. Zhang, M. Bernhardt, G. Biscontin, R. Luo, and R. L. Lytton, "A generalized Drucker–Prager viscoplastic yield surface model for asphalt concrete," *Materials and Structures/Materiaux et Constructions*, vol. 48, no. 11, pp. 3585–3601, Nov. 2015, doi: 10.1617/s11527-014-0425-1.
- [10] S. Kumar Srirangam, "Numerical Simulation of Tire-Pavement Interaction."
- [11] C.-W. Huang, ; Rashid, K. A. Al-Rub, ; Eyad, A. Masad, and D. N. Little, "Three-Dimensional Simulations of Asphalt Pavement Permanent Deformation Using a Nonlinear Viscoelastic and Viscoplastic Model", doi: 10.1061/ASCEMT.1943-5533.0000022.
- [12] J. Yi, S. Shen, B. Muhunthan, and D. Feng, "Viscoelastic-plastic damage model for porous asphalt mixtures: Application to uniaxial compression and freeze-thaw damage," *Mechanics of Materials*, vol. 70, pp. 67–75, Mar. 2014, doi: 10.1016/j.mechmat.2013.12.002.
- [13] Z. Yang, H. Yang, L. Wang, and D. Cao, "The development and application of an interfacial cohesive zone model of the pavement interlayer considering the characteristics of adhesive materials," *Case Studies in Construction Materials*, vol. 18, Jul. 2023, doi: 10.1016/j.cscm.2022.e01775.
- [14] X. Wang and Y. Zhong, "Influence of tack coat on reflective cracking propagation in semi-rigid base asphalt pavement," *Eng Fract Mech*, vol. 213, pp. 172–181, May 2019, doi: 10.1016/j.engfracmech.2019.04.015.

- [15] E. Offei, K. Ksaibati, R. K. Young, and D. Apronti, "Evaluating base widening methods," *International Journal of Pavement Engineering*, vol. 17, no. 6, pp. 517–527, Jul. 2016, doi: 10.1080/10298436.2015.1007227.
- [16] "Petri Varin, Timo Saarenketo ROAD WIDENING GUIDELINES A ROADEX IV report for Task D2 'Widening of Roads' 2 PREFACE."
- [17] J. Zhang, J. Zheng, and B. Huang, "Fracture Mechanics Analysis of Cracking in Asphalt Pavement Widening."
- [18] H. Wang, Y. Wu, J. Yang, and H. Wang, "Numerical simulation on reflective cracking behavior of asphalt pavement," *Applied Sciences (Switzerland)*, vol. 11, no. 17, Sep. 2021, doi: 10.3390/app11177990.
- [19] S. Yang, Y. Zhang, O. Kaya, H. Ceylan, and S. Kim, "Investigation of longitudinal cracking in widened concrete pavements," *Baltic Journal of Road and Bridge Engineering*, vol. 15, no. 1, pp. 211–231, 2020, doi: 10.7250/bjrbe.2020-15.468.
- [20] A. Thombre, "Study of Structural Failure of Road after Widening and its Remedial Measures," *Int J Res Appl Sci Eng Technol*, vol. 11, no. 5, pp. 5726–5733, May 2023, doi: 10.22214/ijraset.2023.53025.
- [21] A. Das, "Structural Design of Asphalt Pavements: Principles and Practices in Various Design Guidelines," *Transportation in Developing Economies*, vol. 1, no. 1, pp. 25–32, Oct. 2015, doi: 10.1007/s40890-015-0004-3.
- [22] M. Projects, "Specifications Design Asphalt pavements," 2016. [Online]. Available: www.onlinedoctranslator.com
- [23] Z. C. Grasley, "VISCOELASTIC-VISCOPLASTIC DAMAGE MODEL FOR ASPHALT CONCRETE," 2009.
- [24] S. P. Panchenko, "NUMERICAL SIMULATION OF VISCOELASTIC MATERIALS," *Science and Transport Progress. Bulletin of Dnipropetrovsk National University of Railway Transport*, vol. 0, no. 5(53), p. 157, Nov. 2014, doi: 10.15802/stp2014/30811.
- [25] P. Mackiewicz and A. Szydło, "Viscoelastic parameters of asphalt mixtures identified in static and dynamic tests," *Materials*, vol. 12, no. 13, Jul. 2019, doi: 10.3390/ma12132084.
- [26] E. Chen and X. Zhang, "Dynamic Analysis of Viscoelastic Asphalt Pavement under Vehicle–Bridge Interaction Load," *Journal of Transportation Engineering, Part B: Pavements*, vol. 147, no. 4, Dec. 2021, doi: 10.1061/jpeodx.0000296.
- [27] R. F. N. Brito, R. D. S. G. Campilho, R. D. F. Moreira, I. J. Sánchez-Arce, and F. J. G. Silva, "Composite stepped-lap adhesive joint analysis by cohesive zone modelling," in *Procedia Structural Integrity*, Elsevier B.V., 2021, pp. 665–672. doi: 10.1016/j.prostr.2021.10.074.
- [28] R. Ktari, F. Fouchal, A. Millien, and C. Petit, "Surface roughness: A key parameter in pavement interface design," *European Journal of Environmental and Civil Engineering*, vol. 21, pp. s27–s42, Mar. 2017, doi: 10.1080/19648189.2017.1304284.
- [29] N. F. Ghaly, I. M. Ibrahim, and E. M. Noamy, "Tack coats for asphalt paving," *Egyptian Journal of Petroleum*, vol. 23, no. 1, pp. 61–65, Mar. 2014, doi: 10.1016/j.ejpe.2014.02.009.
- [30] R. F. N. Brito, R. D. S. G. Campilho, R. D. F. Moreira, I. J. Sánchez-Arce, and F. J. G. Silva, "Composite stepped-lap adhesive joint analysis by cohesive zone modelling," in *Procedia Structural Integrity*, Elsevier B.V., 2021, pp. 665–672. doi: 10.1016/j.prostr.2021.10.074.

- [31] Y. Li and B. Zeng, "Modeling of masonry structures using a new 3D cohesive interface material model considering dilatancy softening," *Eng Struct*, vol. 277, Feb. 2023, doi: 10.1016/j.engstruct.2022.115466.
- [32] C. Du, Y. Sun, J. Chen, H. Gong, X. Wei, and Z. Zhang, "Analysis of cohesive and adhesive damage initiations of asphalt pavement using a microstructure-based finite element model," *Constr Build Mater*, vol. 261, Nov. 2020, doi: 10.1016/j.conbuildmat.2020.119973.
- [33] R. Michalczyk, "Implementation of generalized viscoelastic material model in Abaqus code," 2015. [Online]. Available: https://www.researchgate.net/publication/270880363
- [34] A. Zbiciak, "APPLICATION OF ELASTO-VISCO-PLASTIC CONSTITUTIVE MODEL FOR ASPHALT PAVEMENT CREEP SIMULATION."
- [35] S. Lelovic, "Conditions for stability of deformation in elasto-plastic materials," *Gradjevinski materijali i konstrukcije*, vol. 58, no. 4, pp. 37–49, 2015, doi: 10.5937/grmk15040371.
- [36] "Abaqus/CAE User's Manual Abaqus 6.11 Abaqus/CAE User's Manual."
- [37] "Finite Element Analysis for pavement widening," 2018.
- [38] R. D. S. G. Campilho, M. D. Banea, J. A. B. P. Neto, and L. F. M. Da Silva, "Modelling adhesive joints with cohesive zone models: Effect of the cohesive law shape of the adhesive layer," *Int J Adhes Adhes*, vol. 44, pp. 48–56, 2013, doi: 10.1016/j.ijadhadh.2013.02.006.
- [39] S. H. Song, G. H. Paulino, and W. G. Buttlar, "A bilinear cohesive zone model tailored for fracture of asphalt concrete considering viscoelastic bulk material," *Eng Fract Mech*, vol. 73, no. 18, pp. 2829–2848, Dec. 2006, doi: 10.1016/j.engfracmech.2006.04.030.